

EFFECT OF ULTRASOUND ON XANTHAN GUM FERMENTATION

By

SHEKHAR PATEL

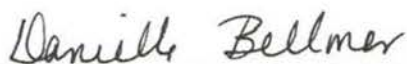
Bachelor of Technology in Dairying
Acharya N. G. Ranga Agricultural University
Hyderabad, India
1996

Master of Technology in Dairying (Dairy Engineering)
National Dairy Research Institute
Karnal, India
1999

Submitted to the Faculty of the Graduate College of the
Oklahoma State University in partial fulfillment
of the requirements for the Degree of
DOCTOR OF PHILOSOPHY
in Biosystems Engineering
December, 2003

EFFECT OF ULTRASOUND ON XANTHAN GUM FERMENTATION

Thesis Approved:

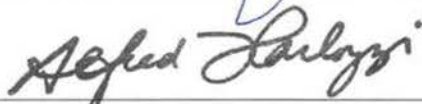


Thesis Advisor









Dean of the Graduate College

ACKNOWLEDGEMENTS

During my pursuit of doctoral study and research I faced many challenges. I must confess that my success in meeting these challenges was not entirely because of my abilities, but because of the people around me. I thus dedicate this thesis to these great people.

I wish to express my respect and admiration for my thesis advisor Dr. Dani Bellmer. She is among the very best persons I have ever known in my professional career. I will like to emulate her as a supervisor. I thank the members of my advisory committee for their suggestions and insights. I am grateful to them for sharing their experiences. Had they not been on my committee, the conclusions of this research would have been less authoritative. My wife Sabitha helped me perfect various biochemical tests and also provided me the motivation to continue whenever I reached a dead-end. I am grateful to God for having made me the recipient of her love and support. I wish to thank Muluken, Dharmendra, Travis, Kean and Nachiket for their invaluable technical assistance and friendship during the course of my research. I express my love and respect for my parents and sister who supported me through out my educational endeavors.

Also, I wish to thank FAPC and the department of biosystems engineering for supporting me during my research study. Finally, as a citizen of India, I will remain indebted to the United States of America for providing me the opportunity to advance my career goals.

TABLE OF CONTENTS

CHAPTER	PAGE
1 INTRODUCTION.....	1
1.1 JUSTIFICATION	1
1.2 OBJECTIVES.....	2
2 REVIEW OF LITERATURE	4
2.1 XANTHAN GUM.....	4
2.1.1 Occurrence.....	5
2.1.2 Physiological Function	5
2.1.3 Structure.....	6
2.1.3.1 Chemical Structure	6
2.1.3.2 Secondary Structure	7
2.2 EFFORTS TO IMPROVE MASS TRASFER.....	8
2.2.1 Foams	9
2.2.2 Oxygen Vectors	9
2.2.3 Headspace Pressurization.....	10
2.2.4 Microbubbles.....	11
2.2.5 Pulsing Agitator	11
2.2.6 Membrane Diffuser.....	11
2.2.7 Hydrogen Peroxide.....	12

2.2.8	<i>Non-conventional Bioreactor Designs</i>	12
2.3	ULTRASOUND.....	13
2.3.1	<i>Theory</i>	13
2.3.2	<i>Mode of Action</i>	14
2.3.3	<i>Sonicator Designs</i>	15
2.3.4	<i>Effect of Sonication on Macromolecules</i>	18
2.3.5	<i>Effect of Ultrasound on Cells</i>	23
2.3.6	<i>Improved Mass Transfer due to Ultrasound</i>	25
3	MATERIALS AND METHODS	26
3.1	EXPERIMENTAL SET-UP	26
3.2	EXPERIMENTAL PLAN	26
3.3	EQUIPMENT DETAILS.....	28
3.3.1	<i>Fermenter</i>	28
3.3.2	<i>Ultrasonic Equipment</i>	29
3.3.3	<i>Sensors</i>	31
3.4	OXYGEN UPTAKE RATE	32
3.5	MAINTENANCE OF MICROORGANISM.....	34
3.5.1	<i>Strain Maintenance</i>	34
3.5.2	<i>Inoculation Procedures</i>	34
3.5.3	<i>Culture Media</i>	35
3.6	FERMENTATION CONDITIONS	36

3.6.1	<i>Fermentations in Shake Flasks</i>	36
3.6.2	<i>Fermentations in Fermenter</i>	36
3.6.3	<i>Sonication Parameters</i>	37
3.7	ANALYTICAL METHODS.....	37
3.7.1	<i>Biomass Concentration</i>	38
3.7.2	<i>Xanthan Concentration</i>	39
3.7.3	<i>Glucose Concentration</i>	39
3.8	DETERMINING PROPERTIES OF XANTHAN MOLECULE.....	40
3.8.1	<i>Retention Time</i>	40
3.8.2	<i>Molecular Weight Distribution</i>	42
3.9	POWER MEASUREMENT	45
3.10	STATISTICAL ANALYSIS.....	45
4	RESULTS AND DISCUSSION	46
4.1	CHARACTERIZATION OF ULTRASONIC EQUIPMENT.....	46
4.1.1	<i>Calorimetric Characterization of Ultrasonic Horn</i>	46
4.1.2	<i>Residence Time Distribution of Ultrasonic Flow Cell</i>	49
4.2	EFFECT OF SONICATION ON <i>XANTHOMONAS CAMPESTRIS</i> AND XANTHAN GUM.....	52
4.2.1	<i>Effect of Sonication on Viability of X. campestris</i>	52
4.2.2	<i>Effect of ultrasound on Xanthan gum quality</i>	54
4.3	DETERMINATION OF ULTRASONIC PROCESSING PARAMETERS	56

4.3.1	<i>Identification of Suitable Values of Xanthan Gum Concentration, Flow rate and Sonication Amplitude</i>	56
4.3.2	<i>Identification of Suitable Growth Phase During Fermentation for Sonication</i>	60
4.3.2.1	Effect of Sonication Immediately After Exponential Growth.....	61
4.3.2.2	Effect of Sonication During Stationary Growth	64
4.3.2.3	Effect of Sonication During Death Phase.....	67
4.3.3	<i>Conclusion</i>	69
4.4	PRELIMINARY FERMENTATION STUDIES	70
4.4.1	<i>Typical Xanthan Fermentation and Its Characteristics</i>	70
4.4.2	<i>Exposure to Ultrasound after Exponential Growth</i>	72
4.5	SONICATED FERMENTATION	75
4.5.1	<i>Single Dose Sonication</i>	75
4.5.2	<i>Intermittent Dose Sonication</i>	77
4.6	OXYGEN UPTAKE RATE DURING SONICATION	79
5	CONCLUSIONS	82
6	FUTURE RESEARCH	84
7	BIBLIOGRAPHY	86

LIST OF FIGURES

FIGURE	PAGE
Figure 2.1 Chemical Structure of Xanthan Gum	7
Figure 2.2 Some Current and Future Concepts of Sonobioreactors.....	16
Figure 2.3 Ultrasonic Degradation of 1% Solutions of Narrow Polydispersity Polystyrenes in Toluene....	19
Figure 2.4 Intrinsic Viscosity $[\eta]$ of Xanthan Gum as a Function of Ultrasonic Irradiation Time	22
Figure 2.5 GPC Chromatograms of a Polymer Solution Undergoing Sonication	22
Figure 3.1 Experimental Set-up.....	26
Figure 3.2 Flow Chart Showing Experimental Plan.....	27
Figure 3.3 Fermenter Dimensions (cm).....	28
Figure 3.4 Turbine Blade.....	29
Figure 3.5 Ultrasonic Flow Cell.....	29
Figure 3.6 Ultrasonic Flow Cell Dimensions (cm)	30
Figure 3.7 DO Sensor Holder for Oxygen Uptake Rate Measurement.....	31
Figure 3.8 Calibration Curve for Biomass	38
Figure 3.9 HPSEC Set-up	44
Figure 4.1 Calorimetric Characterization of Ultrasonic Horn Using Water.....	47
Figure 4.2 Calorimetric Characterization of Ultrasonic Horn Using 1%(w/v) Xanthan Gum Solution	48
Figure 4.3 Approximate Specific Power Corresponding to Percentage Amplitude in Xanthan Broth	49
Figure 4.4 Residence Time Distribution of a Tracer in Ultrasonic Flow Cell (flow rate = 100 ml/min)	50

Figure 4.5 Hypothetical Flow Zones in Ultrasonic Flow Cell.....	51
Figure 4.6 Effect of Sonication on viability of <i>X. campestris</i>	53
Figure 4.7 SEC Chromatograms of Xanthan Gum obtained from Control and Sonicated Fermentation.....	55
Figure 4.8 A Typical Size Exclusion Chromatogram of Xanthan Gum.....	57
Figure 4.9 Growth Curve of Sonicated <i>X. campestris</i> Obtained Immediately After Exponential Growth...	61
Figure 4.10 Xanthan Production by <i>X. campestris</i> Sonicated Immediately After Exponential Growth	62
Figure 4.11 Specific Substrate Consumption Immediately After Exponential Growth	63
Figure 4.12 Specific Xanthan Production Immediately After Exponential Growth.....	63
Figure 4.13 Growth Curve of <i>X. campestris</i> Sonicated During Stationary Growth	64
Figure 4.14 Xanthan Production by <i>X. campestris</i> Sonicated During Stationary Growth	65
Figure 4.15 Specific Substrate Consumption by <i>X. campestris</i> Sonicated During Stationary Growth	66
Figure 4.16 Xanthan Production by <i>X. campestris</i> Sonicated During Stationary Growth.....	66
Figure 4.17 Growth Curve of <i>X. campestris</i> Sonicated During Death Phase	67
Figure 4.18 Xanthan Production by <i>X. campestris</i> Sonicated During Death Phase.....	68
Figure 4.19 Specific Substrate Consumption by <i>X. campestris</i> Sonicated During Death Phase.....	68
Figure 4.20 Xanthan Production by <i>X. campestris</i> Sonicated During Death Phase.....	69
Figure 4.21 A Typical Xanthan Fermentation	71
Figure 4.22 Xanthan Gum Fermentation with Prolonged Exposure to 20% Amplitude After Exponential Growth	73
Figure 4.23 Intermittent Exposure to 20% Amplitude Ultrasound After Exponential Growth	74
Figure 4.24 Single Dose Sonication Immediately after Exponential Growth Phase.....	76

Figure 4.25 Single Dose Sonication during Stationary Phase	76
Figure 4.26 Intermittent Dose Sonication with Shorter and Frequent Treatments.....	77
Figure 4.27 Intermittent Dose Sonication with Occasional Treatments.....	78
Figure 4.28 Dissolved Oxygen Profiles in Fermenter and Recycle Pipeline after Sonication	80
Figure 4.29 Increase in Oxygen Uptake Rate due to Sonication During Various Growth Phases.....	80

LIST OF TABLES

TABLE	PAGE
Table 4.1 Three Factor Full Factorial Design.....	58
Table 4.2 Analysis of Variance.....	59
Table 4.3 Comparison of Different Levels of Processing Parameters.....	59

NOMENCLATURE

α	probability of the outcome under the null hypothesis
λ	wavelength (μm)
ω	wave energy density ($\text{J}\cdot\text{m}^{-3}$)
η	intrinsic viscosity (ml/g)
μ	specific growth rate (h^{-1})
ρ_L	density (g/cc)
η_{sp}	specific viscosity
ΔT	rise in temperature (deg C)
Δt	time taken for a particle to move between the two measuring points (s)
ADI	acceptable daily intake
ADP	adenosine-5'-diphosphate
AFFF	asymmetrical flow field fractionation
ANOVA	analysis of variance
ATTC	American type culture collection
ATP	adenosine-5'-triphosphate
c	wave velocity ($\text{m}\cdot\text{s}^{-1}$)
C	xanthan gum solution concentration ($\text{g}\cdot\text{L}^{-1}$)
C_{in}	molar fraction of oxygen entering the system ($\text{mg O}_2\cdot\text{L}^{-1}$)

C_{out}	molar fraction of oxygen leaving the system ($\text{mg O}_2\cdot\text{L}^{-1}$)
C_p	heat capacity ($\text{J}\cdot\text{g}^{-1}\cdot\text{deg C}^{-1}$)
D	diffusion constant
DF	degree of freedom
DO	dissolved oxygen (%)
DRI	refractive index detector
E	energy absorption rate ($\text{J}\cdot\text{s}^{-1}$)
EU	European Union
f	Frequency (Hz)
FAO	food and agricultural organization
g	gravitational constant
$G-6-P$	D-glucose-6-phosphate
$G6P-DH$	glucose-6-phosphate dehydrogenase
GPC	gel permeation chromatography
HK	hexokinase
$HPLC$	high-performance liquid chromatography
I	intensity of ultrasound (W m^{-2} or $\text{kW}\cdot\text{L}^{-1}$)
i	index
Kla	volumetric oxygen transfer coefficient (h^{-1})
$LALLS$	low angle laser light scattering

m	mass of fluid (kg)
M_i	molecular weight (Da)
M_{lim}	limiting molecular weight (Da)
M_n	number-average molecular mass (Da)
M_w	weight-average molecular mass (Da)
MALLS	multi-angle laser light scattering
MS	mean square for error
MWD	molecular weight distribution
NADP	nicotinamide adenine dinucleotide phosphate
NADPH	reduced nicotinamide adenine dinucleotide phosphate
N_i	number of molecules
NRRL	Northern Regional Research Laboratory (now the National Center For Agricultural Utilization Research)
OTR	oxygen transfer rate ($\text{mg O}_2\cdot\text{L}^{-1}\cdot\text{h}^{-1}$)
OUR	oxygen uptake rate ($\text{mg O}_2\cdot\text{L}^{-1}\cdot\text{h}^{-1}$)
p	alpha value arising out of a statistical test
P	pressure amplitude of sound wave (Pa)
PDI	polydispersity index
pfc	perfluorocarbon
q_{o_2}	specific rate of oxygen consumption ($\text{mmol O}_2\cdot\text{g}^{-1}\text{ dry wt. h}^{-1}$)
R^2	square of the Pearson product moment correlation coefficient

RMS	root mean square
RTD	residence time distribution
SEC	size exclusion chromatography
SS	sum of squares
t	sonication time (s)
v/v	volume to volume
w/v	weight to volume
w/w	weight to weight
W_i	weight of molecules (Da)
X	cell concentration (g. L ⁻¹)
Y_{X/O_2}	oxygen yield coefficient

Units

%	percentage
μm	micrometer
atm	atmosphere
cm	centimeter
°C	degree centigrade
cfu	colony forming unit
g	gram

h	hour
Hz	hertz
J	joule
k	kilo
L	liter
m	meter
mg	milligram
min	minutes
ml	milliliter
mm	millimeter
mol	mole
MDa	million dalton
MHz	mega hertz
Pa	pascal
rpm	revolutions per minute

1 Introduction

In the last few decades, many new and useful polysaccharides of scientific and commercial interest have been discovered which can be obtained from microbial fermentations.

Microorganisms such as bacteria and fungi produce three distinct types of polymers:

- i. Extracellular polysaccharides, which can be found either as a capsule that envelops the microbial cell or as an amorphous mass secreted into the surrounding medium
- ii. Structural polysaccharides, which can be part of the cell wall
- iii. Intracellular storage polysaccharides

Xanthan gum is an extracellular polysaccharide produced by the bacterium *Xanthomonas campestris*. Xanthan gum has unique properties that are useful in diverse applications such as food, pharmaceutical, oilfield, cosmetics, and other industrial fields. Commercial production occurs in a conventional aerobic batch fermentation process involving air sparging.

1.1 JUSTIFICATION

Most known microbial exopolysaccharides with industrial significance are produced in aerobic submerged fermentation systems. In almost every case, the viscosity of the fermentation liquor progressively increases to a high level as a result of product formation (Sutherland, 1993). This progressively increasing viscosity makes the fermentation process inefficient due to increased resistance to mass transfer to the growing microbes and thus

increased power consumption. Though many different physical, chemical and biological methods have been applied to increase the mass transfer in the viscous xanthan fermentation broth, no study has been reported which evaluates the effect of ultrasound. Since ultrasound is capable of producing strong shear forces in liquid media, sonication might help in reducing resistance to mass transfer around the bacteria, which in turn might facilitate higher production rates of the exopolymer. In this study, the term “sonication” implies exposing a fluid to ultrasonic energy transferred from a hard surface vibrating at ultrasonic frequency (higher than 20 kHz).

Ultrasound is widely used in medical imaging, sonochemical processing, ultrasonic cleaning of surfaces, and as the basis for underwater sonar ranging. Medical imaging applications use megahertz range (1–10 MHz), *low power*, diagnostic ultrasound. High energy or *power ultrasound* in the 20–100 kHz frequency range is used in many sonochemical processes. At sufficiently high acoustic power inputs, ultrasound is known to rupture cells and ultrasonication is a well-established laboratory technique for cell disruption (Chisti and Moo-Young, 1986). A cell can be inactivated by ultrasound at intensities less than those needed to cause disruption (Dakubu, 1976). However, new research suggests that ultrasound at certain power levels enhances bacterial growth, and in some instances helps to improve productivity of fermentation processes (Francko, Taylor et al., 1990; Francko, Al-Hamdani et al., 1994).

1.2 OBJECTIVES

The overall goal of this research study was to determine whether sonication of viscous xanthan fermentation broths at specific power levels of less than 5 kW/L could improve xanthan production. The specific objectives of this study were to:

- i. Characterize a suitable ultrasonic system for treating fermentation broth.
- ii. Determine the impact of ultrasound on *Xanthomonas campestris* and the quality of xanthan gum.
- iii. Identify the processing variables such as exposure time (flow rate), ultrasonic intensity (amplitude), and bacterial growth phase to be used for sonication during fermentation.
- iv. Determine the extent to which production of xanthan gum could be improved through application of ultrasound.
- v. Study the effect of sonication on oxygen uptake rate.

2 Review of literature

2.1 XANTHAN GUM

Xanthan gum, a microbial biopolymer produced by the *Xanthomonas* bacterium, is important because of its extraordinary properties as well as its contribution to the successful establishment of an industrial production process. Xanthan gum was discovered in the 1950s at Northern Regional Research Laboratory of the U.S. Department of Agriculture in the course of a screening which aimed at identifying microorganisms that produced water-soluble gums of commercial interest (Born, Langendorff et al., 2001). Xanthan gum was first industrially produced in 1960, and it became available commercially in 1964. The approval for food use was given by the U.S. Food and Drug administration in 1969, and the FAO specification followed in 1974. Approval in Europe was obtained in 1982, under the E number E415. The official definition of the EU food regulations for E415 is: Xanthan gum is a high molecular weight polysaccharide gum produced by a pure culture fermentation of a carbohydrate with natural strains of *Xanthomonas campestris*, purified by recovery with ethanol or propane-2-ol, dried and milled. It contains d-glucose and d-mannose as the dominant hexose units, along with d-glucuronic acid and pyruvic acid, and is prepared as the sodium, potassium or calcium salt. Its solutions are neutral. The molecular weight must be approximately 1 MDa and the color must be cream. Xanthan gum is approved as a food additive with no limit for acceptable daily intake (ADI) and the gum may be used quantum satis, which means with just the quantity useful for the application. Xanthan is produced

commercially by several companies, such as Monsanto/Kelco, Rhodia, Jungbunzlauer, Archer Daniels Midland, and SKW Biosystems. Annual volumes worldwide are estimated to be about 35,000 tons in 2001.

2.1.1 OCCURRENCE

Xanthan is produced by *Xanthomonas campestris*, a plant-associated bacterium that is generally pathogenic for plants belonging to the family Brassicaceae. *Xanthomonas* does not form spores, but it is very resistant to desiccation during relatively long periods. The resistance is usually due to the protective effect of the xanthan gum produced and exuded by the bacteria. Xanthan also protects the bacteria from the effects of light, and generally causes wilting of the leaves by blocking water movements (Born, Langendorff et al., 2001). The polysaccharide is not a reserve energy source because in general the bacterium is not able to catabolize its own extracellular polysaccharide.

2.1.2 PHYSIOLOGICAL FUNCTION

The physiological function of the exopolysaccharide xanthan has received little attention compared with investigations into the molecule's production, properties, and applications. The bacteria (*Xanthomonas* sp.) that produce xanthan gum as a secondary metabolite are usually phytopathogenic, or may live in asymptomatic association with plant tissues or epiphytes. *Xanthomonas* infections have been observed in over 120 monocotyledonous and over 150 dicotyledonous plant species (Born, Langendorff et al., 2001). In general, bacterial exopolysaccharide induce water-soaking of the intercellular space which is important for bacterial colonization. It is also possible that xanthan forms a gel-like slime in the

intercellular space as a result of synergy with other plant polysaccharides. This gel may then promote bacterial colonization of plant tissue by retarding the desiccation of the bacterial colony, by protecting the bacteria from bacteriostatic compounds, and by preventing close morphological contact of the colony with the cell wall, thus preventing the triggering of plant defense reactions. The amount of exopolysaccharide produced by *Xanthomonas* is correlated to the organism's virulence; strains with attenuated virulence usually produce less exopolysaccharide and the distribution of the polysaccharide in infected leaves coincides with that of bacteria (Born, Langendorff et al., 2001).

2.1.3 STRUCTURE

2.1.3.1 Chemical Structure

Xanthan is a heteropolysaccharide with a very high molecular weight, consisting of repeating units (Figure 2.1). The sugars present in xanthan are D-glucose, D-mannose, and D-glucuronic acid. The glucoses are linked to form a β -1,4-D-glucan cellulosic backbone, and alternate glucoses have a short branch consisting of a glucuronic acid sandwiched between two mannose units. The side chain consists therefore of β -d-mannose-(1,4)- β -d-glucuronic acid-(1,2)- α -d-mannose. The terminal mannose moiety may carry pyruvate residues linked to the 4- and 6-positions. The internal mannose unit is acetylated at C-6. Acetyl and pyruvate substituents are linked in variable amounts to the side chains, depending upon which *Xanthomonas campestris* strain the xanthan is isolated from. The pyruvic acid content also varies with the fermentation conditions. On average, about half of the terminal mannoses carry a pyruvate, with the number and positioning of the pyruvate and acetate residues conferring a certain irregularity to the otherwise very regular structure. Usually, the degree of

substitution for pyruvate varies between 30 and 40%, whereas for acetate the degree of substitution is as high as 60 to 70%. Some of the repeating units may be devoid of the trisaccharide side chain.

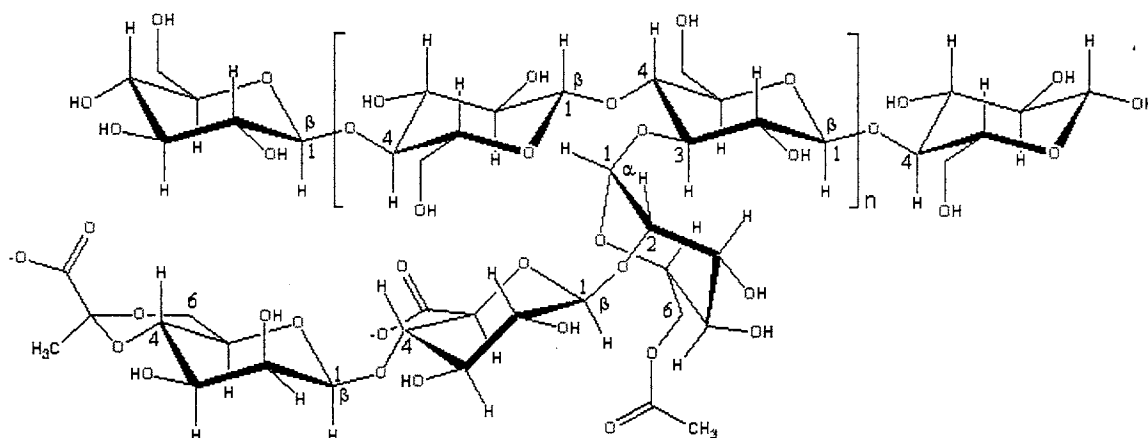


Figure 2.1 Chemical Structure of Xanthan Gum

2.1.3.2 Secondary Structure

The secondary structure of xanthan depends on the conditions under which the molecule is characterized. The molecule may be in an ordered or in a disordered conformation. The ordered confirmation can be either native or renatured; in the native form the conformation is present at temperatures below the melting point of the molecule, a temperature which depends on the ionic strength of the medium in which xanthan is dissolved. Two models, a single-strand helix and a doublestrand or multi-strand helix, have been proposed, though most authors currently support the idea of a double helix. The helix is stabilized by noncovalent bonds, such as hydrogen bonds, electrostatic interaction, and steric effects; its structure can be described as a rigid rod. In aqueous solution, the molecule may undergo a conformational transition which can be driven by changes in temperature and ionic strength,

and which depends on the degree of ionization of the carboxyl groups and acetyl contents. The temperature-induced transition from an ordered to a disordered conformation is generally attributed to a complete or partial separation of the double-strand form. Renaturation may occur under favorable conditions, which means temperatures below the transition temperature and high salt concentrations. The transition from the denatured to the renatured state is reversible, whereas that from the native to the denatured state is irreversible.

2.2 EFFORTS TO IMPROVE MASS TRASFER

Numerous experiments have been conducted aimed at improving the production of the commercially important xanthan gum. Various physical, chemical and biological methods have been employed to improve the yield. Few of them being altering agitation and type of impellers (Funahashi, Maehara et al., 1987; Peters, Herbst et al., 1989; Umasankar, Annadurai et al., 1996; Amanullah, Tuttiett et al., 1998), altering the feeding strategy (Amanullah, Satti et al., 1998), changing the genetic make-up of the cells (Tseng, Ting et al., 1992), use of growth agents such as citric acid (Jana and Ghosh, 1997) , detergents (Galindo and Salcedo, 1996), etc. However, one of the most critical aspects of any aerobic fermentation is the supply of oxygen to the growing cells. Oxygen supply was not studied much during the 1980s. However, as the biotechnological revolution started gaining momentum, and as more and more microbial products started to enter the commercial market more and more attention has been directed toward the problem of oxygen transfer during fermentation. In the case of xanthan fermentation, oxygen transfer is widely recognized as a bottleneck during the production process. By improving oxygen transfer the total yield of the process can be significantly improved (Garcia-Ochoa, Castro et al., 2000).

2.2.1 FOAMS

Only now researchers are paying attention to solving the problem by using novel and varied methods. For instance stabilized foams have been generated to increase the gas-liquid interfacial area by slowly introducing coarse bubbles into media. One example involves the use of fetal bovine serum. With 10% fetal bovine serum and a bubble sparging rate of 50 mL/h, K_La increased approximately 90% compared with no foaming (Ju and Armiger, 1990). This approach might be feasible for small scale fermentations. Obtaining fetal bovine serum for large commercial applications like xanthan gum production is not possible and obviously unfeasible.

2.2.2 OXYGEN VECTORS

Limitations of oxygen transfer in fermentation can also be solved using auxiliary liquids immiscible in the aqueous phase. The liquids (called oxygen-vectors) used in one such study were hydrocarbon (n-dodecane) and perfluorocarbon (forane F66E) in which oxygen is highly soluble (54.9 mg/L in n-dodecane and 118 mg/L in forane F66E at 35°C in contact with air at atmospheric pressure). It has been demonstrated that the use of n-dodecane emulsion in a culture of *Aerobacter aerogenes* enabled a 3.5-fold increase of the volumetric oxygen transfer coefficient (k_La) calculated on a per-liter aqueous phase basis (Rols, Condoret et al., 1990). In another study two-phase aqueous/perfluorocarbon dispersions were studied (Junker, Hatton et al., 1990). These dispersions were examined for their oxygen transfer enhancement capability in the absence and presence of an oxygen-consuming reaction. For the pfc-in-water dispersions, oxygen uptake rate (OUR) enhancements were

equal both with and without oxygen-consuming cells present in the aqueous phase. In contrast, for water-in- perfluorocarbon dispersions, OUR enhancements in the presence of reaction were limited by oxygen diffusion across the aqueous phase droplets. Nevertheless, enhancement factors of 5-10 on an aqueous phase volume basis were obtained in 75% perfluorocarbon dispersion. In yet another study the feasibility of enhancing oxygen transfer in bioreactors by introduction of adequate amounts of perfluorocarbon emulsions was clearly demonstrated (Ju, Lee et al., 1991). Even though there are conflicting reports in the literature with respect to perfluorocarbons, the effect of perfluorocarbons on the environment has not yet been studied. The technical feasibility of using the oxygen-vectors might have been demonstrated but the disadvantage of such oxygen vectors seems to be the high cost of chemicals and separation from fermentation media, which has to be further processed to produce xanthan.

2.2.3 HEADSPACE PRESSURIZATION

Bioreactor headspace pressurization represents an excellent means of enhancing oxygen mass transfer to a culture. This method is particularly effective in situations where stirring or vigorous aeration is difficult (Yang and Wang, 1992). This method is simple, clean, inexpensive, and easily implemented, and can be applied alongside other existing methods of oxygen mass transfer enhancement. However, it does not offer a solution to the problem of eliminating the oxygen transfer resistance.

2.2.4 MICROBUBBLES

Mass balance and transfer of oxygen through the use of oxygen microbubbles has been studied (Michelsen, 1991). The potential problem with this method is that it uses surfactants for generating microbubbles which in turn form a barrier in gas to liquid mass transfer. The trade-off between increased surface area and the degree of resistance to mass transfer has to be studied further in Xanthan fermentation systems. Also the energy required to generate the microbubbles needs to be investigated.

2.2.5 PULSING AGITATOR

Oxygen transfer in a novel pulse bioreactor has been evaluated. The agitator consists of a series of alternately fixed and movable parallel plates mounted so that the movable plates vibrate at 30 Hz causing a pulsating fluid motion. The main feature of this bioreactor is high oxygen transfer with low shear to prevent damage to fragile animal cell membranes (Monahan and Holtzapple, 1993). Though this is a promising area its efficiency in xanthan fermentation system might be limited considering the scale of commercial systems and the fact that there are dead zones within the fermenter and all the vibrational energy might not be evenly distributed in the dead zones.

2.2.6 MEMBRANE DIFFUSER

The oxygen transfer efficiency was examined using fine bubble membrane diffusers and large blade slow speed mixers. An increase in the air flow rate resulted in a decrease of the oxygen transfer efficiency (Gillot and Heduit, 2000).

2.2.7 HYDROGEN PEROXIDE

A method of oxygen supply that completely eliminates the gas-liquid transport resistance has been presented recently (Sriram, Rao et al., 1998). The method involves a need-based liquid-phase decomposition of hydrogen peroxide to provide the necessary oxygen. The maximum specific growth rate and xanthan yields in the novel cultivation were 89% and 169%, respectively, of those obtained in conventional cultivation. However, in another study (Christensen, Myhr et al., 1996) it was shown that conformationally ordered, double-stranded xanthan, degraded in the presence of H_2O_2 and Fe^{2+} (at 20°C). It is common knowledge that the water used industrially for xanthan fermentation is the normal sterilized potable water, which depending on location will have Fe^{2+} ions. Thus this method does involve some complexity. Also H_2O_2 is well known for neutralizing bacteria if used in large proportions. In industrial plants where mixing is a problem, addition of H_2O_2 might create pockets of high concentration of H_2O_2 . This might impact the cell growth.

2.2.8 NON-CONVENTIONAL BIOREACTOR DESIGNS

Other alternative methods of improving oxygen supply, especially in viscous fermentations and shear-sensitive fermentations have been investigated using non-conventional bioreactor designs (Suh, Schumpe et al., 1992; Kessler, Popovic et al., 1993; Xu, Lin et al., 1994; Yang, Lo et al., 1996). However, for the industry to improve its xanthan productivity the adoption of such new designs might involve huge investments and may also involve complete redesign of the processing plant. The aim of current research is to modify the process minimally without modifying the basic design of the production plant design in a significant way.

2.3 ULTRASOUND

Ultrasonication is generally associated with damage to cells but evidence is emerging for beneficial effects of controlled sonication on conversions catalyzed by live cells (Chisti, 2003). Discussed below is the current state-of-the-art in this field.

2.3.1 THEORY

Ultrasound is defined as acoustic energy or sound waves with frequencies above 20 kHz. The energy imparted to the fluid by ultrasound depends on the intensity (I , W m^{-2}) of the sound that is the energy passing through an area in unit time. The intensity is related to the velocity of the wave and its energy density, ω :

$$I = \omega \cdot c$$

The energy density is calculated as follows:

$$\omega.(J \cdot m^{-3}) = \frac{1}{2} \frac{P}{\rho_L c^2}$$

P (Pa) is the pressure amplitude of the sound wave (pressure amplitude is the difference between maximum and minimum pressure at the wave peak and trough, respectively). An ultrasound wave can be a propagating wave or a non-propagating standing wave. A standing wave is produced when a wave traveling in one direction encounters a wave of the same frequency traveling in the opposite direction. All points on a propagating wave undergo displacement. By contrast, certain fixed points or nodes on a standing wave undergo no displacement. Particles suspended in a medium sonicated with standing wave ultrasound accumulate at the nodes.

2.3.2 MODE OF ACTION

Ultrasound effects are either chemical or physical or both, depending upon the intensity used. Acoustic cavitation (the formation, growth, and collapse of bubbles) provides the primary mechanism for ultrasonic effects. During cavitation, bubbles collapse and produce intense local heating, high pressures, and very short lifetimes; these transient, localized hot spots drive high-energy chemical reactions. As described in detail elsewhere (Flint and Suslick, 1991), these hot spots have temperatures of approximately 5000°C, pressures of about 1000 atm, and heating and cooling rates above 10^{10} K/s. Cavitation, often accompanied by emission of light, can break apart relatively robust small molecules. Chemical reactions are not generally seen in the ultrasonic irradiation of solids or solid-gas systems. Ultrasonic cavitation in liquid-solid systems produces high-energy phenomena. The physical effects include:

- i. increased mass transport from turbulent mixing and acoustic streaming
- ii. the generation of surface damage at liquid-solid interfaces by shock waves and microjets
- iii. the generation of high-velocity inter-particle collisions in slurries
- iv. the fragmentation of macromolecules

Cavitation near extended liquid-solid interfaces is very different from cavitation in pure liquids (Leighton, 1994). Near a solid surface, bubble collapse becomes non spherical, driving high-speed jets of liquid into the surface and creating shockwave damage to the surface. Because most of the available energy is transferred to the accelerating jet, rather than the bubble wall itself; this jet can reach velocities of hundreds of meters per second. In addition, shock waves created by cavity collapse in the liquid may also induce surface damage and the fragmentation of brittle materials. The impingement of micro jets and shockwave on the

surface creates the localized erosion responsible for ultrasonic cleaning and many of the sonochemical effects on heterogeneous reactions. Usually cells do not survive cavitation for long. However, intermittent power ultrasound of short duration can cause a productivity enhancing effect in live systems (Chisti, 2003). In a sonobioreactor the cavitation threshold energy is not exceeded in most of the reactor volume. Cavitation threshold values can vary widely depending on the fluid being sonicated. Typical cavitation threshold values are between 15 and 65 kW m⁻³ (Chisti, 2003).

2.3.3 SONICATOR DESIGNS

The absorption of sonic energy by a fluid depends on the prevailing pressure. An increase in ambient pressure up to a certain limit increases the conversion of sound energy to shock wave energy. This suggests that an ultrasound transducer should be positioned close to the base of a sonobioreactor vessel where the hydrostatic pressure is high (Chisti and Moo-Young, 2002). Ultrasound is produced using magneto-restrictive or piezoelectric transducers, which convert the alternating current of an electric oscillator into mechanical waves that are transmitted to the suspension through a cylindrical rod-shaped probe or 'horn' (Figure 2.2). The horn, usually made from titanium, vibrates with the same frequency as the oscillator and might take the shape of a flat plate. A simple probe-type ultrasound horn delivers power ultrasound to a distance of only 70–100 mm. For a given effect, the total input of the acoustic power required will increase with increasing volume of the fluid. For small bioreactor vessels, an ultrasound horn with the tip submerged in the fluid can be sufficient. Large volumes of fluids can be sonicated in continuous or recycle-flow sonobioreactors, some of which are shown in Figure 2.2 (Chisti, 2003). Mechanically mixed bioreactors with a

polymer membrane base can be sonicated using an alloy transducer placed next to the membrane and outside the bioreactor vessel (Wang, Sakakibara et al., 1996). Immersing the bioreactor vessel in a water bath provides a means of transmitting energy to the fluid in the bioreactor and through the membrane base. Similar setups for use without a water bath have been described (Schlafer, Sievers et al., 2000).

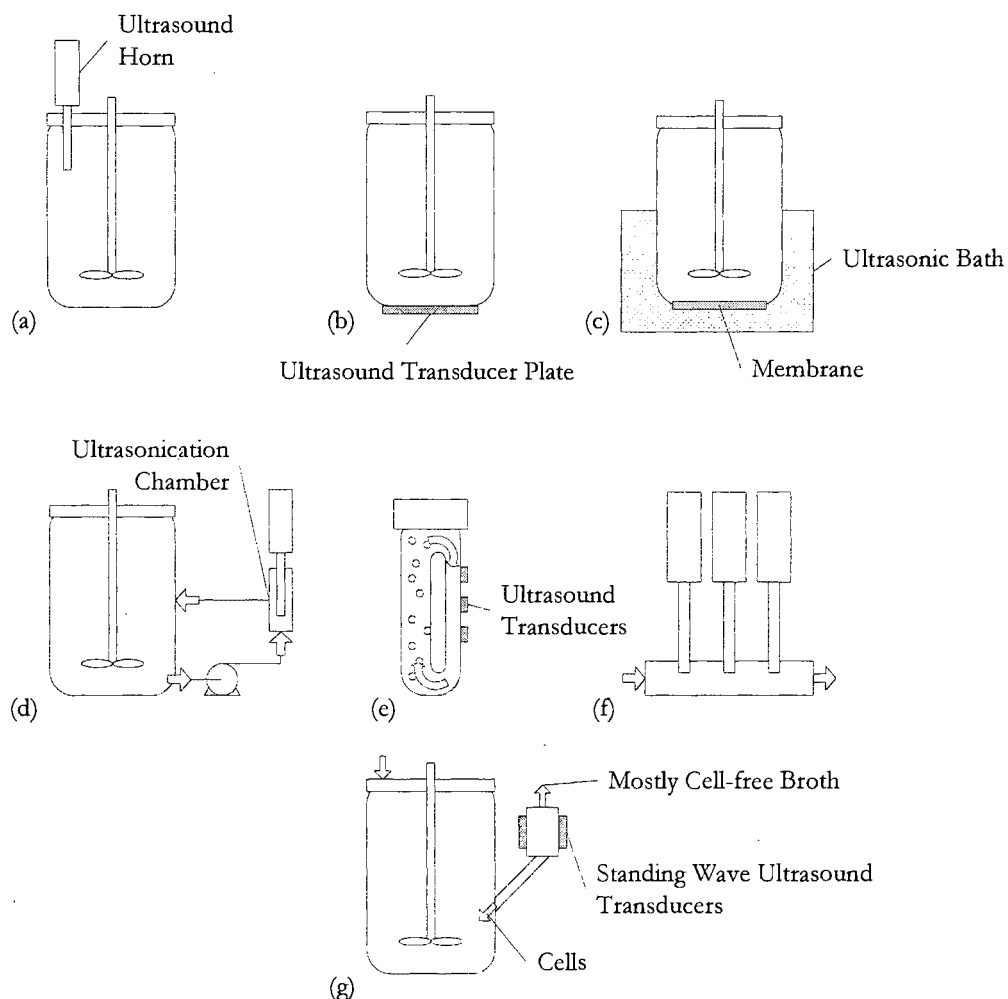


Figure 2.2 Some Current and Future Concepts of Sonobioreactors

(a) Stirred bioreactor with an ultrasound horn; (b) stirred reactor with flat-plate ultrasound transducer; (c) ultrasound transmission from an ultrasonic bath through a membrane or plate sonocoupling; (d) external ultrasound irradiation of broth in a recycle bioreactor; (e) airlift sonobioreactor; (f) tubular flow sonobioreactors; (g) high-density cell culture with ultrasonic retention of cells using a standing wave. All devices except (g) can be used for continuous or intermittent sonication.

Most of the effects of sonication are linked with the energy imparted to the culture broth and cells in a sonobioreactor. Other relevant factors in assessing the effects of sonication include the spatial variation of the sonic energy dissipation rate in the bioreactor. The amplitude of the sound waves and the viscosity of the broth influence the outcome of sonication. The amplitude of the wave relates directly with the acoustic power delivered to the broth. Some processes are influenced in linear proportion to the acoustic power imparted to the fluid (Chisti, 2003).

At present, a satisfactory comparison of the ultrasonication results of different groups is not readily possible. This is mainly because of the several different and not necessarily correct ways the various authors have reported the ultrasonic energy input to the fermentation broth. Different sonobioreactors are probably best compared in terms of equal specific absorption (W m^{-3}) of ultrasound energy (Chisti, 2003). In some cases, only the value of the electrical power (W) of the ultrasound device has been reported (Radel, McLoughlin et al., 2000). In other instances, an absence of information on the quantity of the fluid sonicated, makes a specific power input calculation impossible. When intensity of ultrasound is reported as W m^{-2} , the area of the transducer tip needs to be known to calculate the power delivered to a given volume of broth. Ideally, the power absorbed by the broth should be determined experimentally by calorimetry. For calorimetric measurements, a microbial broth or other fluid in a thermally insulated sonobioreactor is sonicated for time t . The resulting rise in temperature (ΔT), the sonication time and the heat capacity (C_p) of the fluid can then be used to calculate the energy absorption rate, E , using the equation:

$$E(W) = \frac{mC_p\Delta T}{t}$$

In the above equation, m is the mass of the fluid. It is noteworthy that the specific power input calculated by the various methods is only an average value. The local power input is position dependent and probably varies greatly with location. This introduces additional difficulty in accurately estimating the activation and damaging thresholds of ultrasound energy for different cells. Because the ultrasound energy absorbed eventually appears as heat, any ultrasonicated bioreactor will require more cooling than a comparable conventional bioreactor. Generally, heat generation is not a major limitation in sonobioreactors for live catalysts because only low inputs of ultrasound energy are sufficient to produce the desired biological effects.

2.3.4 EFFECT OF SONICATION ON MACROMOLECULES

The effects of ultrasound on large molecules like proteins and polymers can be both physical and chemical. Examples of physical changes induced by ultrasound in polymer systems include the dispersal of fillers and other components into base polymers (as in the formulation of paints), the encapsulation of inorganic particles with polymers, modification of particle size in polymer powders, and welding and cutting of thermoplastics (Price, 1996). In contrast, chemical changes can also be created during ultrasonic irradiation, invariably as a result of cavitation, and these effects have been used to benefit many areas of polymer chemistry. The basic effects (Price and Smith, 1993) of irradiating a polymer solution with power ultrasound are shown in Figure 2.3, with polystyrene in toluene as an example. The degradation proceeds more rapidly at higher molecular weights and approaches a limiting value, M_{lim} , below which no further degradation takes place (in this case $\sim 30,000$). Polymers

with this value or lower values are unaffected by ultrasound under these conditions. These effects have been reported in all types of macromolecules in solution and include both organic and inorganic polymers in organic solvents and various polymers in aqueous media (such as polyethylene oxide, cellulose, polypeptides, proteins, and DNA).

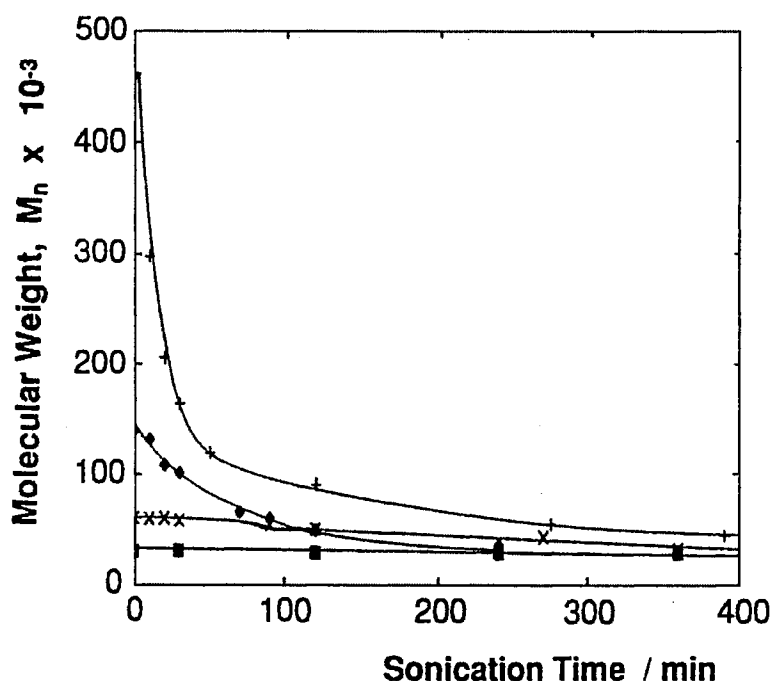


Figure 2.3 Ultrasonic Degradation of 1% Solutions of Narrow Polydispersity Polystyrenes in Toluene

This common behavior is a result of a physical process that is independent of the chemical nature of the polymer, but rather depends on the polymer chain dimensions in solution. A large number of studies have demonstrated that the rate of degradation and M_{lim} are insensitive to the nature of the polymer when sonicated under the same conditions. Also, the degradation proceeds faster and to lower molecular weights at lower temperatures, in more dilute solutions, and in solvents with low volatility. This pattern follows the effect of the parameters on cavitation bubble collapse. Sonication at higher temperatures or in volatile

solvents results in more vapors entering the bubble and so cushioning the collapse, making it less violent. In dilute solutions, the polymer chains are not entangled and so are free to move in the flow fields around the bubbles. As expected, the degradation is more efficient at high ultrasonic intensities, owing to the greater number of bubbles with larger radii (Suslick and Price, 1999). Many authors have found that as the power delivered to the reaction mixture increases, the rate of the reaction increases to a maximum and then decreases with a continued increase in power (Gutierrez and Henglein, 1990). A possible explanation for the observed decrease at high powers is the formation of a dense cloud of cavitation bubbles near the probe tip which acts to block the energy transmitted from the probe to the fluid (Contamine, Faid et al., 1994; Ratoarinoro, Contamine et al., 1995). Hence, by suitable manipulation of the experimental conditions, one can manipulate a sonicated process.

Although there is still some debate about the precise origins of the degradation, it has been shown that under conditions that suppress cavitation, degradation does not occur. The polymer chains are subjected to extremely large forces in the rapid liquid flows near collapsing cavitation bubbles and in the shock waves generated after bubble implosion; these can result in the breakage of a bond in the chain. There is no evidence that the extreme conditions of temperature found in cavitation bubbles contribute to polymer degradation in nonaqueous liquids, because the polymer chains have negligible vapor pressure and are unlikely to be found at the bubble interface. In contrast, however, pyrolysis can occur in aqueous solutions in which hydrophobic polymers concentrate at the bubble-air interface. Degradation can be used as an additional processing parameter to control the molecular-weight distribution. Sonication has been used for obtaining different molecular weight fractions of Xanthan gum. Figure 2.4 illustrates the intrinsic viscosities of four different

fractions as a function of the ultrasonic irradiation time, where data at the initial time indicate that of the unsonicated xanthan gum. Intrinsic viscosity (η) is a function of the polymer molecular weight as given by Mark–Houwink equation (Holzwarth, 1978):

$$\eta = \lim_{C \rightarrow 0} \frac{\eta_{sp}}{C} = 6.6 \times 10^{-6} \left(\bar{M}_v \right)^{1.35} [ml / g]$$

The specific viscosity η_{sp} is obtained from the relative viscosity, which is the ratio of the viscosity of xanthan gum solution at a certain concentration (C) to that of the solvent. Using the Ubbelohde viscometer (Schott-Geräte, Germany, Capillary No. 52610/I), the flow times of each xanthan gum solution and pure solvent (deionized water) were measured at several different polymer concentrations. The temperature was accurately kept at $20.00 \pm 0.005^\circ\text{C}$ by a constant temperature circulating system (Haake F6, Germany). The plot of η_{sp}/C versus C gave a straight line, the intercept of which was η . Therefore, the viscosity-average molecular weight is obtained from intrinsic viscosity. Intrinsic viscosity decreases with ultrasonic irradiation time as shown in Figure 2.4. The following viscosity-average molecular weights were obtained: 3.61×10^6 for unsonicated xanthan gum, 3.41×10^6 after 15 min irradiation, 3.25×10^6 after 30 min irradiation, and 2.80×10^6 after 60 min irradiation (Sohn, Kim et al., 2001).

Another example of a polymer solution undergoing sonication is shown in Figure 2.5 (Suslick and Price, 1999). The degradation narrows the distribution markedly, and after 24 h of sonication, no material with molecular weight greater than 100,000 remains.

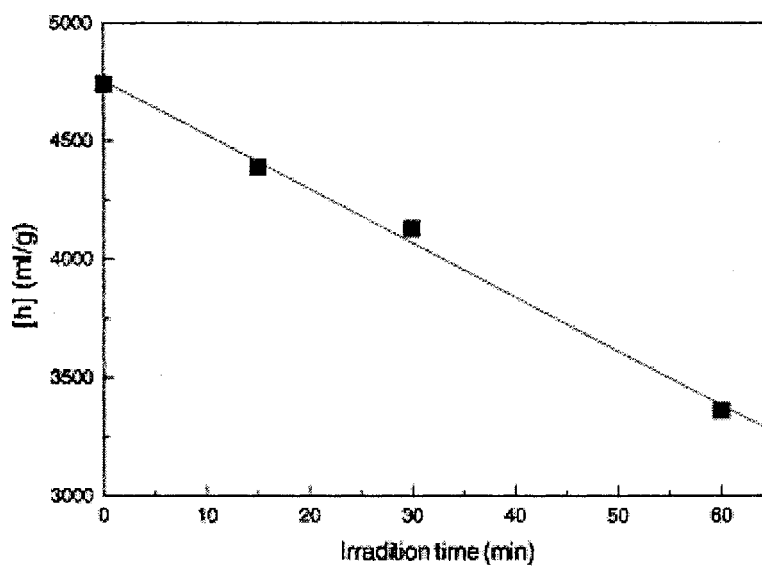


Figure 2.4 Intrinsic Viscosity $[\eta]$ of Xanthan Gum as a Function of Ultrasonic Irradiation Time

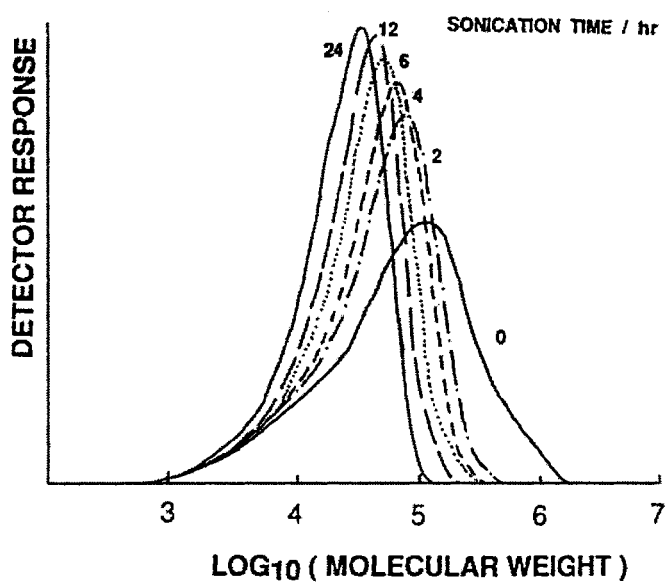


Figure 2.5 GPC Chromatograms of a Polymer Solution Undergoing Sonication

2.3.5 EFFECT OF ULTRASOUND ON CELLS

Distortions of bubble collapse depend on a surface several times larger than the resonance bubble size. Thus, for ultrasonic frequencies of approximately 20 kHz, damage associated with microjet formation cannot occur for solid particles smaller than 200 μm (Suslick and Price, 1999). Since microorganisms are much smaller than 200 μm , it would mean that they might not be drastically affected by ultrasound of frequencies around 20 kHz. However, cells can differ significantly in their sensitivity to ultrasound. For example, a 5 min daily exposure to ultrasound (20 kHz, 50 W pulse) has enhanced growth rate and the final biomass yield of *Anabaena flos-aquae*, a cyanobacterium (Francko, Taylor et al., 1990; Francko, Al-Hamdani et al., 1994). The same treatment reduced the growth rate of the microalga *Selenastrum capricornutum*. For both microorganisms, the ultrasonic treatment enhanced the protein content of the cells but levels of chlorophyll a and the uptake of ^{14}C -labelled bicarbonate were not affected (Francko, Taylor et al., 1990). A 46% increase in biomass yield of *Anabaena flos-aquae* was attained relative to controls. Effects of this magnitude for only short periods of sonication during culture suggest substantial commercial potential for ultrasound enhanced bioprocesses. Continuous and intermittent ultrasonication at 200 kHz and 17.2 kW m^{-2} power input has damaged *Lactobacillus delbrueckii* cells, causing them to leak intracellular β -galactosidase (Sakakibara, Wang et al., 1994; Wang, Sakakibara et al., 1996). Cells can respond differently to propagating and standing wave ultrasounds of equal intensity (Radel, McLoughlin et al., 2000). Standing wave sound appears to be less damaging than propagating ultrasound. Animal cells are perhaps the most fragile of live biocatalysts (Chisti, 2000; Chisti, 2001) but they withstand standing wave ultrasound of considerable power. A power input of 220 kW m^{-3} did not affect viability, the glucose uptake rate and antibody production of a hybridoma culture exposed to megahertz-range standing wave. The relatively less cell

damage in standing wave fields is explained by the migration of the particles suspended in such a field, to positions of low acoustic pressure and mechanical stress. The particles then remain in zones of low stress. By contrast, in a propagating wave field, the cells remain uniformly distributed in the fluid and experience a greater mean acoustic pressure (Bohm, Anthony et al., 2000). Cavitation, microstreaming and other effects of ultrasound are generally more intense in a propagating wave field. Stimulation of *Panax ginseng* suspended cells with short duration (0.5–6.0 min) ultrasound (power less than or equal to 100 kW m^{-3} , 38.5 kHz) affected cross-membrane ion fluxes within 2 min after exposure. Low doses of ultrasound ($600\text{--}800 \text{ kJ m}^{-3}$) were sufficient to induce these responses. Ultrasound stimulated the synthesis of secondary metabolites, without reducing the net biomass yield (Wu and Lin, 2002). Similar enhancements in metabolite productivity by low-power ultrasound have been reported with *Panax ginseng* (Lin, Wu et al., 2001) and *Lithospermum erythrorhizon* cells (Lin and Wu, 2002).

Whether sonication is continuous or intermittent also affects the survival behavior of cells in a sonic field. During production of ethanol by *S. cerevisiae*, intermittent sonication at 300 W m^{-3} and 25 kHz more than doubled the yield of ethanol but this effect did not occur in continuously sonicated culture. Cell growth and ethanol production persisted at higher intensity sonication (12 kW m^{-3}) but at rates comparable with nonsonicated controls (Schlafer, Sievers et al., 2000). Continuous ultrasonication at low power (300 W m^{-2} , 43 kHz) reduced fermentation time by 50 to 64% in producing of wine, beer and sake using various strains of the yeast *S. cerevisiae*. Ultrasound enhanced yeast growth and decreased the concentration of inhibitory dissolved carbon dioxide possibly through improved degassing (Matsuura, Hirotsune et al., 1994). Ultrasound has stimulated sterol synthesis in bakers' yeast

(Bujons, Guajardo et al., 1988). In another study, intermittent ultrasound treatment for a cumulative period of 150 s using a 25 kHz tube resonator (constant 80 W effective output) caused a ~76% increase in the release of intracellular gentamicin during production by *Micromonospora echinospora*. The broth was sonicated by continuous recirculation between a stirred bioreactor and an externally located sonication chamber (Chu, Li et al., 2000).

2.3.6 IMPROVED MASS TRANSFER DUE TO ULTRASOUND

As discussed earlier, ultrasound enhances mass transfer and reaction rates. Under typically used regimens of operation of conventional bioreactors, a stagnant film of liquid invariably surrounds small microbial cells suspended in the culture fluid. This film can impede mass transfer of nutrients and products. In other cases, solid–liquid and gas–liquid mass transfer of substrates and nutrients can be a rate controlling factor (Chisti, 1999). In a sonicated bioreactor, the pulsation of microbubbles of gas in the fluid generates micro streaming and other effects that can thin the fluid boundary layer around cells positioned close to the bubbles (Kilby and Hunter, 1990), thus enhancing mass transfer. Ultrasound has the potential for enhancing mass transfer within a cell. At certain intensities of ultrasound, intracellular micro streaming has been reported inside animal and plant cells (Bar, 1988). Similarly, rotation of organelles and induced circulation within vacuoles of plant cells, have been associated with ultrasound (Nyborg, 1982). Distinct from enhancing transport through the fluid boundary layer around cells, ultrasound can greatly increase the rates of gas–liquid oxygen transfer, removal of carbon dioxide and dissolution of suspended solids and drops. This increases the supply of low solubility substrates and, indirectly, enhances a culture's productivity.

3 Materials and Methods

3.1 EXPERIMENTAL SET-UP

This study involves comparing a new ultrasonicated fermentation process with a conventional fermentation process. To achieve the objectives of the study an experimental set-up was designed as shown in Figure 3.1.

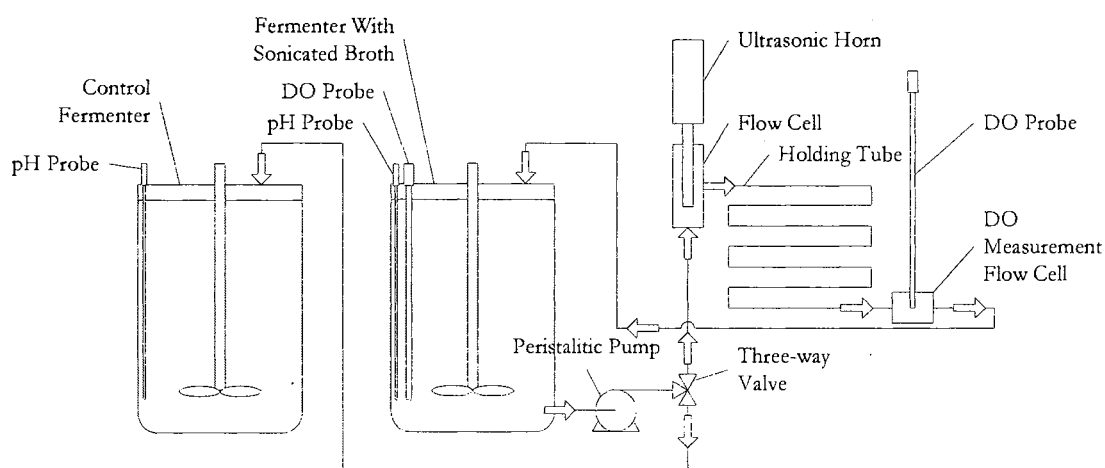


Figure 3.1 Experimental Set-up

3.2 EXPERIMENTAL PLAN

The experiment plan is shown as a flow chart in Figure 3.2. The rectangular boxes represent processes. The parallelograms represent data derived from the processes and the diamonds represent decisions made based on the data and processes. All the experiments involving the

biomass were initiated by using the same mother culture of *Xanthomonas campestris*. The purpose of the preliminary study was to ascertain whether the fermentation was normal during continuous or intermittent recycling of fermentation broth on a larger scale, with processing parameters obtained from earlier experiments.

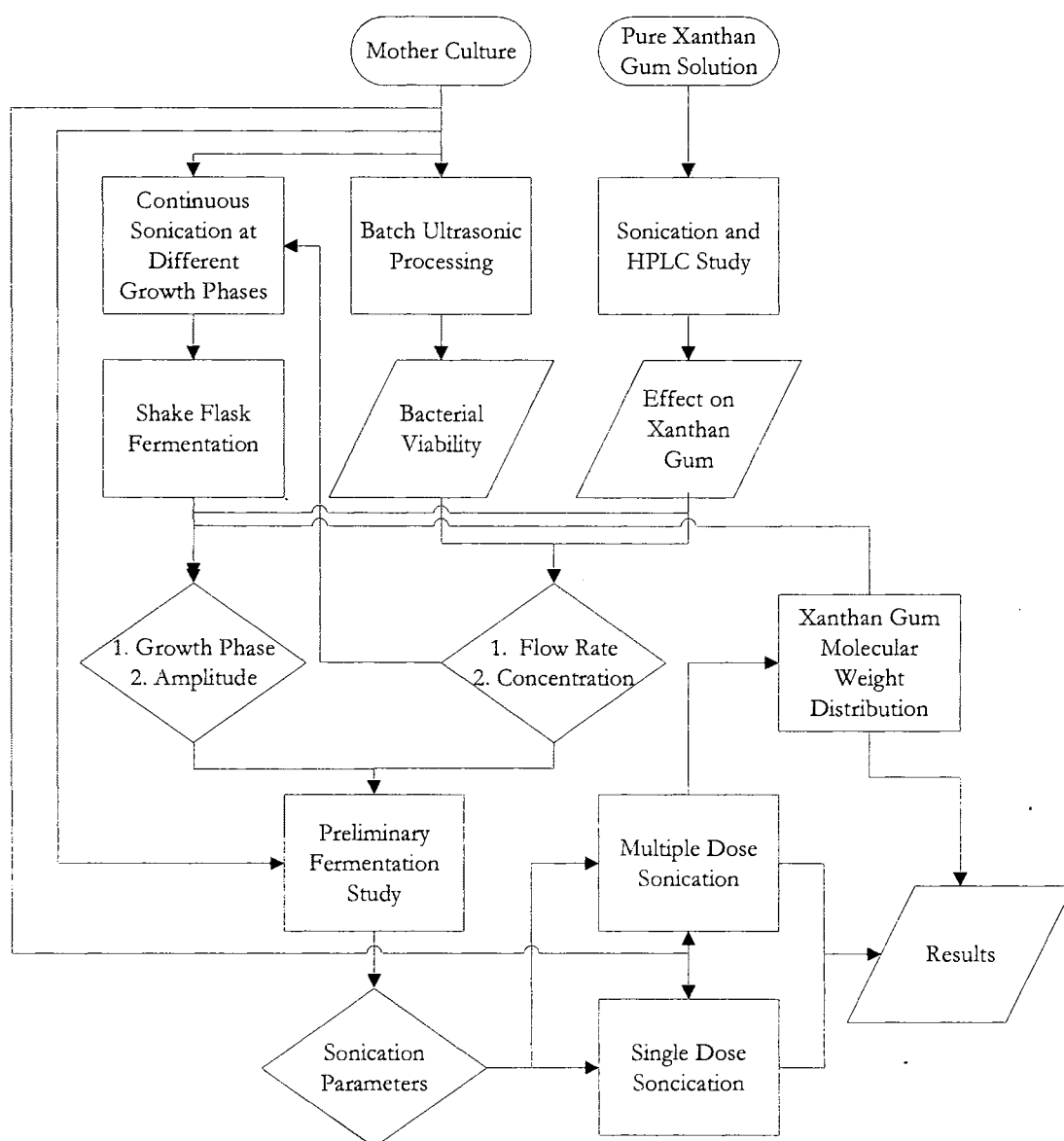


Figure 3.2 Flow Chart Showing Experimental Plan

3.3 EQUIPMENT DETAILS

3.3.1 FERMENTER

Xanthan gum fermentation using *Xanthomonas campestris* was conducted in two identical 14L turbine blade agitated fermenters (New Brunswick Scientific Microferm). The dimensions of the fermenter are shown in Figure 3.3, and that of the turbine blade is shown in Figure 3.4. The distance between the turbine blades was twice the diameter of the blades. Temperature control in the fermenter was achieved by a hollow tube heat exchanger, having controlled water supply. Input to the temperature controller was provided by a thermocouple immersed in a thermo-well on the head-plate of the fermenter. The fermenter was also equipped with a single-nozzle integrated sparger for air supply. The sparger was placed 1 cm below the turbine blades and axially centered to the shaft of the fermenter.

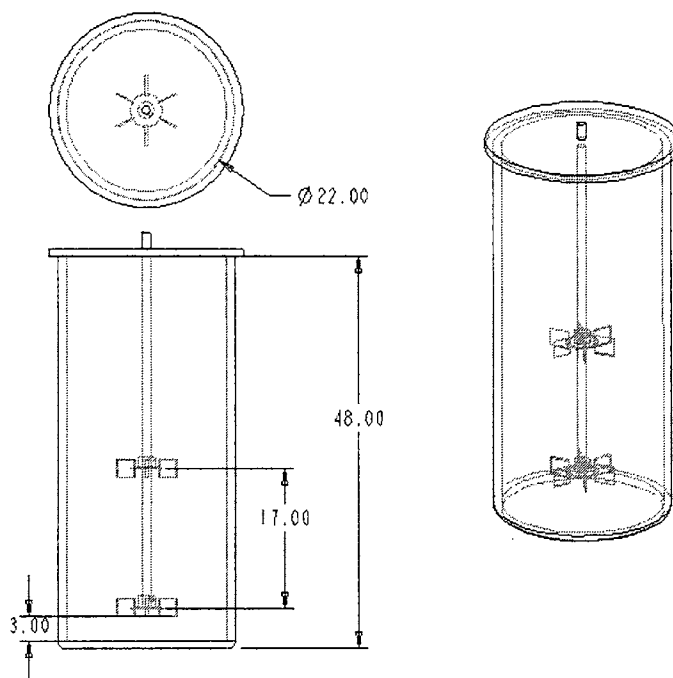


Figure 3.3 Fermenter Dimensions (cm)

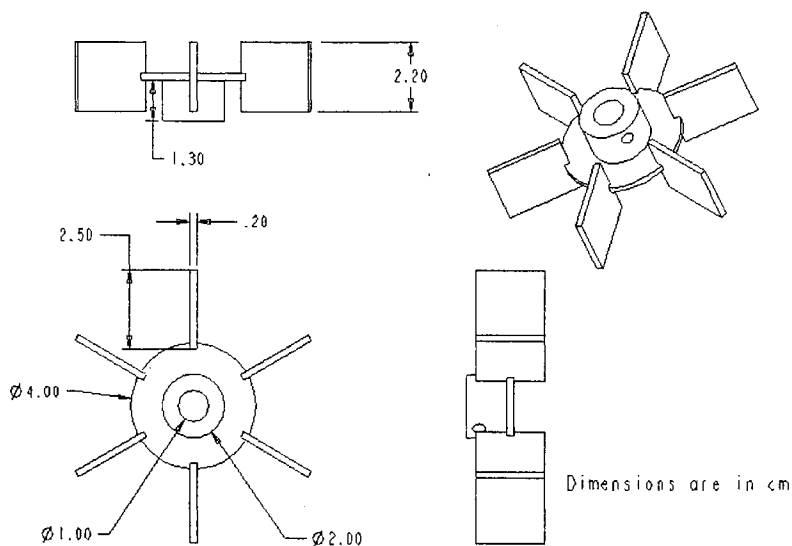


Figure 3.4 Turbine Blade

3.3.2 ULTRASONIC EQUIPMENT

Ultrasonic equipment used was a VCX 750 Watt Ultrasonic Processor. It comprised of two components -- ultrasonic flow cell (Figure 3.5) and a control unit.

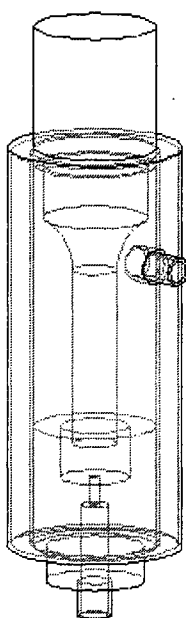


Figure 3.5 Ultrasonic Flow Cell

The details of the autoclavable stainless steel ultrasonic flow cell, equipped with an inlet (A) and outlet (B) are shown in greater detail in Figure 3.6.

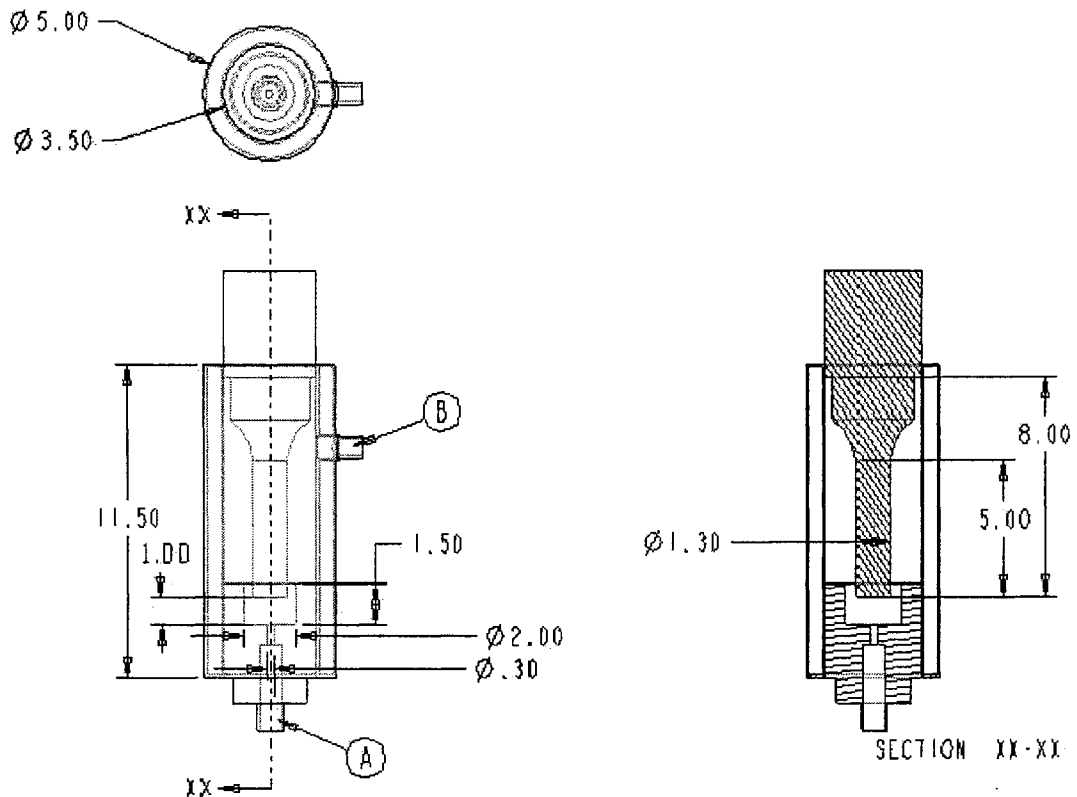


Figure 3.6 Ultrasonic Flow Cell Dimensions (cm)

The flow cell is capped from the top by ultrasonic horn, which delivers ultrasonic energy to the incoming liquid from the bottom end of the cell. The ultrasonic horn has a narrow low intensity solid tip (tip diameter: 13mm) that can vibrate at maximum amplitude of 6 μm . Ultrasonic horn is connected to an ultrasonic generator, which in turn is connected to a control unit that allows for manual amplitude control.

Generally, two types of ultrasonic equipment are commonly available: ultrasonic baths and narrow tip ultrasonic generators. Since a narrow tip ultrasonic generator is more effective

than an ultrasonic bath/reactor (Mermillod-Blondin, Fauvet et al., 2001), it was the equipment of choice. An external loop allows for more flexibility in controlling the exposure levels and in scalability, and at the same time keeps the costs of system design at a minimum.

3.3.3 SENSORS

The pH was measured using Mettler Toledo’s sterilizeable pH probes, and the oxygen concentration in the outlet air was analyzed using zirconium oxide sensor (EX-2000 Gas Analyzer, New Brunswick Sc Co., Inc.). Dissolved oxygen (DO) was measured using polarographic Ingold probes. For measuring DO in the pipeline a DO probe holding assembly was designed and fabricated. Figure 3.7 depicts the DO probe holding assembly.

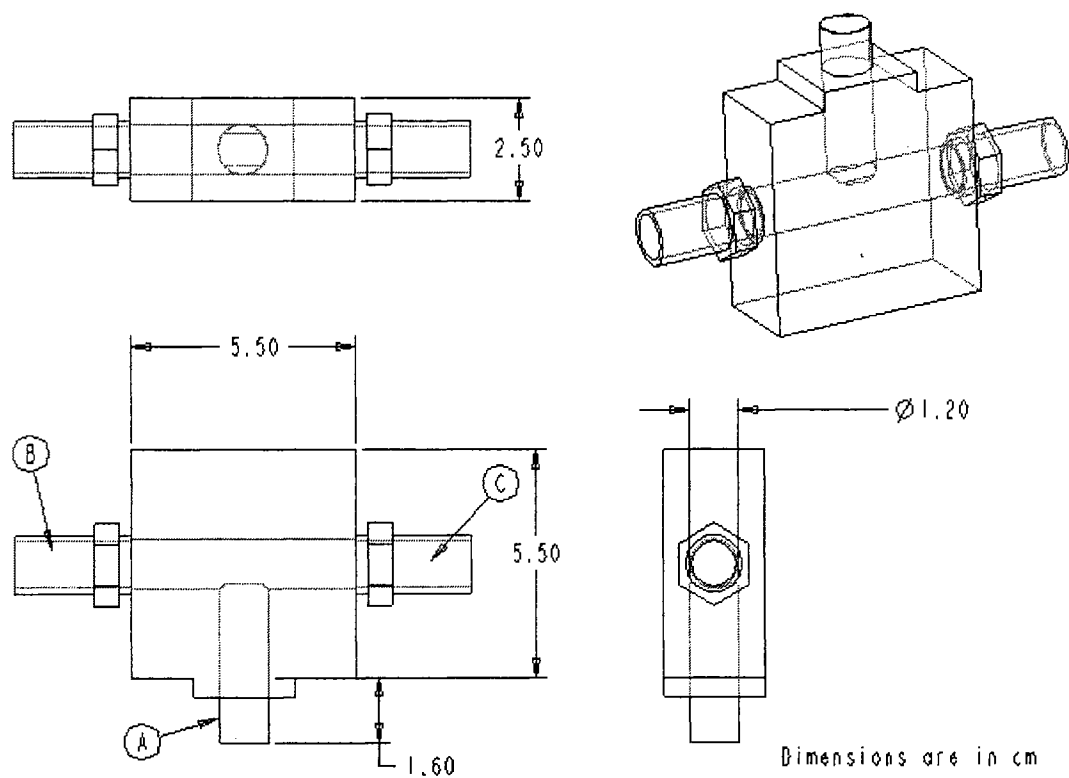


Figure 3.7 DO Sensor Holder for Oxygen Uptake Rate Mesurement

The DO probe holder allows the DO probe to measure the DO level from the axial center of the fluid stream passing through it.

3.4 OXYGEN UPTAKE RATE

Oxygen is usually introduced to fermentation broth by sparging air through the broth. The rate of oxygen transfer from the gas bubbles through the liquid film surrounding the gas bubbles is generally referred to as the Oxygen Transfer Rate (OTR). The rate of oxygen consumption by the biomass from the broth is usually referred to as Oxygen Uptake Rate (OUR), which is mathematically defined as:

$$\text{Oxygen uptake rate (OUR)} = q_{O_2} X = (\mu X)/(Y_{X/O_2})$$

Where, q_{O_2} = specific rate of oxygen consumption ([mol or mg O_2]/g dry wt cells · h); X = cell concentration (g dry wt cells/ L); Y_{X/O_2} = oxygen yield coefficient (g dry weight cells/g O_2); μ = specific growth rate (h^{-1})

The microbe more or less intrinsically controls oxygen uptake rate. This rate can be decreased if the Oxygen Transfer Rate becomes the limiting factor. The measurement of OUR is difficult due to many different reasons. In particular, the very low specific consumption rate, the sensitivity of the cells to variations in dissolved oxygen concentration and the difficulty to provide oxygen without damaging the cells are problems which must be taken into account while using any particular OUR measurement methods. It has been extensively reported in the literature that oxygen transfer rates measured by dynamic methods using dissolved oxygen probes may lead to errors in hundreds of percents (J.B. Hubbard, 1990). It has also been specifically reported that the dynamic method for oxygen uptake determination is unsuitable even for moderately viscous xanthan broth (Amanullah,

Tutti et al., 1998). One author has cautioned that for accurate measurement using the mass balance method, the change of the oxygen mole fraction in the gas has to be sufficiently high for accurate measurements (Suh, Herbst et al., 1990). Also, this method requires accurate measurements of pressure, temperature and flow rates. A dynamic method, which is relatively inexpensive and straightforward, has been reported (Yoon and Konstantinov, 1994). This method is based on dissolved oxygen (DO) measurement at two points. The OUR is calculated from the following equation:

$$\text{OUR} = (\text{C}_{\text{in}} - \text{C}_{\text{out}})/\Delta t$$

Where, C_{in} and C_{out} are the molar fraction of oxygen entering and leaving the system, and Δt is the time taken for a particle to move between the two measuring points. The monitoring scheme is applicable to both microbial and mammalian cell bioprocesses of laboratory or industrial scale. It enables the continuous and undisturbed monitoring of OUR, which is conventionally impossible without gas analyzers. The technique does not require knowledge of $k_L a$. It provides smooth, robust, and reliable signal. Also, there is no 'headspace' available for phenomena like surface aeration. The only major difficulty is the requirement for careful calibration of the two pO_2 electrodes, since the OUR determination is based on the difference between the signals of the two electrodes. The latter might necessitate a system for the sterile removal, washing, calibration, re-sterilization and re-insertion of the probes from/to the bioreactor /tubes at intervals during the culture. One significant advantage of this technique over others is that the OUR measurements can be performed only on the broth that has been ultrasonically treated in the continuous flow cell. The two points between which the measurement will be taken will be located at the exit of the continuous flow cell and the inlet of the fermenter. In other employed methods the actual OUR is masked by the dilution that occurs due to only a fraction of the total volume being

subjected to ultrasound at a time. In this cases, the external loop meant for ultrasonic treatment can be advantageously used to measure the OUR. Thus this method is used for measurement in this study.

3.5 MAINTENANCE OF MICROORGANISM

3.5.1 STRAIN MAINTENANCE

Xanthomonas campestris NRRL B-1459 was obtained in a lyophilized state from ATCC (Manassas, VA, USA). The lyophilized culture was aseptically removed from the ampule and transferred to liquid Yeast and Mold broth (3 g/L yeast extract, 3 g/L malt extract, 5 g/L glucose, 10 g/L peptone) medium and incubated for 48 h at 27°C. This was then used to produce a large number of freeze-dried bead suspensions, which were subsequently stored at -20°C. The contents of a single ampule was transferred to liquid Yeast and Mold broth, incubated for 48 h at 27°C and then used to inoculate Yeast and Mold broth agar slopes. These served as the master slopes and were stored at 4°C in a refrigerator for a maximum of 3 months before being discarded.

3.5.2 INOCULATION PROCEDURES

Triplicate Yeast and Mold broth agar plates were prepared by inoculating each plate with a loop of solution from dilution blanks ($1:10^6$ or $1:10^8$), prepared from one loop of culture from the master slopes. After growing bacterial colonies on these agar plates for 48 h at 27°C, two loops of the largest colonies were further transferred to shake 200ml flasks (50ml Yeast and Mold broth), which were incubated at 27°C and agitated at 200 rpm for 48 h. The

final mother inoculum was prepared by inoculating 500ml of Yeast and Mold broth with this incubated broth.

3.5.3 CULTURE MEDIA

Three types of culture media were used for various stages of fermentation. To maintain the bacterial strain for long periods, Yeast and Mold agar was used. For cultivation of in the shake flask a different media similar in composition to yeast and mold agar media was used. For fermentation in 14 L fermenter a well defined medium (based on (Peters, Herbst et al., 1989)) was used as the production medium in order to keep the variability of results due to medium components to a minimum. The compositions of these three media are given below.

Yeast and Mold agar media: Yeast extract: 3 g L⁻¹, malt extract: 3 g L⁻¹, peptone: 5 g L⁻¹, glucose: 10 g L⁻¹; and agar: 28 g L⁻¹.

Shake Flask media: Yeast extract: 3 g L⁻¹, malt extract: 3 g L⁻¹, peptone: 5 g L⁻¹, and glucose: 15 g L⁻¹.

Fermenter media: Glucose: 50 g L⁻¹, citric acid: 2.3 g L⁻¹, KH₂PO₄: 5 g L⁻¹, NH₄Cl: 2 g L⁻¹, Na₂SO₄: 0.114 g L⁻¹, MgCl₂·5H₂O: 0.163 g L⁻¹, FeCl₃·6H₂O: 0.0014 g L⁻¹, ZnCl₂: 0.0067 g L⁻¹, CaCl₂·2H₂O: 0.012 g L⁻¹, H₃BO₃: 0.006 g L⁻¹, Na₂CO₃: 0.5 g L⁻¹, antifoam: 0.5 g L⁻¹. Glucose was sterilized separately to avoid the Maillard reaction. The two solutions were autoclaved at

121°C and 15 psig for 15 minutes. After they cooled to room temperature, they were aseptically mixed in the fermenter and their pH adjusted to 7.0 using NaOH.

3.6 FERMENTATION CONDITIONS

Fermentations were carried out both in 14 L fermenters as well as shake flasks. The shake flask fermentations were necessary to carry out multiple fermentations simultaneously.

3.6.1 FERMENTATIONS IN SHAKE FLASKS

Fermentations in the shake flasks were carried out in 250 ml Erlenmeyer glass shake flasks. The maximum quantity of broth used in each flask was 100 ml. The Erlenmeyer flasks were mounted on a shaking platform that in turn was enclosed in a temperature controlled chamber maintained at 27 deg C. The speed of the shaking platform was maintained at 200 rpm.

3.6.2 FERMENTATIONS IN FERMENTER

The experiment was initiated with 10 L of fermentation medium in a single fermenter. At the end of exponential growth phase of the bacteria, 5 L of fermentation broth was transferred to another fermenter. From this point on, the fermentation conditions in both the fermenters were kept identical. Of these two fermenters, one fermenter (sonicated fermenter) was attached to a recirculation pipeline and the ultrasonic processor, while the other (control fermenter) was left undisturbed. Temperature and pH were maintained at $27^{\circ}\text{C} \pm 1.5^{\circ}\text{C}$ and 7, respectively, as these conditions have been determined optimum for growth (Shu and Yang, 1991; GarciaOchoa, Santos et al., 1997). Solutions of 5N NaOH and

1N HCl were used as base and acid, respectively, to automatically maintain the pH. Sterile air (passed through a 0.2 μ m filter) flow was kept constant at 1.0 vvm. Dissolved oxygen was measured using polarographic Ingold probes and maintained at levels above 20% of air saturation by manual increases in impeller speed (400-500 rpm). A recirculation peristaltic pump connected between the fermenter and the flow cell was used to maintain a flow rate of about 100 ml/min. Samples were collected immediately after inoculation and every 8 hours thereafter for 60 hours from both the fermenters. Each sample was analyzed for the concentrations of xanthan gum, biomass and glucose (g/L).

3.6.3 SONICATION PARAMETERS

Biological activity is increases or decreases based upon the type of ultrasonic treatment (Schlafer, Sievers et al., 2000). Microbes are more likely to be killed by increasing ultrasonic intensity and are less effected at higher frequency (Peterson and Pitt, 2000). Also it has been reported that microbes/micelial cells, exposed for about 30 to 150 sec to ultrasound at a frequency of 25 KHz and 80 W constant output, remained intact (Chu, Li et al., 2000). Thus, it is proposed to use sub-lethal levels of ultrasonic energy at a lower frequency of 20 KHz. Three levels of amplitude will be evaluated at a flow rate of about 100ml/min: 20% (1.2 μ m), 35% and 50% (3 μ m) of the maximum achievable amplitude (6 μ m).

3.7 ANALYTICAL METHODS

During the course of the experiment, several variables such as – biomass formation rate, xanthan production rate, and glucose uptake rate were monitored. In the following sections the methods used to determine their concentrations in the broth are described.

3.7.1 BIOMASS CONCENTRATION

Biomass concentration was determined by 10-20 fold sample dilution and measurement of absorbance at 565 nm using a spectrophotometer. The contribution of gum to this measurement was determined by the 565 nm absorbance of the centrifuged cell free supernatant as described earlier. The centrifuged pellet was resuspended in distilled water to remove undesired soluble material and centrifuged at 38 000g for 20 min. The resulting pellet was dried on a watch glass in a 100 C oven until constant weight was achieved. A calibration of dry cell weight versus absorbance at 565 nm for triplicates resulted in a linear relationship with a regression coefficient of 0.99 (Figure 3.7).

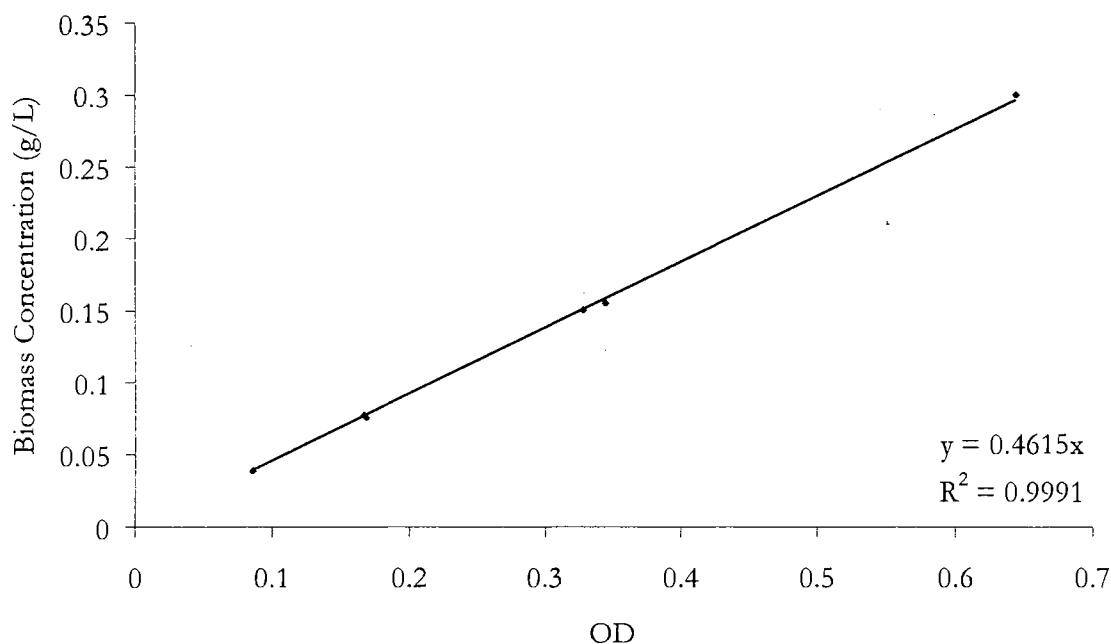


Figure 3.8 Calibration Curve for Biomass

3.7.2 XANTHAN CONCENTRATION

Xanthan concentration was determined from the broth's viscosity. Xanthan gum extracted from 60 h fermentation was used to create calibration curves. The calibrations were performed at three shear rates (0.1 Pa.s; 0.31 Pa.s; 1.0 Pa.s). Viscosity of the xanthan solutions was determined with a rheometer (AR 1000N TA Instruments, New Castle, DE, USA) attached with a stainless steel recessed end concentric cylinder (internal diameter of the sample holder -- 15mm, outer diameter of concentric cylinder -- 14mm, cylinder immersion height -- 42mm, gap -- 4mm). An equilibration time of 30 sec was given to each sample. The temperature of the system was maintained at 25°C using a constant temperature circulator water bath. The xanthan gum concentration obtained from each calibration was averaged to give the final xanthan gum concentration. Xanthan gum was extracted by adding three volumes of alcohol and 10% (v/v) of 2% w/v KCl solution to the cell free supernatant (obtained after centrifugation at 30,000 g for 45 min) to precipitate xanthan gum. The solution was centrifuged at 30,000 g for 10 min and the precipitate was collected and dried for 24 h at 80°C. The dried xanthan was ground into a powder form. Standard solutions (0.1%, 0.5%, 1.0%) were prepared in shake flasks which were mixed for 24 hr at 200 rpm.

3.7.3 GLUCOSE CONCENTRATION

Glucose in fermentation broth was determined using Boehringer Mannheim (R-Biopharm GmbH, Germany) Enzymatic BioAnalysis/Food Analysis test kit. The principle of glucose determination is that the D-Glucose is phosphorylated to D-glucose-6-phosphate (G-6-P) in the presence of the enzyme hexokinase (HK) and adenosine-5'-triphosphate (ATP) with the simultaneous formation of adenosine-5'-diphosphate (ADP). In the presence of the enzyme

glucose-6-phosphate dehydrogenase (G6P-DH), G-6-P is then oxidized by nicotinamide-adenine dinucleotide phosphate (NADP) to D-gluconate-6-phosphate with the formation of reduced nicotinamideadenine dinucleotide phosphate (NADPH). The amount of NADPH formed in this reaction is stoichiometric to the amount of D-glucose. The increase in NADPH is measured by means of its light absorbance at 334, 340 or 365 nm. This is then correlated to the glucose amount in the fermentation broth.

3.8 DETERMINING PROPERTIES OF XANTHAN MOLECULE

To differentiate and characterize xanthan gum, most often, properties such as molecular weight distribution, molar mass, and root mean square radius are used. In this study two different approaches were used to aid in understanding the effect of ultrasound on xanthan molecule. In the first approach, pure xanthan solutions were subject to varying degrees of ultrasonic intensities. The effect of ultrasound was measured by comparing the change in retention time in two size exclusion chromatography columns connected in series. In the second approach, during a sonicated fermentation, a feasible, ultrasonic treatment on the higher end was given to the broth. The xanthan obtained from a regular fermentation was compared to xanthan obtained sonicated fermentation. The molecules were differentiated based on their weight average molecular weight, number average molecular weight, and root mean square radius.

3.8.1 RETENTION TIME

Size exclusion chromatography (SEC) is an extremely important technique for characterizing macromolecules. SEC is a high-performance liquid chromatographic (HPLC) technique in

which molecules are separated according to differences in hydrodynamic volume. This separation mechanism is made possible by the packing material in the column. The packing material is made of porous spherical particles. The retention in SEC is governed by the partitioning (or exchange) of the macromolecular solute molecules between the mobile phase (the eluent flowing through the column) and the stagnant liquid phase that occupies the interior of the pores. The range of macromolecular sizes that can be separated with a given column depends on the size (or size distribution) of the pores. The resulting chromatogram in an SEC experiment thus represents a molecular size distribution. The distance of the peak of the molecular weight distribution from the origin is called retention time. The lowest-molecular-weight molecules permeate all of the pores within the SEC column, and thus take longer to elute. The larger molecules elute first. Thus if a polymer is broken down then the peak of the molecular weight distribution curve is delayed. In this study to differentiate among various ultrasonic treatments, absolute molecular weight techniques (such as MALLS) could have been employed, but these efforts would have been costly and time-consuming (considering that there were 81 unique treatments). In this instance, the absolute values of molecular weights were not important because the interest was only in comparing samples to determine whether there is a relative difference in molecular weight. Hence retention time was chosen as an appropriate measure to compare different sonicated xanthan solutions.

The xanthan molecule's retention time was determined by size exclusion chromatography on two PL aquagel-OH 60 15 μ m, 300x7.5 mm columns (Polymer Laboratories Ltd., Church Stretton, U.K.), connected in series using a conventional HPLC system (Alliance 2690) equipped with a differential refractometer (Waters 410 Differential Refractive Index

Detector). Large particle size packing columns (15 μ m) were used to avoid on-column shear degradation of very high molecular weight xanthan molecules, and high pore size was required to fully resolve all the sample components. The eluent used was 0.2M NaNO₃/0.01M NaH₂PO₄ (pH=7), at a flow rate of 1.0ml/min. The sample loading was 0.01% w/v, 100 μ l. The concentration of the sample solution injected is minimized in order to avoid viscous streaming effects, which distort elution profile (Yau, Kirkland et al., 1979). Millennium-32 Version 4.0 Software carried out data handling automatically.

3.8.2 MOLECULAR WEIGHT DISTRIBUTION

The molecular weight distribution (MWD) is characterized by either the number, or weight of chains, with N repeating units. Number-average molecular weight is obtained by weighting each molar mass by the number of molecules of that molar mass present in the molecule.

$$M_n = \frac{\sum N_i M_i}{\sum N_i} = \frac{1}{N} \sum N_i M_i = \frac{\sum W_i}{\sum W_i / M_i}$$

Weight-average molecular mass is

$$M_w = \frac{\sum N_i M_i^2}{\sum N_i M_i} = \frac{\sum W_i M_i}{\sum M_i}$$

Here N_i and W_i are the number and weight, respectively, of molecules having molecular weight M_i . The subscript i is an index representing all molecular weights present in the ensemble of chains. Molecular weight distribution is represented by Polydispersity index (MWD or PDI) is:

$$PDI = M_w / M_n$$

Accurate determination of the Mw of xanthan is difficult for several reasons, including: (1) the very high molecular weight; (2) the stiffness of the molecule; and (3) the presence of aggregates. Nonetheless, several techniques have been used to determine the molecular weight of xanthan, including GPC-MALLS (gel- permeation chromatography with multi-angle laser light scattering), AFFF-MALLS (asymmetrical flow field fractionation combined with multiangle laser light scattering) and electron microscopy.

GPC-MALLS is a technique that permits the estimation of absolute molecular weight and gyration radius of polysaccharides, without the need for column calibration methods or standards. Often used in the field of polymer analysis, this technique is constituted by a GPC system, which allows molecules to be separated as a function of their molecular size, and also by MALLS, which allows information to be obtained on the molecular weight of the fraction eluted from the column. There are two classical methods to determine the molecular weight: the Zimm method; and the Debye method. The Debye method is preferable for xanthan (Born, Langendorff et al., 2001). LALLS (low-angle laser light scattering) provides a measure at a very low angle (5°) and avoids this problem, but this type of apparatus does not provide any information on the gyration radius. Wyatt (1993) has described the theory and practice of online light scattering measurements in detail. The equations described by Wyatt (1993) are used as the basis for rigorous fitting of the light scattering and concentration data by the ASTRA® software to retrieve the molar mass and rms radius for the xanthan gum in solution.

Three different samples of xanthan were used for characterization. One of the two was a commercial sample, obtained from Sigma Chemical Co., St Louis, MO. The two other

samples were obtained from intermittent dose sonication with shorter and frequent treatments (shown in Figure 4.23). 0.01% (w/v) xanthan gum solutions were prepared in nano pure water. For light scattering measurements, the chromatography system (Figure 3.8) consisted of Agilent HP1100 HPLC System; two chromatography columns; MALLS detector -- DAWN EOS; Concentration detector – Optilab; refractive index detector (DRI) from Wyatt -- UV@280 nm; DLS detector -- Wyatt QELS (Wyatt Tech., Santa Barbara, CA). The serially placed chromatography columns were two PL aquagel-OH 60 15 μ m, 300x7.5 mm columns (Polymer Laboratories Ltd., Church Stretton, U.K.).

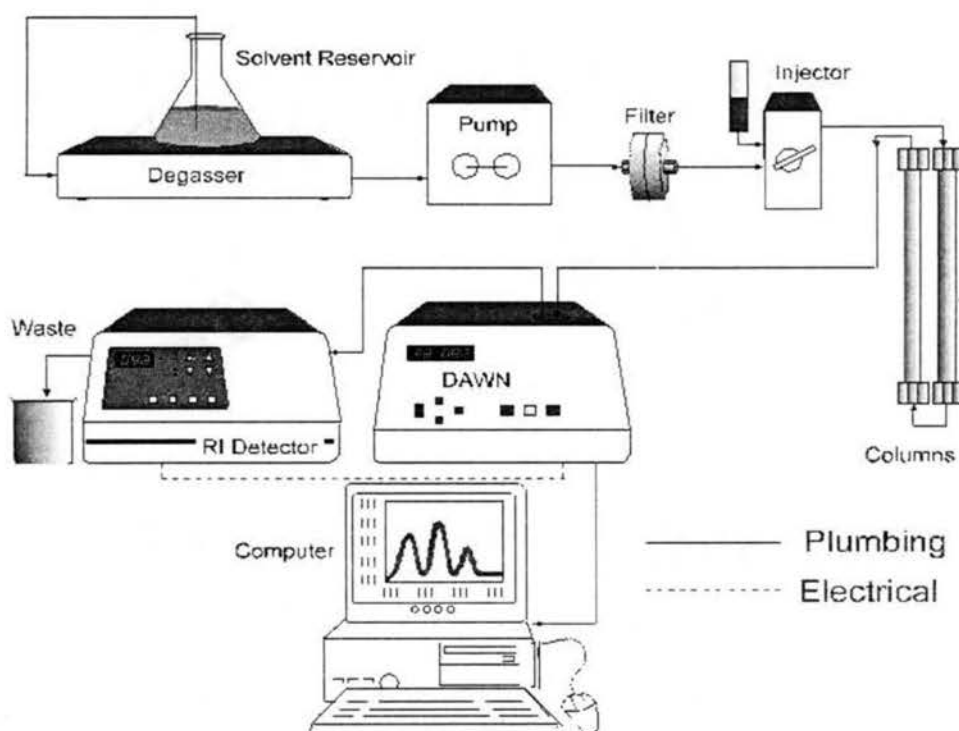


Figure 3.9 HPSEC Set-up

The electronic outputs of the DRI and the MALLS were processed using ASTRA® (Wyatt Tech). The scattering angles in degrees available for intensity measurements were 14.5, 25.9,

34.8, 42.8, 51.5, 60.0, 69.3, 79.7, 90.0, 100.3, 110.7, 121.2, 132.2, 142.5, 152.5, and 163.3.

Molar masses and radii were extracted from data fit to Debye equations.

3.9 POWER MEASUREMENT

Power measurement was required for calorimetric study of the sonicating equipment. The sonicating device was equipped with a timer and an energy meter. The instrument automatically displayed the amount of electrical energy delivered to the ultrasonic horn in Joules and the duration of operation of the ultrasonic horn. Power was calculated by dividing the energy in Joules by the time of operation of the ultrasonic horn. Specific power per unit surface area, of the ultrasonic horn, was calculated by dividing the power delivered to the horn by the cross-sectional surface area of the ultrasonic horn. To measure the amount of power absorbed by the broth or water, the rise in temperature due to sonication per unit mass of liquid was used to calculate the amount of energy absorbed by water (described in section 2.3.3).

3.10 STATISTICAL ANALYSIS

Three-way analysis of variance (ANOVA) was applied to the retention time obtained from chromatograms of sonicated pure xanthan gum solutions to evaluate whether there was any evidence that the means of the populations differed. The three treatments applied were amplitude, concentration and flow rate. Each treatment had three levels (Amplitude: 20%, 35%, 50%; Flow rate: 50 ml/min, 100 ml/min, 150 ml/min; Concentration: 0.5%, 1.0%, 1.5%). Results from ANOVA were subjected to Tukey's multiple comparison test with significance for $p < 0.05$ to investigate which of the means were different.

4 Results and Discussion

4.1 CHARACTERIZATION OF ULTRASONIC EQUIPMENT

4.1.1 CALORIMETRIC CHARACTERIZATION OF ULTRASONIC HORN

The amount of energy transferred by an ultrasonic horn depends on the resistance applied to its surface. The sonication equipment can be set to operate at constant amplitude, but the energy consumed by the sonicator is variable depending upon the medium in which the horn operates. Also, not all the energy delivered to the horn is transferred to the sonicated media. Thus, to quantify the efficiency of the sonication process, calorimetric studies were conducted using water and a 1% xanthan gum solution.

Figure 4.1 shows the results of sonicating 10 ml of water in a thermally insulated container for 60 seconds. Electrical energy delivered to the horn was directly read from the instrument panel. The rise in water temperature due to sonication was used to calculate the amount of specific power absorbed by the water. As shown in Figure 4.1, a linear relationship [$y = 0.07879x - 0.81917$; $R^2 = 0.99$] was observed between the amplitude and the power delivered to the ultrasonic horn. However, a second order relationship [$y = -0.0007x^2 + 0.09807x - 0.89214$; $R^2 = 0.99$] was found between the amplitude and the power absorbed by water. The reason for inefficient energy transfer at higher sonication intensities could be resistance to energy transfer at the interface between water and the horn due to cavitation.

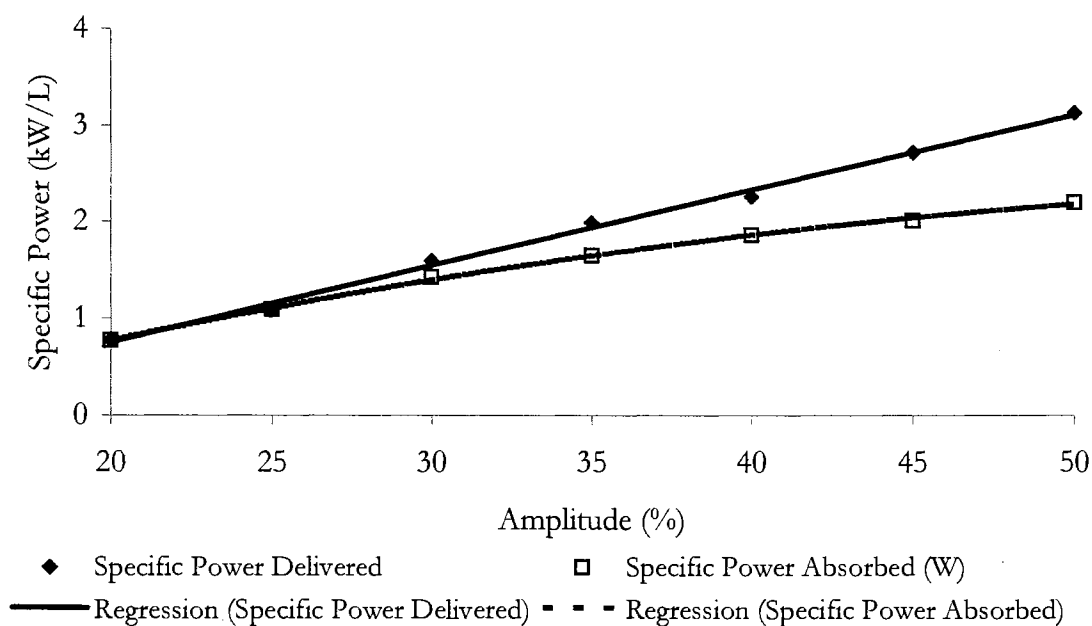


Figure 4.1 Calorimetric Characterization of Ultrasonic Horn Using Water

The results of an experiment using 1% (w/v) xanthan gum solution are shown in Figure 4.2. A linear relationship [$y = 1.0576x - 16.681$; $R^2 = 0.99$] was observed between the amplitude and the power delivered to the ultrasonic horn. A second order relationship [$y = -0.0102x^2 + 1.69x - 26.714$; $R^2 = 1$] was observed between the amplitude and the power absorbed by the xanthan solution. Comparison of Figure 4.1 and Figure 4.2 reveals that at amplitudes greater than 35% the power delivered by the ultrasonic horn and the power absorbed by the liquid is higher for the xanthan solution. Also, energy transfer efficiency in the xanthan solution is better than that in water. In this case the energy transfer from the sonicating horn in the viscous solution is more efficient than in a non-viscous solution. Also, at constant amplitude, the input power required for sonicating solutions varies depending on solution viscosity.

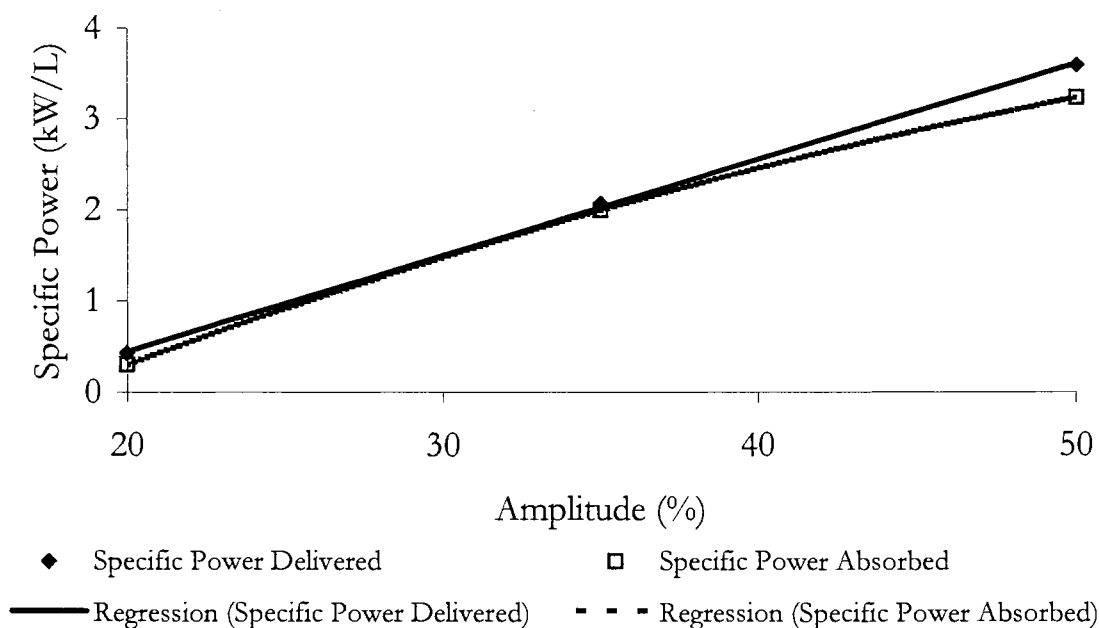


Figure 4.2 Calorimetric Characterization of Ultrasonic Horn Using 1%(w/v) Xanthan Gum Solution

Thus, due to the variability in the power absorbed with varying viscosity, and also due to the difficulty in measuring the actual energy absorbed during a fermentation run, this study will use the term “percentage amplitude” as a measure of intensity of the ultrasonic power.

The amount of specific power absorbed by the xanthan fermentation broth varies depending on the concentration of xanthan gum, which in turn depends on the concentration of xanthan gum produced. Figure 4.3 shows the specific power absorbed at different amplitudes. The variation in power absorbed at the same amplitude is due to variation in xanthan concentration during the course of fermentation.

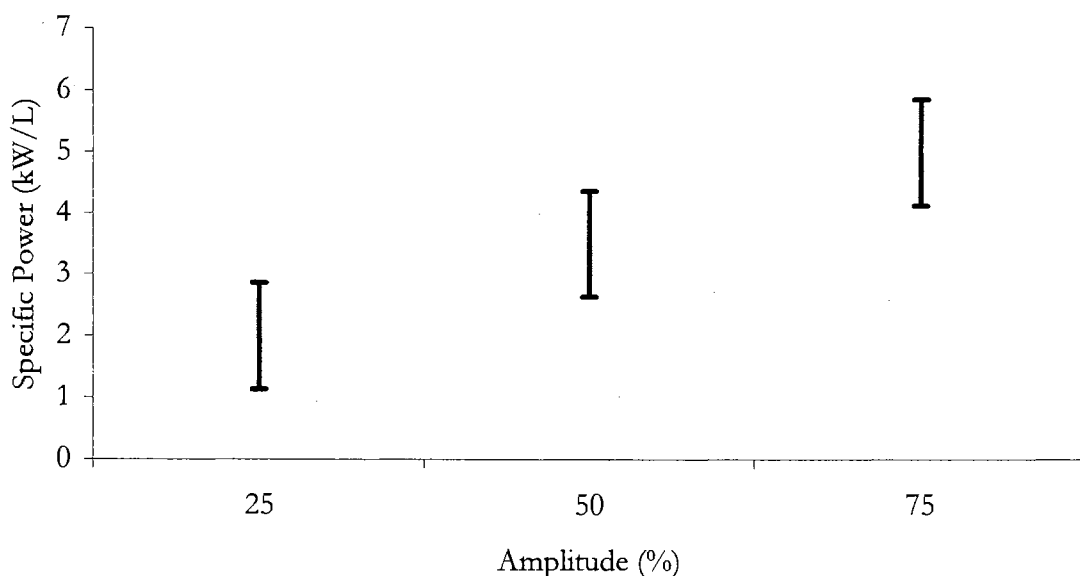


Figure 4.3 Approximate Specific Power Corresponding to Percentage Amplitude in Xanthan Broth

4.1.2 RESIDENCE TIME DISTRIBUTION OF ULTRASONIC FLOW CELL

The residence time distribution (RTD) can provide a useful assessment of the performance of the ultrasonic flow cell by characterizing the fluid flow through it. Thus, a residence time distribution study was conducted to characterize the flow cell at a flow rate of 100 ml/min. The total liquid hold-up volume of the flow cell was experimentally determined to be 75 ml. A stable red food dye with maximum absorbance at 521 nm was used as a tracer with water as the experimental liquid. A linear calibration curve was used to determine the concentrations of the dye at the outlet. A pulse input at the flow cell's inlet was achieved by rapid injection of 1ml pure tracer. The discrete data generated directly from the experiment was used to calculate the area under the curve using the trapezoid rule. Comparative responses to the pulse input at the cell outlet, when the flow-cell is idle and when being

sonicated (50% amplitude), are shown in Figure 4.4. The mean residence times during sonication and during idle conditions were found to be 38.5 s and 46.7 s respectively.

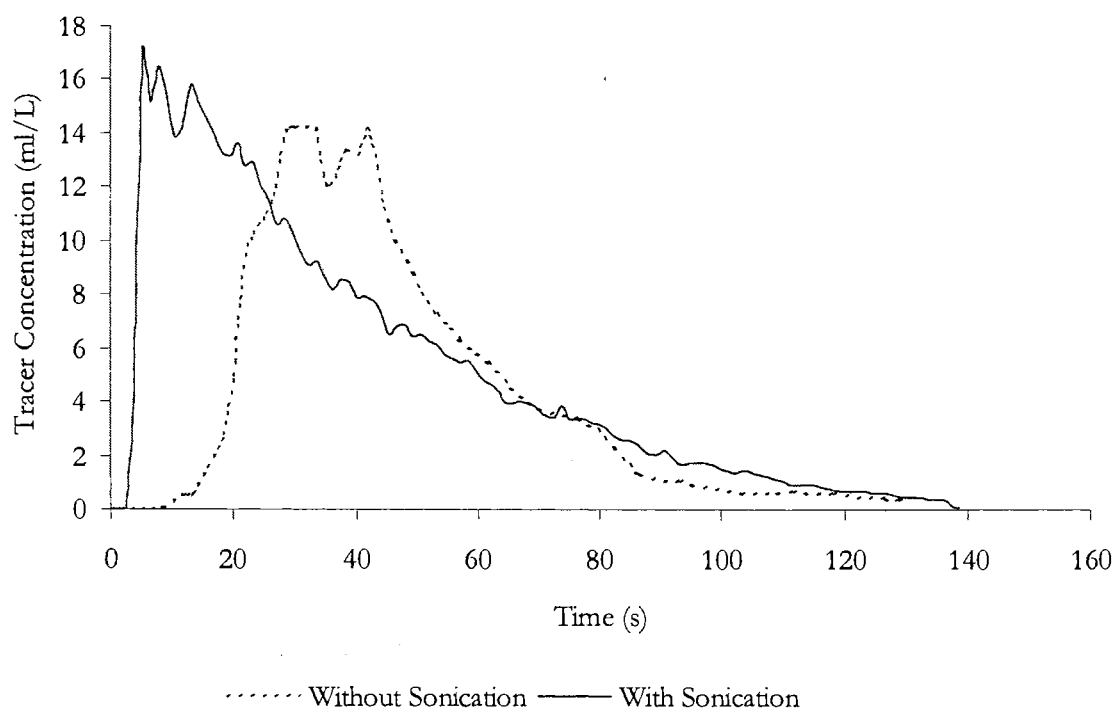


Figure 4.4 Residence Time Distribution of a Tracer in Ultrasonic Flow Cell (flow rate = 100 ml/min)

The curve representing the idle condition shows channeling (wave formation in graph peak) as well as a stagnation effect (gradual lowering of concentration), whereas the one representing the sonicated condition shows only stagnation. Channeling is generally due to uneven distribution of the fluid (short-circuiting from inlet to outlet). These effects can be explained by considering the flow cell as three different flow zones -- A, B, and C. Figure 4.5 shows these zones. Zone A can be thought of as a completely mixed zone where complete instantaneous mixing occurs at the inlet due to the acoustic energy emitted from the tip of the ultrasonic horn. This zone is the only region in the flow cell where the liquid is exposed to ultrasonic energy. Due to continuous inflow and the narrow annular space of zone B, it can be assumed to have a plug flow profile, which means no or minimal axial mixing. Thus,

zone B acts like a one-way valve between zone A and zone C, thereby effectively preventing recycling between the two zones.

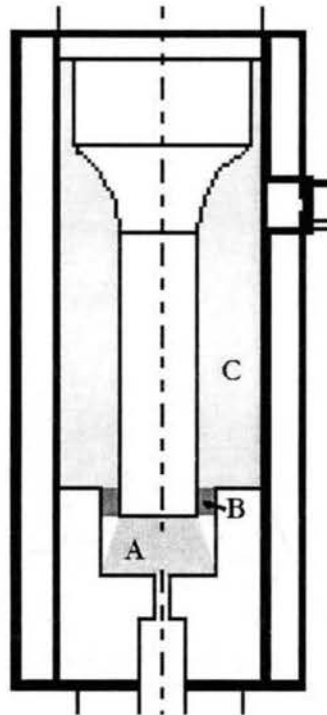


Figure 4.5 Hypothetical Flow Zones in Ultrasonic Flow Cell

With this information the reasons for stagnation and channeling can be explained. During the idle conditions, zone A is not a completely mixed zone and is responsible for channeling, whereas zone C causes stagnation irrespective of the conditions in zone A. Thus, the actual exposure time can be calculated directly from the volume of zone A (3.14 ml) and the flow rate. The residence time of a bacterium in a liquid flowing at 100 ml/min through the flow cell will be approximately 1.9 s.

4.2 EFFECT OF SONICATION ON *XANTHOMONAS* *CAMPESTRIS* AND XANTHAN GUM

4.2.1 EFFECT OF SONICATION ON VIABILITY OF *X. CAMPESTRIS*

To determine the effect of sonication on *Xanthomonas campestris*, 100 ml shake flask medium was prepared and inoculated with 10 ml *Xanthomonas campestris* culture. The shake flask was agitated at 200 rpm and simultaneously incubated at 27°C for 24 h. After the incubation period, 10 ml broth was transferred to a 20 ml beaker with 20 mm internal diameter. The beaker was placed in an ice bath to keep the broth cool during sonication. Samples of the sonicated broth were drawn at one-minute intervals. These samples were further diluted in 1:10², 1:10⁴, 1:10⁶, and 1:10⁸ ratios. Samples from each dilution were immediately plated on YM agar plates in triplicate, which were incubated at 27°C for 48 h. Plates having colony forming units (cfu) less than 30 and more than 300 were rejected. The total number of colony forming units per milliliter broth (cfu/ml) was calculated based on the dilutions performed. The results of sonication at two amplitudes (25% and 50%) are shown in Figure 4.6. Sonication at 75% amplitude produced more heat than what could be taken away by heat transfer in the ice bath. Hence samples taken at amplitude levels above 50% were not considered in this study. It is apparent that sonicating at 25% amplitude has a more detrimental effect than at an amplitude of 50%. This finding is contrary to a previously reported finding that ultrasonically-enhanced killing, or the 'bioacoustic effect', increases with increasing power density (Peterson and Pitt, 2000).

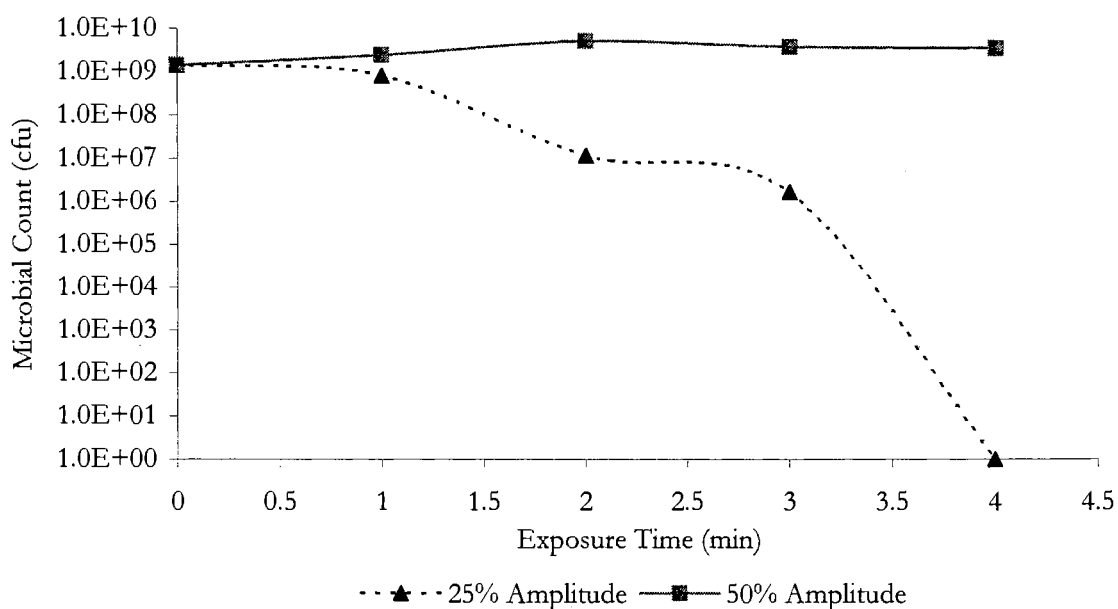


Figure 4.6 Effect of Sonication on viability of *X. campestris*

A possible reason for stable cfu counts at higher power intensity might be formation of standing waves during experimentation. It has been reported that living cells can respond differently to propagating and standing wave ultrasound of equal intensity (Radel, McLoughlin et al., 2000). Standing wave appears to be less damaging than propagating ultrasound. In another study of *Petunia hybrida* plant cell suspensions (Bohm, Anthony et al., 2000), the increased cell damage caused by propagating waves compared with standing waves was explained by their different spatial amplitude patterns and, consequently, the different spatial distribution of cells in the acoustic field. The decreased cell damage in standing wave fields is explained by the migration of the particles suspended in such a field to positions of low acoustic pressure and mechanical stress. The particles then remain in zones of low stress. By contrast, in a propagating wave field, the cells remain uniformly distributed in the fluid and experience a greater mean acoustic pressure.

It is important to note that the decrease in colony forming units does not necessarily mean that a drastic reduction in the number of live bacteria occurred. It is possible that with increased exposure to ultrasound, the bacteria might have gone into a dormant state. The cfu count is based on the ability of bacteria to grow vibrantly within 48h. Damaged or dormant cells take longer to recuperate or grow on agar plates.

4.2.2 EFFECT OF ULTRASOUND ON XANTHAN GUM QUALITY

The Size Exclusion Chromatography (SEC) chromatograms of the xanthan samples obtained from the control and intermittently sonicated (20% amplitude) fermentations are shown in Figure 4.7. The signals from the 90° light scattering (LS) and differential refractive index (DRI) detectors along with the values of RMS radius as a function of elution time are superimposed. Though only the 90° LS signal is shown, data from 15 LS detectors were used to calculate molar mass and RMS radius. Notice that the peaks given by the LS and concentration detectors are of different sizes and shapes. This is mainly due to the fact that the intensity of scattered light from the xanthan solution is proportional to both molar mass and concentration of the molecules eluting at any particular point. At the same time, the signals from the DRI detector are proportional only to the concentration of the molecules. For both samples, there are two main light scattering peaks at elution times of 12.5-14 minutes and 15-16 minutes, indicating the elution of the main xanthan molecular components. However, after the 15-minute mark, the DRI signal is weak, indicating the elution of components whose molar mass is high but concentration is low.

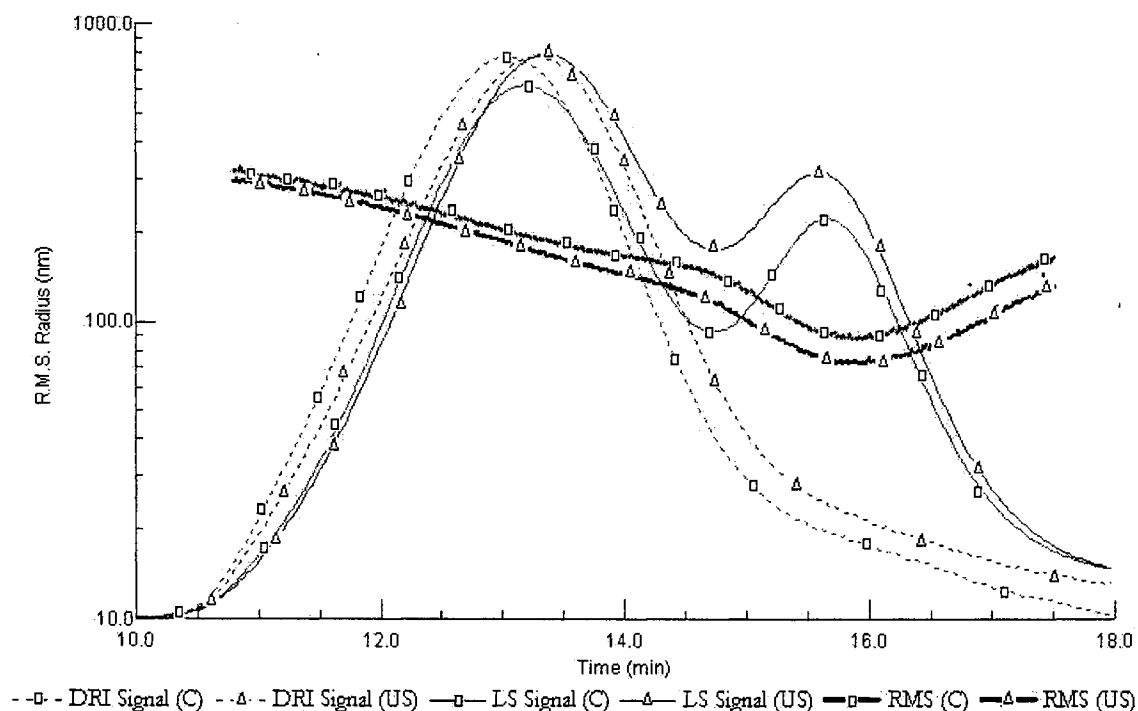


Figure 4.7 SEC Chromatograms of Xanthan Gum obtained from Control and Sonicated Fermentation

From the above figure it can be noted that the RMS radius of sonicated samples is slightly lower than non-sonicated xanthan samples. The calculated weight averaged molecular weight (M_w) of Xanthan produced from the sonicated run was $M_w 6.2 \pm 0.2 \times 10^6$ g/mol and number averaged molecular weight (M_n) was $5.6 \pm 0.1 \times 10^6$ g/mol. Whereas, the calculated weight averaged molecular weight (M_w) of xanthan produced from non-sonicated fermentation was $7.8 \pm 0.2 \times 10^6$ g/mol and number averaged molecular weight (M_n) was $7.3 \pm 0.1 \times 10^6$ g/mol. For comparison purposes, a commercial xanthan gum sample was also analyzed. The weight averaged molecular weight (M_w) of the commercial xanthan gum $3.8 \pm 0.3 \times 10^6$ g/mol and number averaged molecular weight (M_n) was $4.1 \pm 0.4 \times 10^6$ g/mol. It is a common knowledge that unless there is a change in order of magnitudes in the molecular weight, no significant change is observed in xanthan gum's physical or chemical property.

These results suggest that intermittent sonication at 20% amplitude during fermentation has no significant detrimental effect on the xanthan molecule.

4.3 DETERMINATION OF ULTRASONIC PROCESSING PARAMETERS

4.3.1 IDENTIFICATION OF SUITABLE VALUES OF XANTHAN GUM CONCENTRATION, FLOW RATE AND SONICATION AMPLITUDE

Since the molecular size of xanthan is critical in determining the quality of xanthan gum, a change in the molecular weight of xanthan can be used as a control parameter to determine acceptable levels of processing variables. Three variables -- xanthan concentration in solution, flow rate of the solution through the flow cell and the amplitude of sonication were identified as ultrasonic processing variables that might have an influence on the molecular weight of xanthan gum.

Xanthan gum contains a broad distribution of molecular sizes. In size-exclusion chromatography (SEC) the different molecules of xanthan gum of varying sizes show up as typically a broad peak (Figure 4.8), with the earlier-eluting species representing the high-molecular-weight species and the late-eluting species representing the low-molecular-weight species.

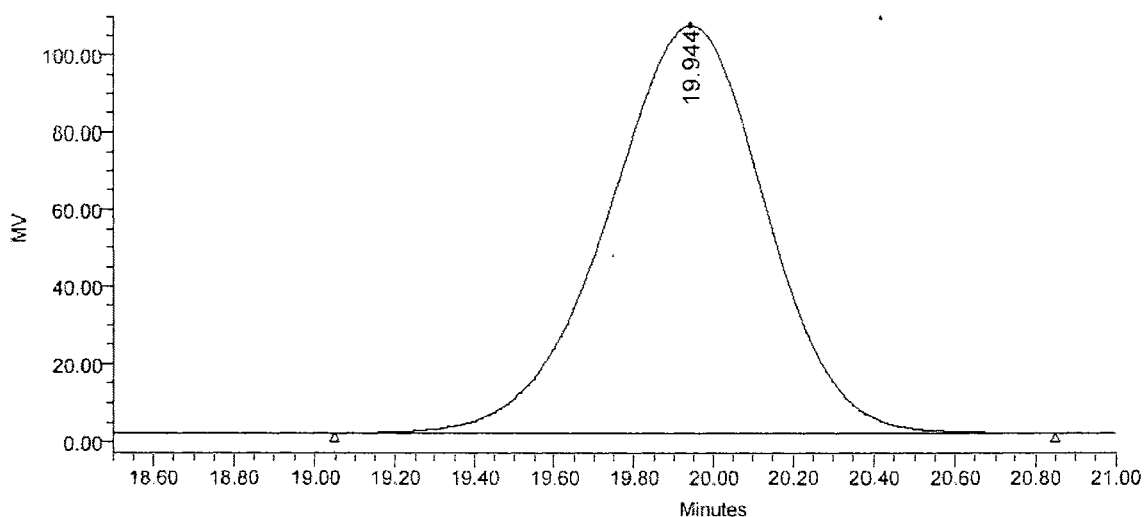


Figure 4.8 A Typical Size Exclusion Chromatogram of Xanthan Gum

Thus, SEC is suitable for comparing the effect of ultrasonic processing on xanthan gum molecular weight based on retention time. In general, the longer the retention time, the smaller the size of the molecule. To determine the effect of ultrasound on the xanthan molecule, 0.5, 1.0 and 1.5% (w/v) concentration solutions of xanthan gum were sonicated at 20, 35 and 50% amplitude in continuous flow mode. Three flow rates of 50 ml/min, 100 ml/min, and 150 ml/min were used. Samples were collected after 5 passes through the flow cell. Retention time was determined using HPLC as described in the materials and methods section. The three-factor full factorial design used for experimentation is shown in Table 4.1. and analysis of variance in Table 4.2. No interaction among the three factors was observed. To isolate which level(s) within the factors differed from the others, Tukey's multiple comparison procedure was used. The comparisons are given in Table 4.3. The differences in the mean values among the different levels of concentration show statistically significant difference ($p = 0.01$). It was found that the effect of

ultrasound on xanthan gum is similar at 1.0% and 1.5% concentration levels when compared to that at 0.5% level.

Concentration (%)	Flow Rate (ml/min)	Amplitude (%)	Retention Time (s)
0.5	50	20	1197.60
0.5	50	35	1197.48
0.5	50	50	1197.78
0.5	100	20	1197.78
0.5	100	35	1197.90
0.5	100	50	1198.50
0.5	150	20	1197.96
0.5	150	35	1197.78
0.5	150	50	1197.84
1	50	20	1197.84
1	50	35	1198.02
1	50	50	1198.14
1	100	20	1198.02
1	100	35	1198.08
1	100	50	1198.20
1	150	20	1198.08
1	150	35	1198.62
1	150	50	1198.80
1.5	50	20	1197.96
1.5	50	35	1198.08
1.5	50	50	1198.14
1.5	100	20	1198.14
1.5	100	35	1198.20
1.5	100	50	1198.08
1.5	150	20	1198.14
1.5	150	35	1198.20
1.5	150	50	1198.14

Table 4.1 Three Factor Full Factorial Design

Similarly, the differences in the mean values among the different levels of flow rate also show statistically significant difference ($p = 0.033$). There was statistically significant difference between samples pumped at 50 ml/min and 150 ml/min. However, the differences in the mean values among the different levels of amplitude do not show any statistically significant difference ($p = 0.08$).

Source of Variation	DF	SS	MS	F	P
Concentration	2	0.618	0.309	8.768	0.01
Flow Rate	2	0.379	0.19	5.385	0.033
Amplitude	2	0.248	0.124	3.523	0.08
Residual	8	0.282	0.0352		
Total	26	2.075	0.0798		

Equal Variance Test Passed: P = 1.000; Normality Test Passed: P=0.288

Table 4.2 Analysis of Variance

Comparisons	Difference of Means	p	q	P<0.05
Concentration				
1.0 vs 0.5	0.353	3	5.647	Yes
1.0 vs 1.5	0.08	3	1.279	No
1.5 vs 0.5	0.273	3	4.369	Yes
Flow Rate				
150 vs 50	0.28	3	4.475	Yes
150 vs 100	0.0733	3	1.172	No
100 vs 50	0.207	3	3.303	No
Amplitude				
50 vs 20	0.233	3	3.729	No
50 vs 35	0.14	3	2.238	No
35 vs 20	0.0933	3	1.492	No

Table 4.3 Comparison of Different Levels of Processing Parameters

Based on these results, a flow rate in the neighborhood of 100 ml/min seems to be the best choice. However, since there was no significant effect on the xanthan due to amplitude, the selection of level of the amplitude will depend on the effects noticed on biomass (discussed in the next section). Regarding concentration, it has been reported that polymers have been found to break-up more at lower concentrations than at higher. Though the results of this study also suggest differences at lower (0.5%) and higher concentrations (1.0% and 1.5%), from the mean value of the retention time it seems that xanthan gum breaks up more at higher concentration than at lower concentration.

4.3.2 IDENTIFICATION OF SUITABLE GROWTH PHASE DURING FERMENTATION FOR SONICATION

During the fermentation process, the broth will be sonicated in a recycle flow cell. As discussed in the residence time distribution study, in a continuous flow mode, the average exposure time is approximately 1.9 s at a flow rate of 100 ml/min. Experiments were conducted on broth at three different stages of bacterial growth – (a) immediately after the exponential growth phase, (b) during the stationary phase and (c) during the death phase. Broth samples, collected from a single fermentation run (to get comparable results), at the three different growth states were sonicated in a non-recycle continuous flow mode (single pass; flow rate = 100 ml/min) at amplitudes of 20%, 35% and 50%. These sonicated samples, along with a control (non-sonicated) sample, were then used as inoculum to further grow the bacteria in fresh production medium in shake flasks at 27°C at 200 rpm without pH control. The growth curves of sonicated inoculum over a 30 h period helped reveal comparative changes brought about by the single pass exposure to ultrasound. The growth curves were obtained from non-linear regression fit of the raw data to a 5 parameter sigmoid function:

$$y = y_o + \frac{a}{\left[1 + e^{-\left(\frac{x-x_o}{b} \right)} \right]^c}$$

where a , b , c , x_o , and y_o are the regression parameters. The xanthan production curves were obtained from a non-linear regression fit of the raw data to a 2 parameter single exponential rise to maximum function:

$$y = a(1 - e^{-bx})$$

where a and b are the regression parameters.

4.3.2.1 Effect of Sonication Immediately After Exponential Growth

The growth of *X. campestris* and production of xanthan gum after sonication immediately following the exponential growth phase are shown in Figure 4.9 and Figure 4.10 respectively.

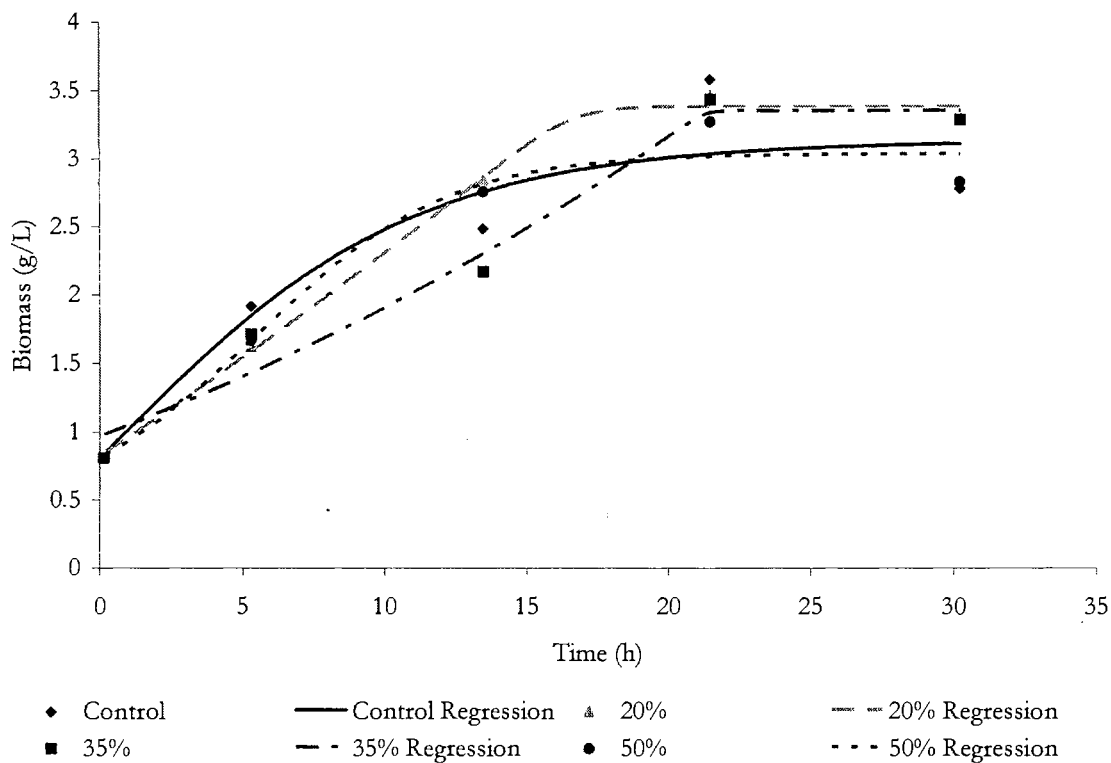


Figure 4.9 Growth Curve of Sonicated *X. campestris* Obtained Immediately After Exponential Growth

Bacteria exposed to 20% amplitude showed a linear increase in biomass throughout the exponential growth phase. Even though the initial growth rate was lower than the control, the linear nature of the growth phase indicates no growth inhibition due to substrate limitation. Bacterial culture exposed to 35% amplitude shows significant lag in growth and suggests damage to the cells at 35% amplitude. However, the bacteria seem to recover at a later stage and reach almost the same cell density as those subjected to 20% amplitude. At an

amplitude level of 50%, the bacteria act more like the control, with a minor lag in growth and show non-linear growth retardation (similar to control), due to a possible substrate limitation.

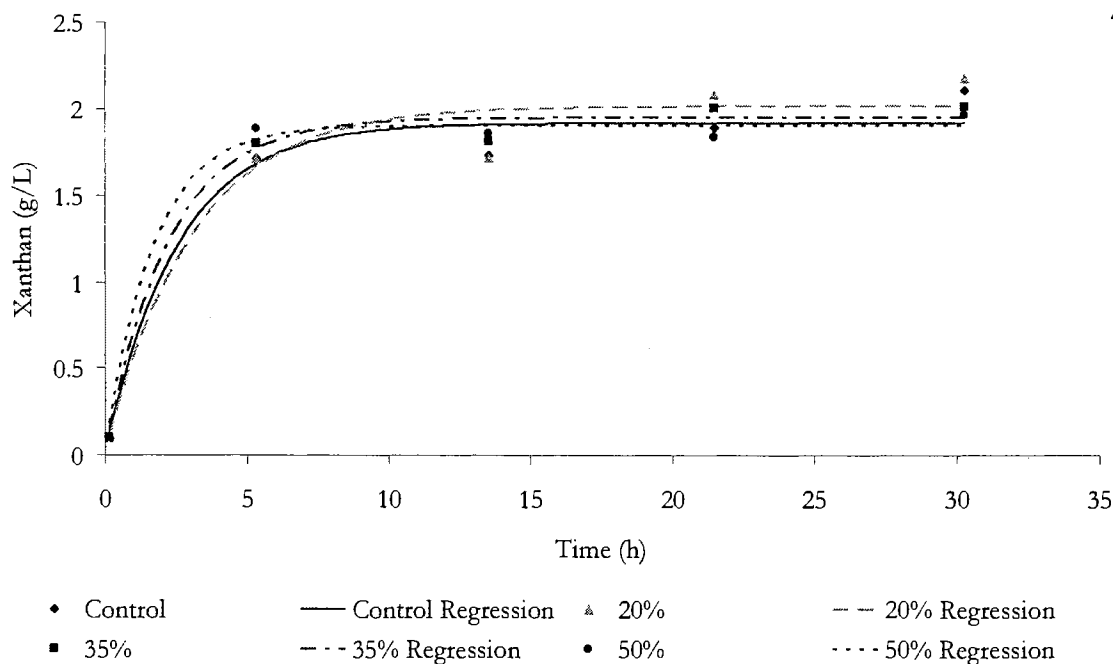


Figure 4.10 Xanthan Production by *X. campestris* Sonicated Immediately After Exponential Growth

While the xanthan production curves (Figure 4.10) are very similar for all amplitudes it appears that with increasing amplitude, the initial rate of xanthan production is higher. However, bacteria treated with lower amplitude levels tend to produce more xanthan at later stages of fermentation. The effect of ultrasonic treatment on xanthan production is evident for the first 6-8 h and that on biomass concentration for 15-20 h. Figure 4.11 shows the specific substrate consumption (per unit mass of biomass) and Figure 4.12 shows the specific xanthan gum production (per 100 g substrate consumed). The control sample's specific substrate consumption curve, during initial growth, shows increased substrate

utilization per gram of biomass produced and lower xanthan yield when compared to sonicated samples.

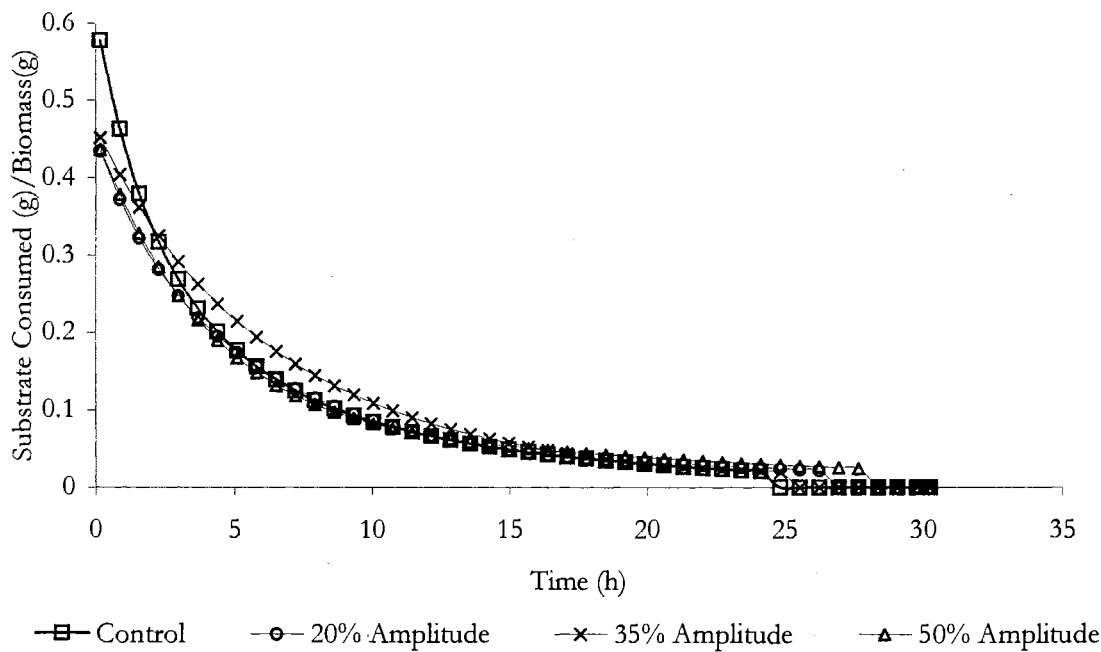


Figure 4.11 Specific Substrate Consumption Immediately After Exponential Growth

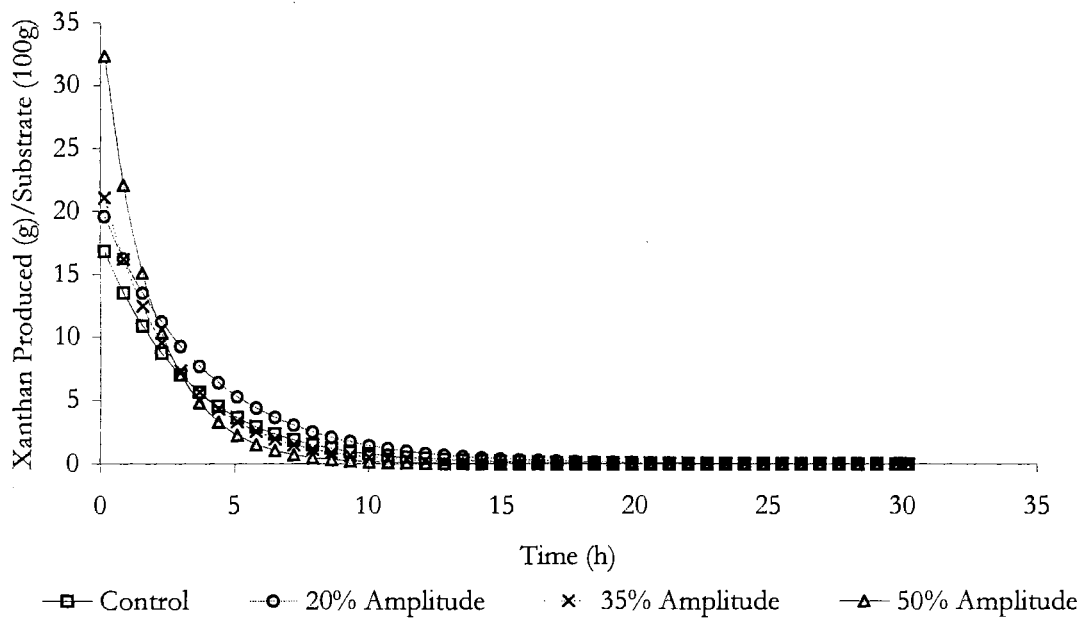


Figure 4.12 Specific Xanthan Production Immediately After Exponential Growth

This suggests a higher maintenance requirement (lower product conversion efficiency) for the control when compared to sonicated samples. After 3 h of fermentation, the sample subjected to 20% amplitude shows higher xanthan production efficiency than the other samples. The sample treated with 35% amplitude shows the least efficiency for product formation.

4.3.2.2 Effect of Sonication During Stationary Growth

The growth of *X. campestris* and production of xanthan gum after sonication during the stationary growth phase are shown in Figure 4.13 and Figure 4.14 respectively.

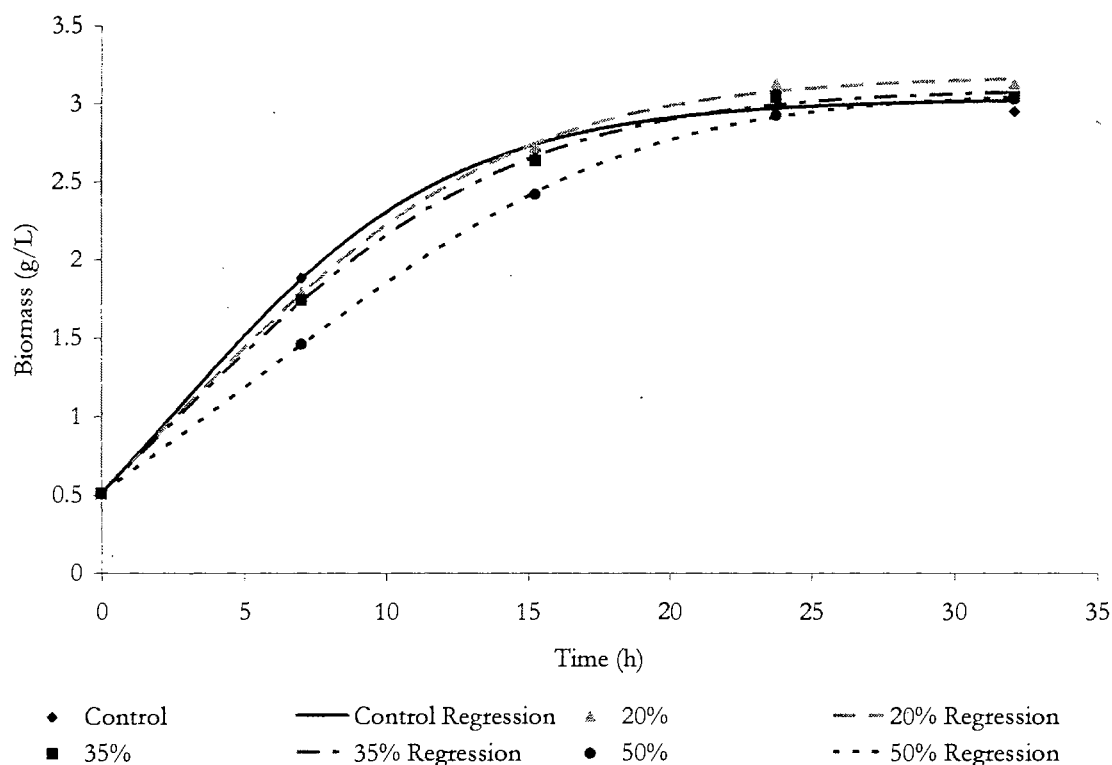


Figure 4.13 Growth Curve of *X. campestris* Sonicated During Stationary Growth

Figure 4.15 shows the specific substrate consumption (per unit mass of biomass) and the Figure 4.16 shows xanthan gum (P) production (per 100 g substrate consumed). The growth curves reveal a progressive reduction in growth rate as the sonication amplitude is increased. As was also noted in the growth curves for samples sonicated after the exponential phase, the initial rate of xanthan production is higher with increasing sonication amplitude. However, bacteria treated with lower amplitude levels tend to produce more xanthan at later stages (after about 10 h) of fermentation. From Figure 4.16 it can also be seen that once again, the sample treated at 20% amplitude shows the greatest xanthan production rate per 100 gm substrate consumed.

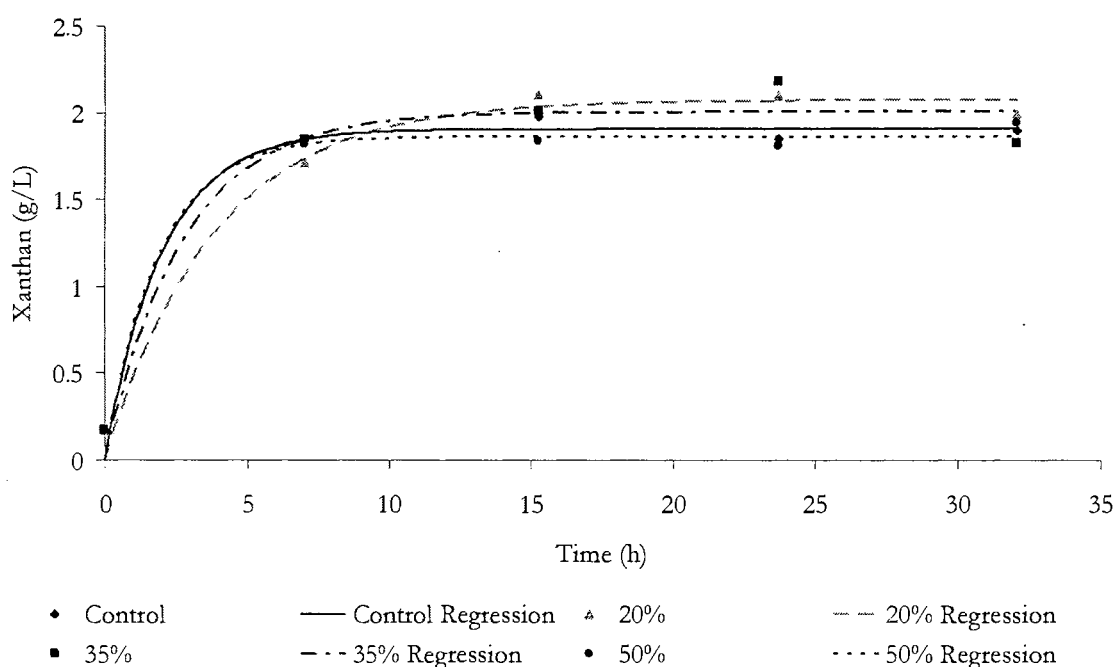


Figure 4.14 Xanthan Production by *X. campestris* Sonicated During Stationary Growth

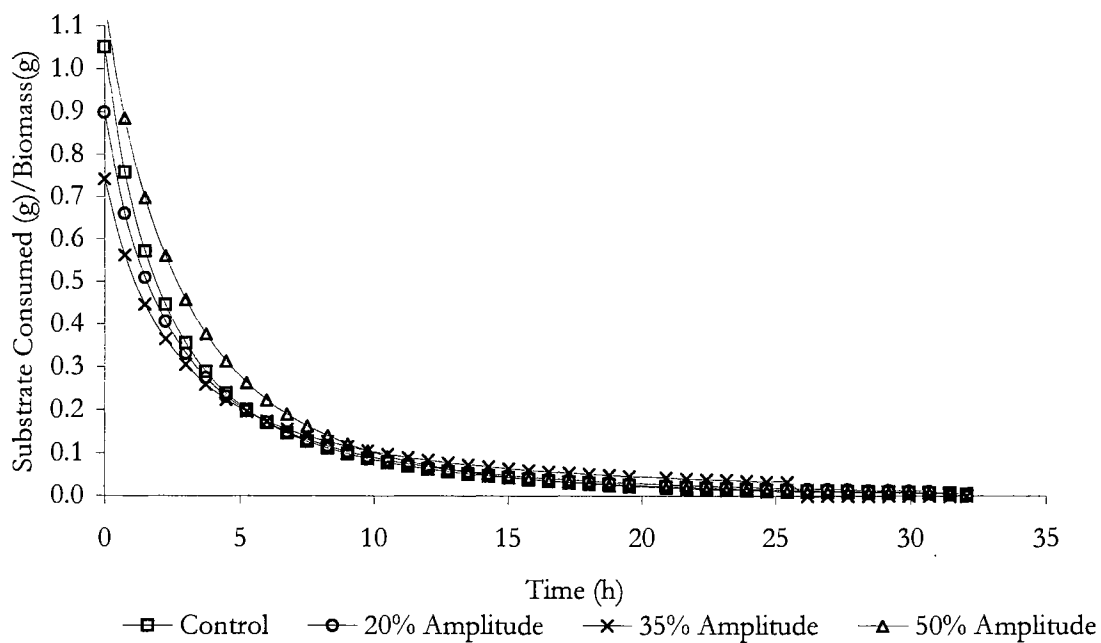


Figure 4.15 Specific Substrate Consumption by *X. campestris* Sonicated During Stationary Growth

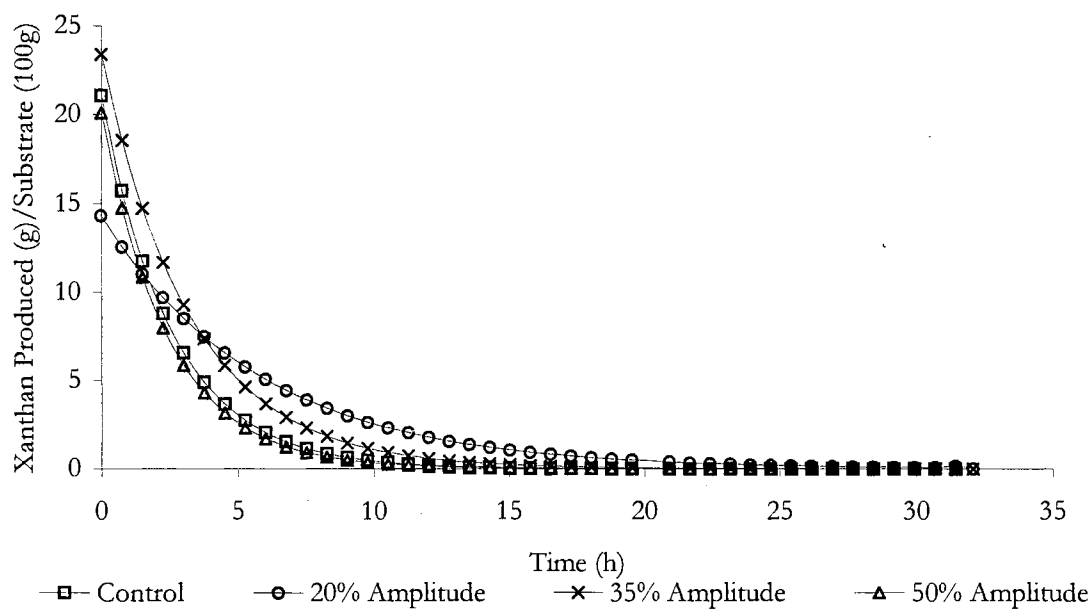


Figure 4.16 Xanthan Production by *X. campestris* Sonicated During Stationary Growth

4.3.2.3 Effect of Sonication During Death Phase

During the death phase, the bacteria are in a fragile state and are susceptible to physical damage. As expected, sonication during the death phase at all amplitudes showed slower growth than the control (Figure 4.17), implying damage to the cells due to sonication. Sonication at 20% amplitude appears to have caused less damage than the 35% and 50% amplitudes during death phase.

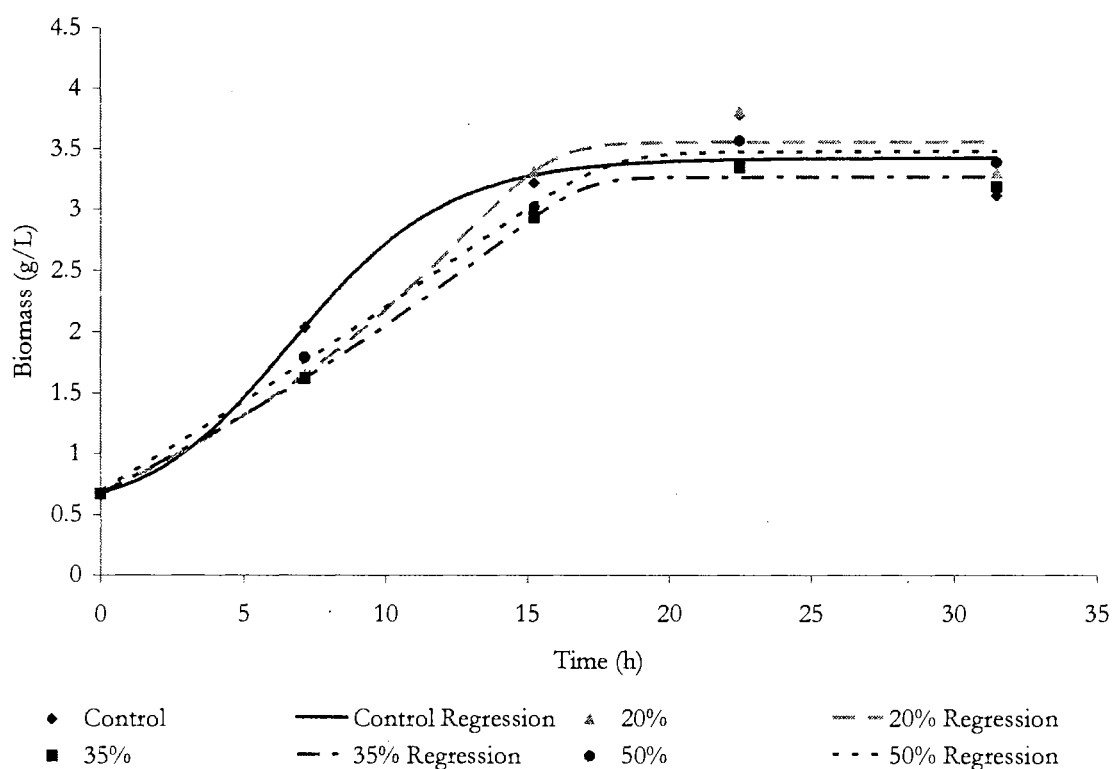


Figure 4.17 Growth Curve of *X. campestris* Sonicated During Death Phase

Figure 4.18 shows xanthan production for the bacterial culture treated with ultrasound during the death phase. At 20% amplitude, the xanthan production remains unchanged when compared to the control. Specific substrate consumption and xanthan production are shown in Figure 4.19 and Figure 4.20 respectively. These figures show no significant differences among the various treatments.

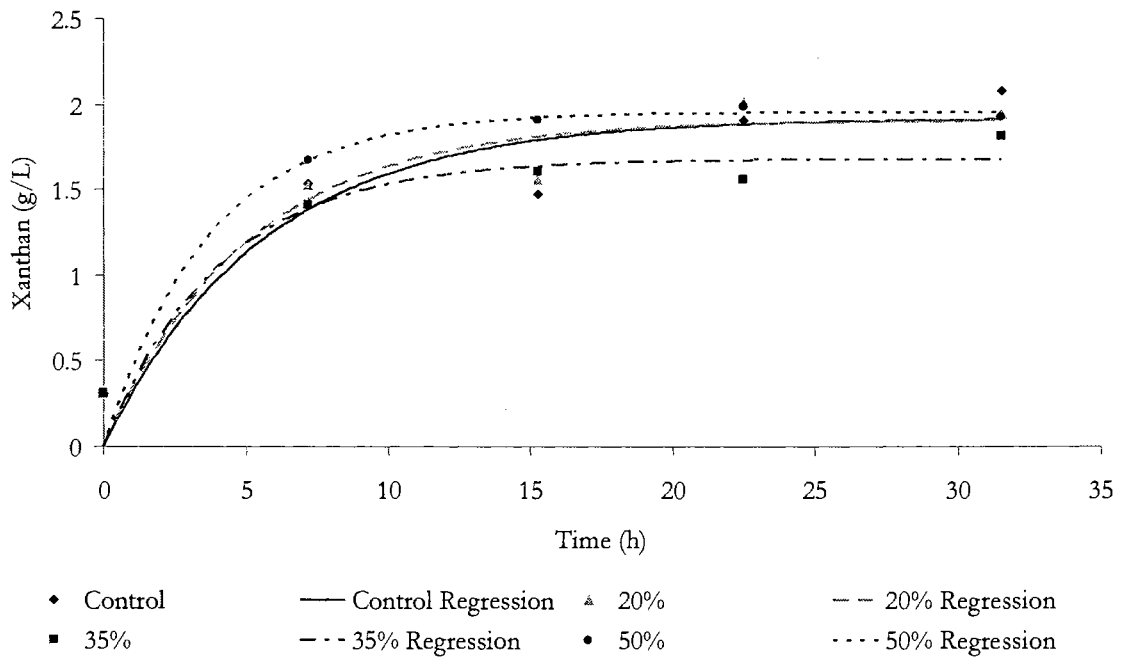


Figure 4.18 Xanthan Production by *X. campestris* Sonicated During Death Phase

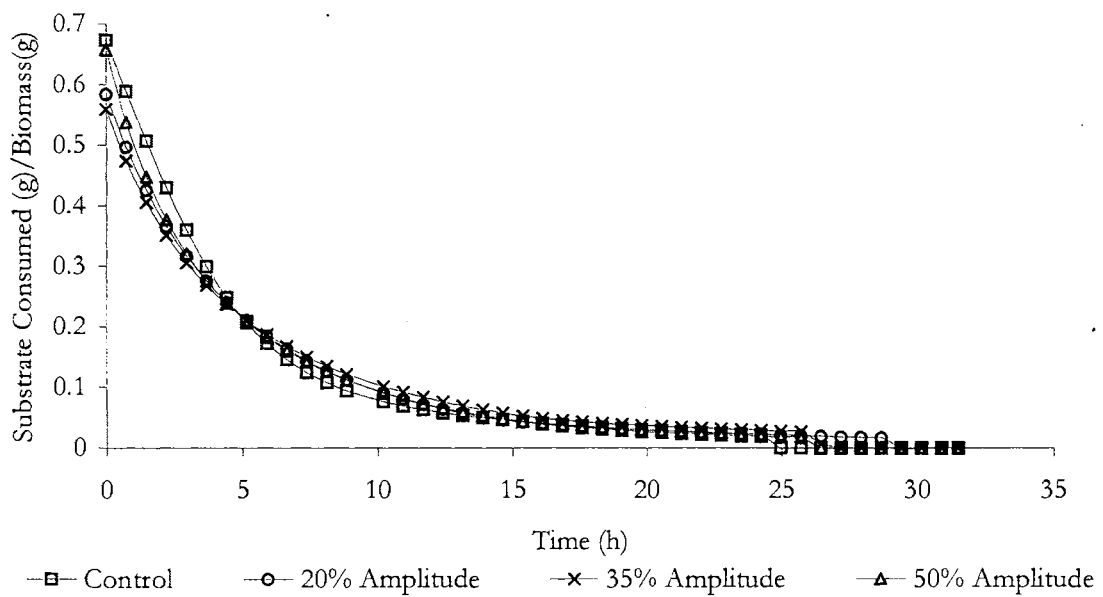


Figure 4.19 Specific Substrate Consumption by *X. campestris* Sonicated During Death Phase

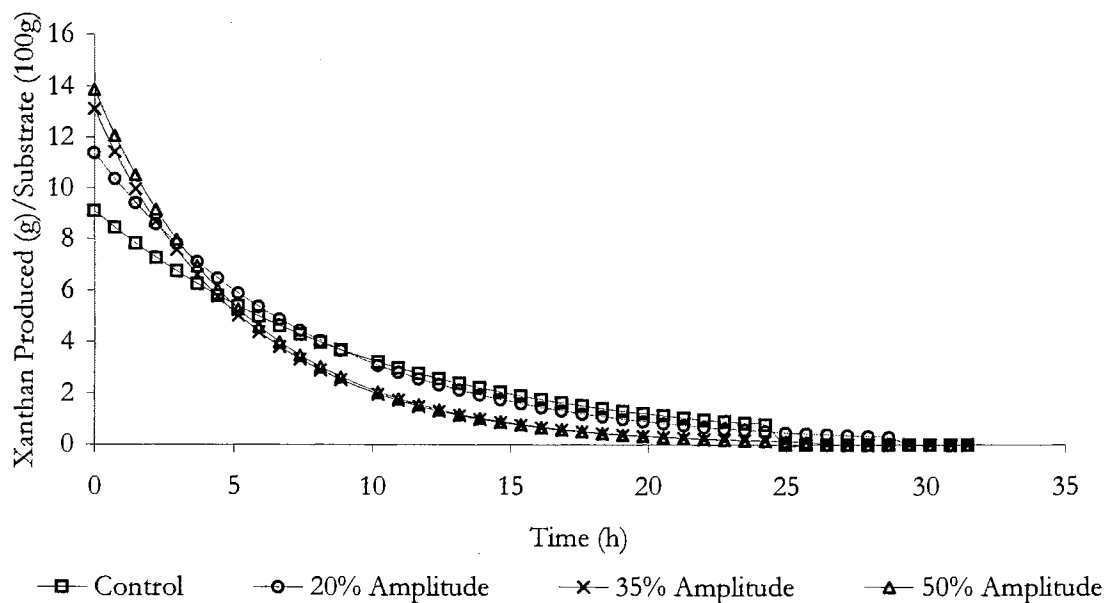


Figure 4.20 Xanthan Production by *X. campestris* Sonicated During Death Phase

4.3.3 CONCLUSION

The goal of this preliminary study was to help identify a suitable growth phase for sonication, and to determine the effect of amplitude of sonication. The amount of substrate consumed per gram of biomass was highest in samples exposed to sonication during the stationary growth phase when compared to the other growth phases. This is an indication of utilization of substrate for purposes other than biomass production during the stationary phase. The excess substrate consumed could be utilized for maintenance and product formation. The specific xanthan production per 100 g of substrate was low during the death phase and was comparable for samples exposed to sonication during the stationary and post-exponential growth phases. The death phase was not the optimum choice for sonication, leaving the other two phases as possibilities. To choose between these two phases, the

studies on xanthan quality can also be used. It was found that xanthan solution of 0.5% had a significantly different ultrasonic effect than 1.0% and 1.5% solutions. Since earlier researchers found that polymers were more likely to disintegrate at lower concentrations, we chose the 1.0% or 1.5% xanthan concentrations, which correspond with stationary growth phase. For these reasons, the stationary growth phase is the portion of the growth phase chosen for further sonication testing.

Also, in all the reported studies the 20% amplitude showed prolonged high xanthan productivity. Thus, sonication amplitude of 20% was selected for use in this investigation.

4.4 PRELIMINARY FERMENTATION STUDIES

4.4.1 TYPICAL XANTHAN FERMENTATION AND ITS CHARACTERISTICS

The various characteristics of the *Xanthomonas campestris* broth, including biomass concentration, xanthan production, and associated mass transfer, have a significant influence on the process. To understand and control the variations, preliminary fermentation runs of *Xanthomonas campestris* were carried out in 14 L bioreactors. After following standard laboratory procedures with respect to inoculum maintenance it was difficult to replicate the runs due to inherent variation in bacterial growth. Thus, an effort was made to improve and standardize the fermentation process for xanthan gum. The operational conditions being studied that needed standardization were agitator speed, airflow rate, batch size of the fermenter and concentration of acid and base. Biomass, glucose, dissolved oxygen and xanthan were measured in the employed experimental set-ups. A typical xanthan fermentation run is shown in Figure 4.21. The best results were obtained using 1-vvm

airflow rate and agitator speeds of 200-600 rpm (depending upon the volume of broth). The bioreactor could handle broth loads from 3.5 liters to 10 liters. If 3.5 – 6.0 L of broth was used, then the fermentation was started at 200 rpm and progressively increased to 600 rpm to maintain at least 20% dissolved oxygen in the broth. For volumes of 6.0 L and above, the agitator speed was maintained at a constant speed of 500 rpm throughout the duration of fermentation. During the initial stages of bacterial growth, the pH of the broth became progressively acidic. During this phase, addition of 5N NaOH to control the pH helped effectively compensate for evaporative moisture losses in the outlet gas. Once bacterial growth slows down and xanthan production begins, the pH of the broth starts shifting toward basic, and if not controlled can reach a pH of 8.5. For controlling the pH, 1N HCL was used. After 50 to 55 hours, the pH of the broth no longer has to be controlled.

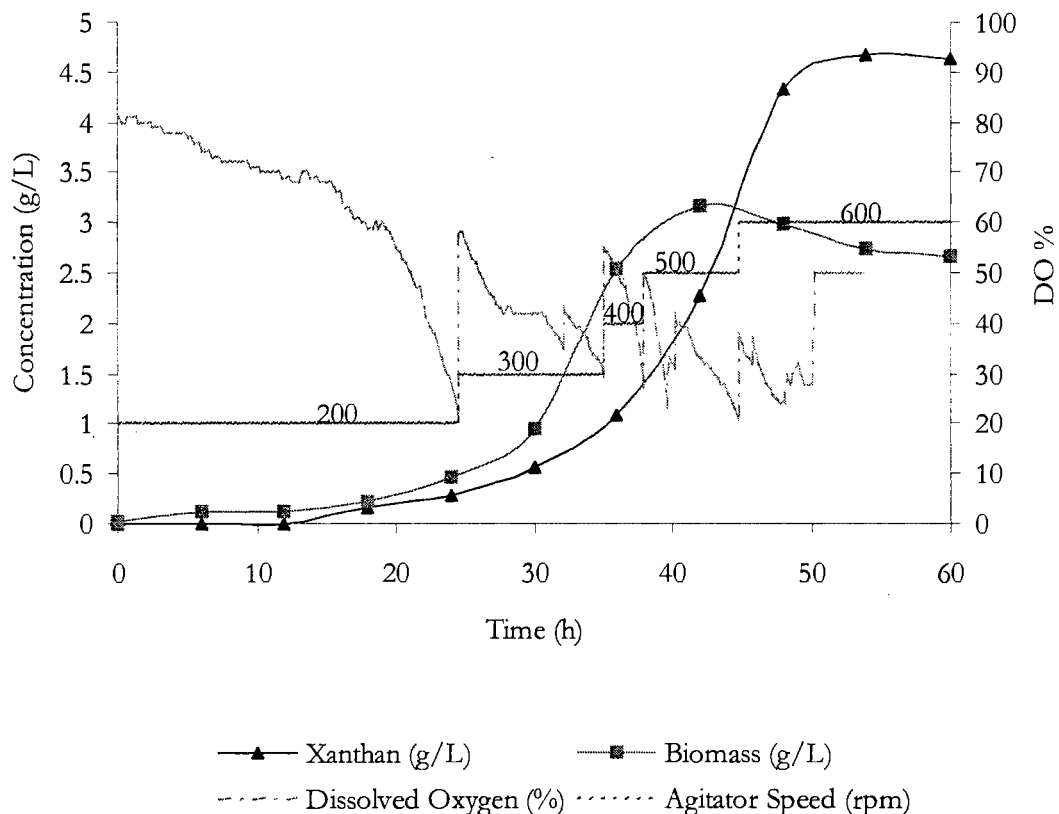


Figure 4.21 A Typical Xanthan Fermentation

Also, the oxygen requirement of the fermentation seems to peak during the logarithmic growth phase of the bacteria, as measured by an online oxygen analyser. This can also be concluded from the observation that the agitation speed had to be increased more frequently during this stage than any other period. The substrate (glucose) consumption curves observed for repeated runs revealed that by the end of the exponential growth phase (25-30 h), about 50% of the substrate in the medium is utilized. The remaining glucose is depleted by about 60 hours. Hence, for all the experiments conducted, only the first 60 h of data are shown and discussed.

4.4.2 EXPOSURE TO ULTRASOUND AFTER EXPONENTIAL GROWTH

To understand the effect of ultrasound in recycle mode, the fermentation broth was sonicated in a recycle loop connected to the fermenter. Due to this recycle loop, the behavior of the biomass in the fermenter is a reflection of both active and dormant bacteria. From studies discussed earlier it is clear that once sonicated, the bacteria have a residual effect over a period of time. If they are sonicated multiple times in a recycle loop then the complex behavior of the bacteria is difficult to predict as it has a carry over effect from an earlier ultrasonic dose.

To determine the upper limit of the recirculation interval that can be used for sonication of the fermentation broth, 20% amplitude was used immediately after the exponential growth phase and continued until the end of fermentation as shown in Figure 4.22. Sonication was applied intermittently in three stages while recycling the broth through the flow cell at a flow

rate of 400 ml/min (Volume in the fermenter = 4 L). The first ultrasonic treatment was 6 h in duration, the second 2.5 h, and the third was for 12 h. It seems that the first recycled sonication treatment caused a reduction in biomass, the second recycle treatment caused the biomass to grow and the third did not have any effect on the biomass density. Because of the reduction in biomass growth during the first ultrasonic treatment there was no xanthan production, indicating that the prolonged recycling had a negative impact on the bacteria. However, it is not clear if the second ultrasonic treatment actually caused an increase in biomass. The third treatment does not seem to affect the xanthan production. The rate of xanthan production remains the same, whereas the biomass density remains constant. Constant biomass density might be possibly due to limitation of substrate at the terminal stage of fermentation.

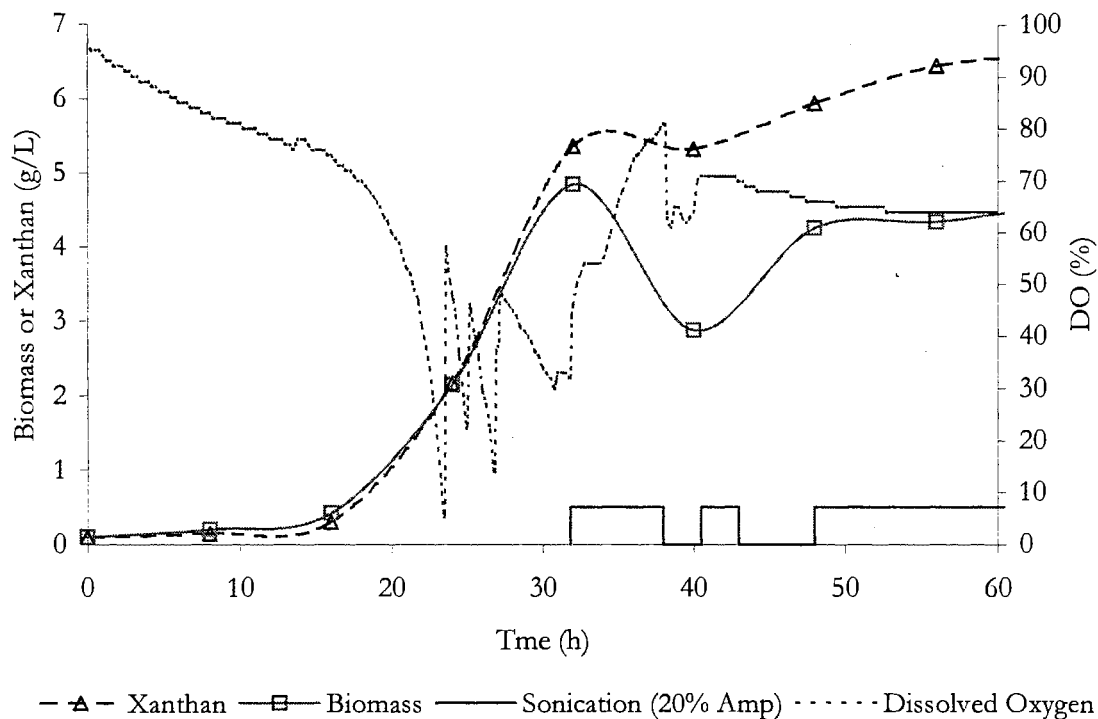


Figure 4.22 Xanthan Gum Fermentation with Prolonged Exposure to 20% Amplitude After Exponential Growth

Based on the results of the above experiment, another experiment was conducted with intermittent sonication with recycling. To better characterize the process two independent identical batch fermentations were run simultaneously. The inoculums of both the fermentation runs were drawn from the same mother culture. The intermittent ultrasonic treatments were each of 1 h duration, and 6-8 h apart, except the last treatment, which was of 4 h duration and 1.5 h from the previous treatment. On comparison with the control (Figure 4.23), it seems that only the first treatment, at the start of the stationary phase, had a major impact on the fermentation. It caused an increased rate of xanthan production (evident from the steeper xanthan production curve in comparison to the control). A feature that was common in prolonged sonication and the intermittent sonication was the re-growth of the bacterial culture after first phase of ultrasonic treatment.

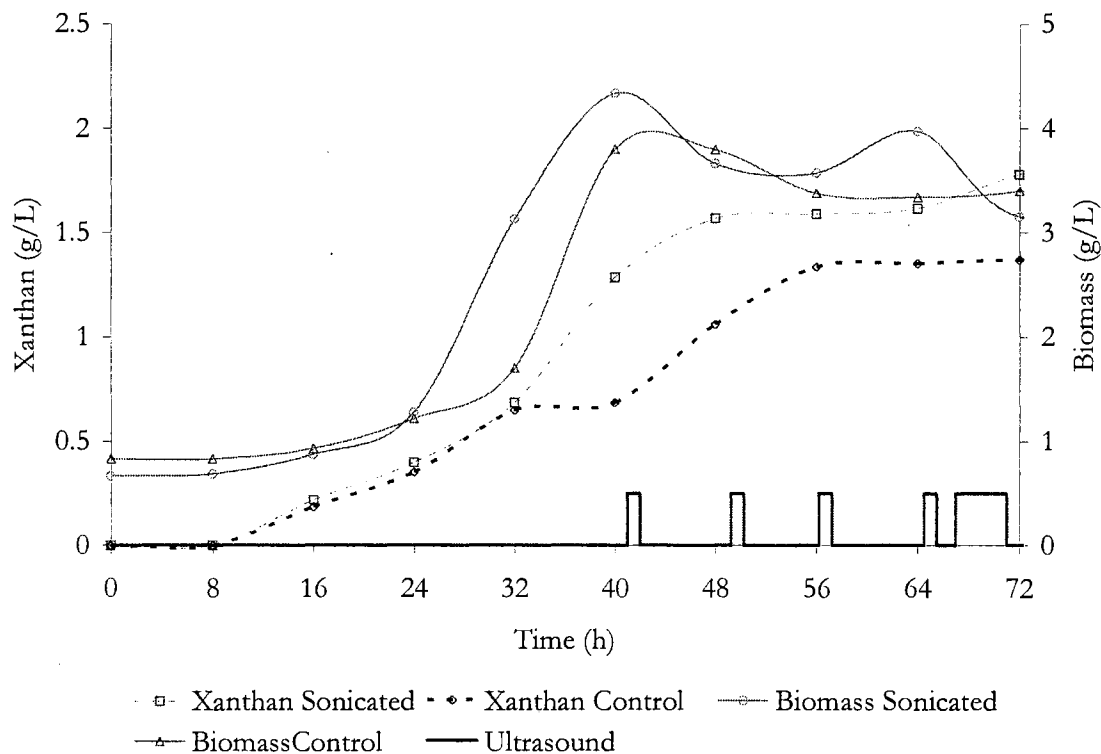


Figure 4.23 Intermittent Exposure to 20% Amplitude Ultrasound After Exponential Growth

4.5 SONICATED FERMENTATION

Based on the experiments discussed in previous sections, it was concluded that to achieve higher xanthan production, the time window during which ultrasonic treatment should be applied is after the exponential phase and before the mid-stationary phase. The duration of recycling through the ultrasonic flow-cell must be short. Two different sonicated fermentation schemes are described below. The first involved sonication in a continuous recycle flow-cell for a short duration (1.5 – 2 h). The second involved intermittent sonication within a period of 15 – 18 h after the completion of exponential growth phase. The flow rate was maintained at 100 ± 20 ml/min. The broth volume in all the runs was 4 L.

4.5.1 SINGLE DOSE SONICATION

Single dose sonication at an amplitude of 20% immediately after the exponential growth phase is shown in Figure 4.24. This treatment seemed to retard biomass growth although the retardation in biomass growth diverts the substrate utilization towards increased xanthan production. Due to retarded biomass growth, the broth has higher substrate levels than the control. This higher xanthan production rate is sustainable only temporarily. The xanthan production rate slows down, as it becomes a function of reduced biomass concentration. It takes about 10-12 h for the bacteria to recover, during which there is no more xanthan production. After the recovery, rest of the substrate is utilized for biomass growth rather than xanthan production. Hence eventually, the sonicated fermentation ends-up less efficient than the non-sonicated control. From this experiment it is evident that sonication must be milder. Thus, another single dose sonication experiment was conducted during the stationary phase (Figure 4.25).

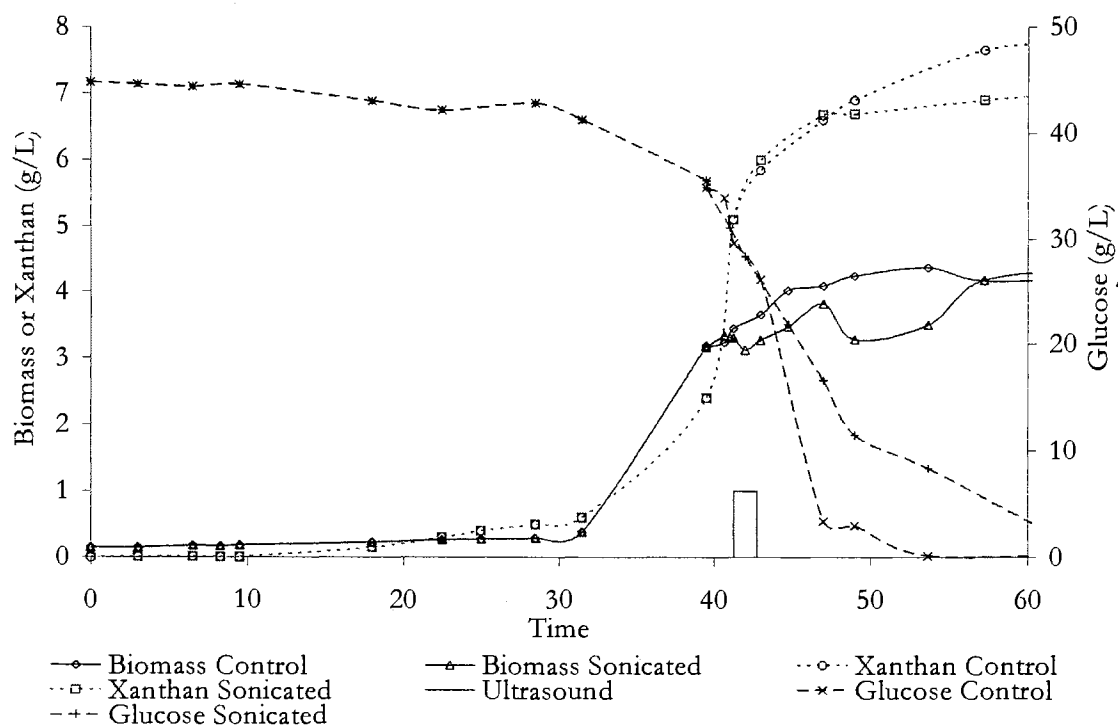


Figure 4.24 Single Dose Sonication Immediately after Exponential Growth Phase

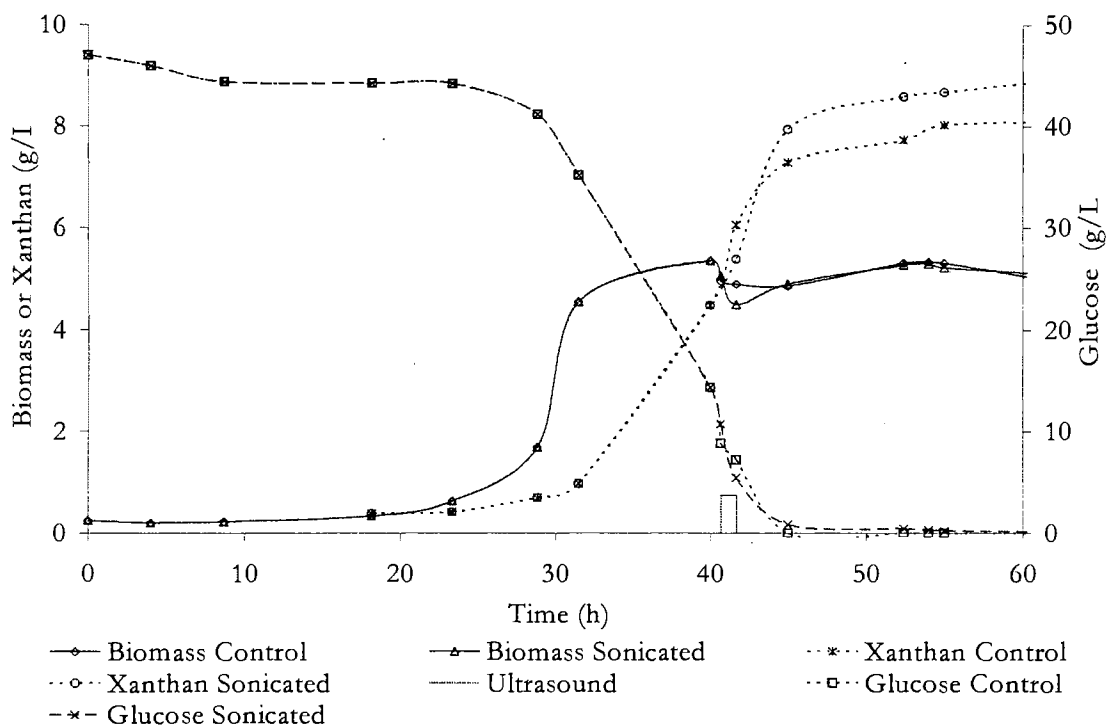


Figure 4.25 Single Dose Sonication during Stationary Phase

In this experiment though increased xanthan production is noticed, there is no significant bacterial growth retardation. Due to the initial jump in xanthan production the sonicated fermentation gives higher xanthan production than the control.

4.5.2 INTERMITTENT DOSE SONICATION

Two types of intermittent dose sonication experiments differing in the frequency of recycle treatment and the length of each recycle dose were performed. The experiment with higher treatment frequency (sonication at intervals of 6 h), is shown in Figure 4.26. It appears that the biomass does not get an opportunity to regrow between the high frequency treatments.

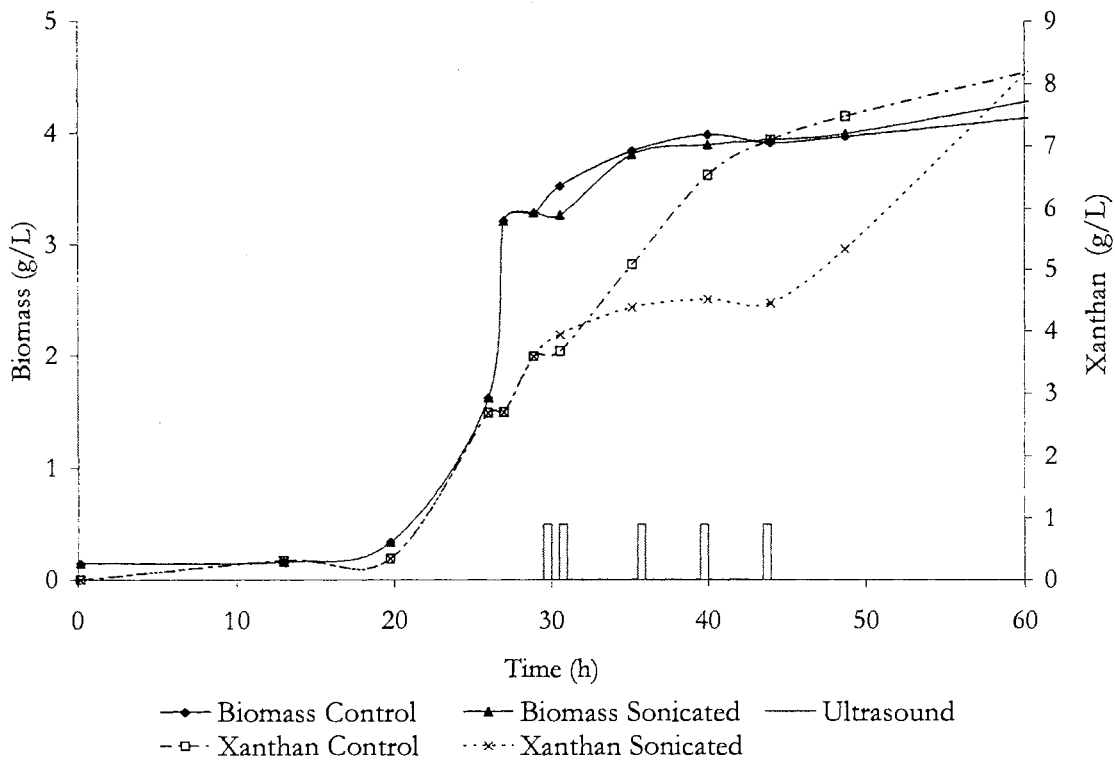


Figure 4.26 Intermittent Dose Sonication with Shorter and Frequent Treatments

After the ultrasonic treatments are stopped, the fermentation proceeds with a higher than usual rate of xanthan production. The linear biomass and xanthan production curves toward the end of fermentation imply that the bacterium does not encounter mass transfer resistance. The fermentations result in equal xanthan production, with or without sonication. However, due to sonication and prolonged stunted growth of the bacteria in the sonicated fermenter, the quality of xanthan gum from the sonicated fermenter is slightly poorer than that obtained from the control. A comparison of the xanthan gum quality from these two fermenters has been discussed in section 4.2.2.

The second sonicated multiple-dose experiment with occasional ultrasonic treatment is shown in Figure 4.27.

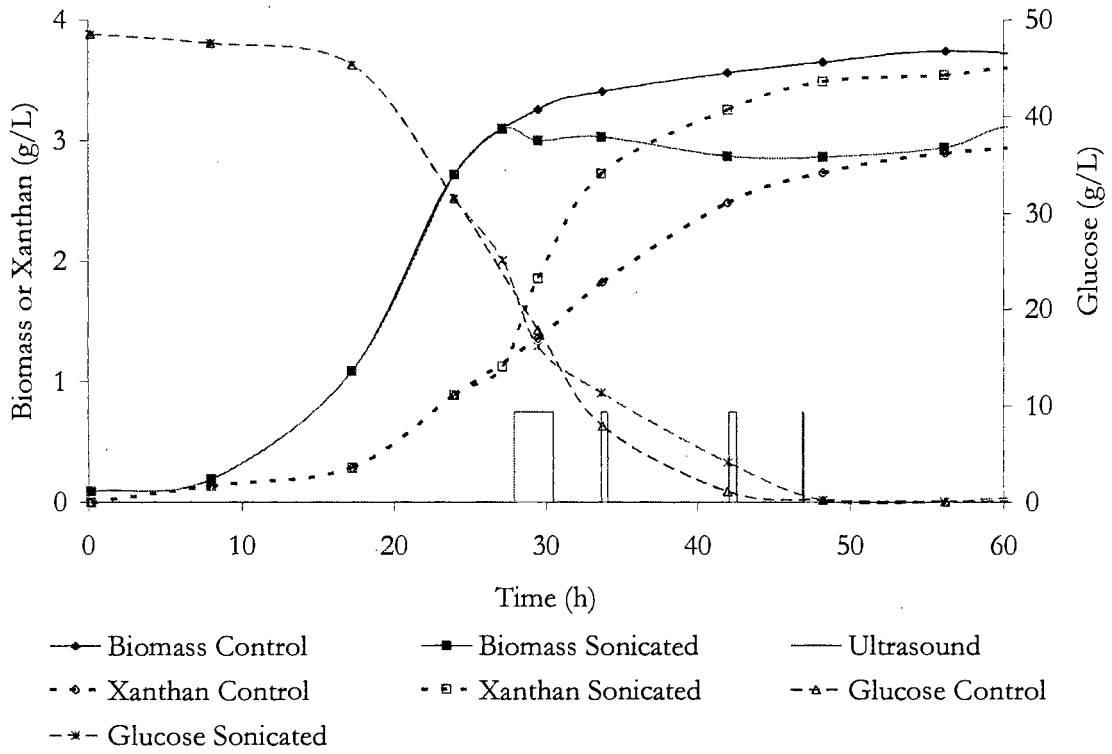


Figure 4.27 Intermittent Dose Sonication with Occasional Treatments

Ultrasonic treatments were applied in four doses (1st for 3h; 2nd for 0.5h; 3rd for 0.5h; and 4th for 0.1h) with three different time intervals between treatments (1st interval for 3h; 2nd interval for 8h; and 3rd interval for 4h). The flow rate and the volume of the fermenter were the same as in earlier experiments. During the application of the first dose, the results show that biomass concentration in the sonicated broth seems to drop off slightly, while xanthan production increases. This shows that the energy from the substrate is being diverted towards the production of xanthan, which is obvious from the steep rise in xanthan concentration. The second ultrasonic treatment seems to retard biomass concentration a little bit but has no significant effect on the rate of xanthan production. The third and fourth ultrasonic treatments have no effect on the fermentation. The rates of xanthan formation and biomass growth are similar to control. Thus it is concluded that one or two ultrasonic doses, with the first one longer than the second, applied early in the stationary growth phase are best to enhance xanthan production.

4.6 OXYGEN UPTAKE RATE DURING SONICATION

Oxygen uptake rate (OUR) was determined by measuring dissolved oxygen (DO) concentration in the fermenter and in the recycle pipeline as described in the materials and methods chapter. A typical dissolved oxygen profile is shown in Figure 4.28. The rate of increase in oxygen uptake rate with growth phase is shown in Figure 4.29. In the example depicted in Figure 4.28, the sonication was started at 35.5 h and stopped at 36 h (mid-stationary growth phase). A probable cause of the rise in DO level in the fermenter might be the microbubbles formed during sonication. As soon as these microbubbles enter the fermenter, diffusion of oxygen into these bubbles and consequent increased oxygen transfer to the fermentation broth due to increased surface area, might cause the rise in DO level.

The most likely reason for the drop in DO level in the recycle pipeline could be the increased oxygen consumption by the bacteria.

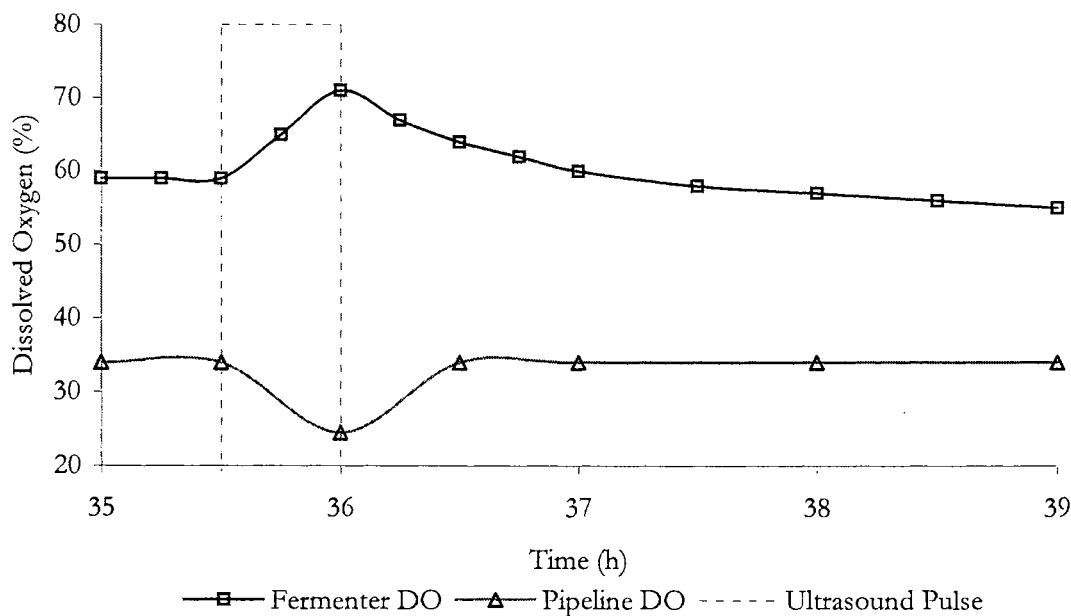


Figure 4.28 Dissolved Oxygen Profiles in Fermenter and Recycle Pipeline after Sonication

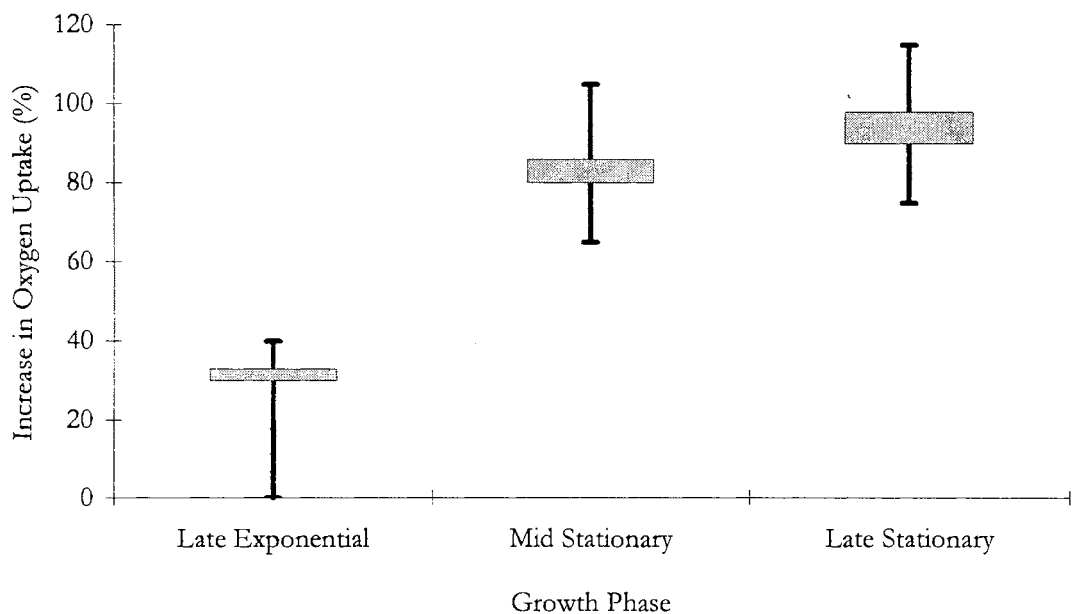


Figure 4.29 Increase in Oxygen Uptake Rate due to Sonication During Various Growth Phases

Intermittent sonication in recycle pipeline showed that sonication had a variable effect on the change in oxygen uptake rate. As the fermentation progressed, sonication seemed to increase the oxygen uptake rate nonlinearly. Immediately after exponential growth, on average sonication helped increase oxygen uptake rate by 27% and this increase was usually in the range of 22 to 32%. During the mid-stationary growth phase, on average oxygen uptake rate increased by 85% and during the late-stationary growth phase the average increase was found to be 95%. The range of increase in oxygen uptake rate for mid- and late-stationary growth phase were 68-102% and 76-114% respectively.

5 Conclusions

Results of this study suggest that appropriate ultrasonic treatment can improve xanthan gum production. The following are the conclusions:

- i. Sonication at amplitudes above 50% (corresponding to 5 kW/L) is not feasible due to excessive heat production. Viscous solutions tend to absorb more energy than non-viscous solutions.
- ii. Though the average residence time in the flow cell was determined to be dependent on the amplitude level, it has little to do with the actual ultrasonic exposure time (which is primarily calculated based on the volume of liquid under the probe exposed to the ultrasonic field and the flow rate of the liquid through the flow cell). At a flow rate of 100 ml/min the actual exposure time was determined to be 1.9 s.
- iii. Due to intermittent sonication, there was no significant change in molecular weight of the xanthan gum molecule. The weight average molecular weight (M_w) of xanthan produced by sonication was $6.2 \pm 0.2 \times 10^6$ g/mol, whereas that of xanthan produced from non-sonicated fermentation was $7.8 \pm 0.2 \times 10^6$ g/mol. Because the difference in the molecular weights of the samples is not in the order of magnitudes, it is concluded that sonication at power level of approximately 1 to 1.5 kW/L with a total residence time of approximately 15 to 20 seconds does not have a significant effect on the physical properties of xanthan gum.

- iv. Xanthan production is dependent on the specific power used during sonication. Power levels between 1 to 1.5 kW/L (corresponding to 20% amplitude) were found to be more suitable than those between 2 to 5 kW/L (corresponding to 35% and 50% amplitudes).
- v. A best time period to sonicate the fermentation broth is after exponential growth phase and before the mid-stationary growth phase.
- vi. Depending upon the acceptable final quality of xanthan, sonication can be either done intermittently or as a single pulse of short duration. Intermittent sonication improved xanthan production by 22% whereas single short dose sonication improved xanthan production by 12%. Continuous sonication does not seem to improve xanthan yield.
- vii. Oxygen uptake rate increased upon sonication by 22 to 114% depending upon the growth state and viscosity of the broth.

6 Future Research

Application of ultrasound to improve yield of biotechnological processes is a fairly new concept and needs further research. An unexpected result in this study was that in a batch system, ultrasound at 20 kHz and 50% amplitude had minimal impact on the viability of bacteria; however, ultrasound at 20% amplitude caused 3 log reductions in viability of bacteria after 3 minutes of continuous sonication. Though this phenomenon can be explained by past research involving stationary waves (Radel, McLoughlin et al., 2000), a method to validate such findings needs to be developed.

During this study it was felt that if the entire volume of the fermenter could be sonicated all at once, it could provide more flexibility in understanding and controlling the process. The effect due to ultrasound seemed to be more due to biochemical changes within the bacteria than mass transfer effects. To achieve an increase in xanthan productivity the control of the quality of energy delivered is critical. The ability to sonicate the whole fermenter will offer more advantages in terms of ability to beneficially exploit the narrow time-window during the stationary phase.

The most critical factor that can aid in faster development and adoption of ultrasonic treatment is the design of new ultrasonic equipment for the biotechnology industry. Currently the equipment used for application of ultrasound in biotechnological research is adapted from the chemical industry. Such equipment does not take into consideration that

living systems cannot survive extreme localized conditions. There is a need for new ultrasonic equipment that delivers the required sonic input with more uniform distribution of energy. For instance, equipment similar to a plate heat exchanger can be fabricated which has alternate vibratory plates. Each of these alternate vibratory plates can have attachments, which deliver ultrasonic energy to the fermentation media in the annular space. The major advantage of such a system will be the even distribution of ultrasonic energy. Also such a system will be easier to control the quality of ultrasonic energy.

7 Bibliography

- Amanullah, A., S. Satti, et al. (1998). "Enhancing Xanthan fermentations by different modes of glucose feeding." *Biotechnology Progress* **14**(2): 265-269.
- Amanullah, A., B. Tuttiett, et al. (1998). "Agitator speed and dissolved oxygen effects in Xanthan fermentations." *Biotechnology and Bioengineering* **57**(2): 198-210.
- Bar, R. (1988). "Ultrasound enhanced bioprocesses: Cholesterol oxidation by *Rhodococcus erythropolis*." *Biotechnology and Bioengineering* **32**(5): 655-663.
- Bohm, H., P. Anthony, et al. (2000). "Viability of plant cell suspensions exposed to homogeneous ultrasonic fields of different energy density and wave type." *Ultrasonics* **38**(1-8): 629-632.
- Born, K., V. Langendorff, et al. (2001). "Xanthan". *Polysaccharides I: Polysaccharides from Prokaryotes*. A. Steinbüchel, Wiley-VCH. **5**: 259-291.
- Bujons, J., R. Guajardo, et al. (1988). "Enantioselective Enzymatic Sterol Synthesis by Ultrasonically Stimulated Bakers' Yeast ." *Journal of the American Chemical Society* **110**(2): 604-606.

- Chisti, Y. (1999). "Mass transfer". *Encyclopedia of Bioprocess Technology: Fermentation, Biocatalysis, and Bioseparation*. S. W. Drew, John Wiley. **3**: 1607–1640.
- Chisti, Y. (2000). "Animal-cell damage in sparged bioreactors." *Trends in Biotechnology* **18**(10): 420-432.
- Chisti, Y. (2001). "Hydrodynamic Damage to Animal Cells." *Critical Reviews in Biotechnology* **21**(2): 67-110.
- Chisti, Y. (2003). "Sonobioreactors: using ultrasound for enhanced microbial productivity." *Trends in Biotechnology* **21**(2): 89-93.
- Chisti, Y. and M. Moo-Young (1986). "Disruption of microbial cells for intracellular products." *Enzyme and Microbial Technology* **8**(4): 194-204.
- Chisti, Y. and M. Moo-Young (2002). "Bioreactors". *Encyclopedia of Physical Science and Technology*. R. A. Meyers, Academic Press. **2**: 247–271.
- Christensen, B. E., M. H. Myhr, et al. (1996). "Degradation of double-stranded xanthan by hydrogen peroxide in the presence of ferrous ions: Comparison to acid hydrolysis." *Carbohydrate Research* **280**(1): 85-99.
- Chu, J., B. L. Li, et al. (2000). "On-line ultrasound stimulates the secretion and production of gentamicin by *Micromonospora echinospora*." *Process Biochemistry* **35**(6): 569-572.

- Contamine, F., F. Faid, et al. (1994). "Chemical reactions under ultrasound: discrimination of chemical and physical effects." *Chemical Engineering Science* **49**(24B): 5865-5873.
- Dakubu, S. (1976). "Cell inactivation by ultrasound." *Biotechnology and Bioengineering* **18**(4): 465-471.
- Flint, E. B. and K. S. Suslick (1991). "The Temperature of Cavitation." *Science* **253**(5026): 1397-1399.
- Francko, D. A., S. Al-Hamdani, et al. (1994). "Enhancement of nitrogen fixation in *Anabaena flos-aquae* (Cyanobacteria) via low-dose ultrasonic treatment." *Journal of Applied Phycology* **6**(5-6): 455-458.
- Francko, D. A., S. R. Taylor, et al. (1990). "Effect of low-dose ultrasonic treatment on physiological variables in *Anabaena flos-aquae* and *Selenastrum capricornutum*." *Biotechnology Letters* **12**(3): 219-224.
- Funahashi, H., M. Maehara, et al. (1987). "Effects of Agitation by Flat-Bladed Turbine Impeller on Microbial-Production of Xanthan Gum." *Journal of Chemical Engineering of Japan* **20**(1): 16-22.
- Galindo, E. and G. Salcedo (1996). "Detergents improve xanthan yield and polymer quality in cultures of *Xanthomonas campestris*." *Enzyme and Microbial Technology* **19**(2): 145-149.

- Garcia-Ochoa, F., E. G. Castro, et al. (2000). "Oxygen transfer and uptake rates during xanthan gum production." *Enzyme and Microbial Technology* **27**(9): 680-690.
- GarciaOchoa, F., V. E. Santos, et al. (1997). "Xanthan gum production in a laboratory aerated stirred tank bioreactor." *Chemical and Biochemical Engineering Quarterly* **11**(2): 69-74.
- Gillot, S. and A. Heduit (2000). "Effect of air flow rate on oxygen transfer in an oxidation ditch equipped with fine bubble diffusers and slow speed mixers." *Water Research* **34**(5): 1756-1762.
- Gutierrez, M. and A. Henglein (1990). "Chemical action of pulsed ultrasound: observation of an unprecedented intensity effect." *Journal of Physical Chemistry* **94**(9): 3625-3628.
- Holzwarth, G. (1978). "Molecular weight of xanthan polysaccharide." *Carbohydrate Research* **66**(1): 173-186.
- J.B. Hubbard, E. J. C., J.M.H. Levelt Sengers (1990). *A survey of selected topics relevant to bioprocess engineering [microform]*, Gaithersburg, MD : U.S. Dept. of Commerce, National Institute of Standards and Technology.
- Jana, A. K. and P. Ghosh (1997). "Stimulation of xanthan production by *Xanthomonas campestris* using citric acid." *World Journal of Microbiology & Biotechnology* **13**(3): 261-264.
- Ju, L.-K. and W. B. Armiger (1990). "Enhancing oxygen transfer in surface-aerated bioreactors by stable foams." *Biotechnology Progress* **6**(4): 262-265.

- Ju, L.-K., J. F. Lee, et al. (1991). "Enhancing oxygen transfer in bioreactors by perfluorocarbon emulsions." *Biotechnology Progress* **7**(4): 323-329.
- Junker, B. H., T. A. Hatton, et al. (1990). "Oxygen transfer enhancement in aqueous/perfluorocarbon fermentation systems. I. Experimental observations." *Biotechnology and Bioengineering* **35**(6): 578-585.
- Kessler, W. R., M. K. Popovic, et al. (1993). "Xanthan Production in an External Circulation Loop Airlift Fermenter." *Canadian Journal of Chemical Engineering* **71**(1): 101-106.
- Kilby, N. J. and C. S. Hunter (1990). "Repeated harvest of vacuole-located secondary product from in vitro grown plant cells using 1.02 MHz ultrasound." *Applied Microbiology and Biotechnology*. **33**(4): 448-451.
- Leighton, T. G. (1994). *The Acoustic Bubble*. London, Academic.
- Lin, L. and J. Wu (2002). "Enhancement of shikonin production in single- and two-phase suspension cultures of *Lithospermum erythrorhizon* cells using low-energy ultrasound." *Biotechnology and Bioengineering* **78**(1): 81-88.
- Lin, L., J. Wu, et al. (2001). "Ultrasound-induced physiological effects and secondary metabolite (saponin) production in *Panax ginseng* cell cultures." *Ultrasound in Medicine & Biology* **27**(8): 1147-1152.

- Matsuura, K., M. Hirotsune, et al. (1994). "Acceleration of cell growth and ester formation by ultrasonic wave irradiation." *Journal of Fermentation and Bioengineering* **77**(1): 36-40.
- Mermillod-Blondin, F., G. Fauvet, et al. (2001). "A comparison of two ultrasonic methods for detaching biofilms from natural substrata." *International Review of Hydrobiology* **86**(3): 349-360.
- Michelsen, D. L. L., Mehran;Velandar, William H.;Mann, James W.;Khalichi, Peyman (1991). "Oxygen mass transfer to flowing ground water using oxygen microbubbles". *2nd International Symposium on Gas Transfer at Water Surfaces*, Minneapolis, MN, USA, Publ by ASCE, New York, NY, USA.
- Monahan, P. B. and M. T. Holtzapple (1993). "Oxygen transfer in a pulse bioreactor." *Biotechnology and Bioengineering* **42**(6): 724-728.
- Nyborg, W. L. (1982). "Ultrasonic microstreaming and related phenomena." *British Journal of Cancer* **45**(5): 156-160.
- Peters, H. U., H. Herbst, et al. (1989). "The Influence of Agitation Rate on Xanthan Production by *Xanthomonas-Campestris*." *Biotechnology and Bioengineering* **34**(11): 1393-1397.
- Peterson, R. V. and W. G. Pitt (2000). "The effect of frequency and power density on the ultrasonically-enhanced killing of biofilm-sequestered *Escherichia coli*." *Colloids and Surfaces B-Biointerfaces* **17**(4): 219-227.

Price, G. J. (1996). *Chemistry Under Extreme or Non-Classical Conditions*. New York, Wiley & Sons.

Price, G. J. and P. F. Smith (1993). "Ultrasonic Degradation of Polymer-Solutions .3. The Effect of Changing Solvent and Solution Concentration." *European Polymer Journal* **29**(2-3): 419-424.

Radel, S., A. J. McLoughlin, et al. (2000). "Viability of yeast cells in well controlled propagating and standing ultrasonic plane waves." *Ultrasonics* **38**(1-8): 633-637.

Ratoarinoro, F. Contamine, et al. (1995). "Power measurement in sonochemistry." *Ultrasonics Sonochemistry* **2**(1): S43-S47.

Rols, J. L., J. S. Condoret, et al. (1990). "Mechanism of enhanced oxygen transfer in fermentation using emulsified oxygen-vectors." *Biotechnology and Bioengineering* **35**(4): 427-435.

Sakakibara, M., D. Wang, et al. (1994). "Effect of ultrasonic irradiation on production of fermented milk with *Lactobacillus delbrueckii*." *Ultrasonics Sonochemistry* **1**(2): S107-S110.

Schlafer, O., M. Sievers, et al. (2000). "Improvement of biological activity by low energy ultrasound assisted bioreactors." *Ultrasonics* **38**(1-8): 711-716.

Shu, C. H. and S. T. Yang (1991). "Kinetics and Modeling of Temperature Effects on Batch Xanthan Gum Fermentation." *Biotechnology and Bioengineering* **37**(6): 567-574.

- Sohn, J. I., C. A. Kim, et al. (2001). "Drag-reduction effectiveness of xanthan gum in a rotating disk apparatus." *Carbohydrate Polymers* **45**(1): 61-68.
- Sriram, G., Y. M. Rao, et al. (1998). "Oxygen supply without gas-liquid film resistance to *Xanthomonas campestris* cultivation." *Biotechnology and Bioengineering* **59**(6): 714-723.
- Suh, I. S., H. Herbst, et al. (1990). "The Molecular-Weight of Xanthan Polysaccharide Produced under Oxygen Limitation." *Biotechnology Letters* **12**(3): 201-206.
- Suh, I. S., A. Schumpe, et al. (1992). "Xanthan Production in Bubble Column and Airlift Reactors." *Biotechnology and Bioengineering* **39**(1): 85-94.
- Suslick, K. S. and G. J. Price (1999). "Applications of ultrasound to materials chemistry." *Annual Review of Materials Science* **29**: 295-326.
- Sutherland, I. W. (1993). *Chapter 4 --Biosynthesis of Extracellular Polysaccharides (Exopolysaccharides); Industrial Gums: Polysaccharides and Their Derivatives*. San Diego, Academic Press Inc., San Diego, California 92101.
- Tseng, Y. H., W. Y. Ting, et al. (1992). "Increase of Xanthan Production by Cloning Xps Genes into Wild- Type *Xanthomonas-Campestris*." *Letters in Applied Microbiology* **14**(2): 43-46.
- Umasankar, H., G. Annadurai, et al. (1996). "Xanthan production - Effect of agitation." *Bioprocess Engineering* **15**(1): 35-37.

- Wang, D., M. Sakakibara, et al. (1996). "Ultrasound-enhanced lactose hydrolysis in milk fermentation with *Lactobacillus bulgaricus*." *Journal of Chemical Technology and Biotechnology* **65**(1): 86-92.
- Wu, J. and L. Lin (2002). "Elicitor-like effects of low-energy ultrasound on plant (*Panax ginseng*) cells: Induction of plant defense responses and secondary metabolite production." *Applied Microbiology and Biotechnology* **59**(1): 51-57.
- Xu, P., J. Q. Lin, et al. (1994). "Xanthan Gum Production with Pumping Static-Mixing Loop Fermenter (Ps-Loop Fermenter)." *Biotechnology Letters* **16**(5): 523-526.
- Yang, J.-D. and N. S. Wang (1992). "Oxygen mass transfer enhancement via fermentor headspace pressurization." *Biotechnology Progress* **8**(3): 244-251.
- Yang, S. T., Y. M. Lo, et al. (1996). "Xanthan gum fermentation by *Xanthomonas campestris* immobilized in a novel centrifugal fibrous-bed bioreactor." *Biotechnology Progress* **12**(5): 630-637.
- Yau, W. W., J. J. Kirkland, et al. (1979). "Chapter 7". *Modern size exclusion liquid chromatography*: 209- 247.
- Yoon, S.-J. and K. B. Konstantinov (1994). "Continuous, real-time monitoring of the oxygen uptake rate (OUR) in animal cell bioreactors." *Biotechnology and Bioengineering* **44**(8): 983-990.

VITA



Shekhar Patel

Candidate for the Degree of

Doctor of Philosophy

Thesis: EFFECT OF ULTRASOUND ON XANTHAN GUM FERMENTATION

Major Field: Biosystems Engineering (Food and Bioprocessing)

Biographical:

Education:

- Bachelor of Technology in Dairying October 1991 – January 1996. Dairy Technology Program, ANGRAU, Tirupati, India
- Master of Technology in Dairying (Dairy Engineering) August 1996 – June 1999. National Dairy Research Institute, Karnal, India
- Completed the requirements for the Ph.D. (Biosystems Engineering) degree of Oklahoma State University in December 2003.

Experience:

- Manager, Process Development and Engineering, Nutrition Business Department, Wyeth Pharmaceuticals, Collegeville, PA. August 2003 onwards
- Research Engineer, Food and Agricultural Products Research and Technology Center, Oklahoma State University. January 2001 – August 2003
- Graduate Research Assistant, Biosystems and Agricultural Engineering Department, Oklahoma State University. January 2000 – December 2000
- Project Management Trainee, L&T-Niro, Vadodara, India. January 1999 – May 1999
- Industrial Trainee, Andhra Pradesh Dairy Development Cooperative Federation, Hyderabad, India. August 1995 – December 1995

Professional Memberships:

- Professional Member, Institute of Food Technologists, Chicago, USA.
- Member, American Institute of Chemical Engineers, New York, USA
- Associate Member Sigma Xi, The Scientific Research Society, NC, USA